5th International Conference on Phosphor Thermometry

Book of Abstracts

A. Mendieta, G. Sutton and C. Winters

National Physical Laboratory

5th International Conference on Phosphor Thermometry
June 24-26th, 2026

The National Physical Laboratory
Teddington, UK

Preface

It is with great pleasure that we present the **5th International Conference on Phosphor Thermometry (ICPT 2026)**, hosted at the National Physical Laboratory in the United Kingdom. This conference continues to provide a focal point for the international community working in luminescence thermometry—bringing together researchers from physics, chemistry, engineering, materials science, and emerging fields.

Since its inaugural meeting in Glasgow in 2018, ICPT has developed into a prominent and collaborative forum for advancing the science and application of thermographic phosphors. In less than a decade, ICPT established a versatile community focused on supporting high-impact applications in extreme environments, advanced manufacturing, energy systems, and nanoscale science. At its core, the conference series has consistently aimed to bridge fundamental materials science with applied measurement science, fostering collaboration and innovation.

The contributions collected in this volume reflect the continued growth and diversification of the field. They demonstrate advances not only in material design and synthesis to metal organic frameworks and nanodiamonds, but also in measurement techniques that integrate luminescence thermometry to complementary diagnostics, emerging computational tools, and new application domains in biology and fire science.

This book contains the programme abstracts, listed in order of Day and Session presented at ICPT 2026. We extend our sincere thanks to all authors, contributors, and participants whose work forms the basis of this volume, and we look forward to the discussions and collaborations that this conference will inspire.

The ICPT2026 organising committee

Presentations

Presenters/ Authors

Posters/presenters

Day 1 – Wednesday 24/06/2026
Sessions 1, 2, 3A, 3B, 4A, and 4B

1. KEYNOTE: The International System of Units, The Kelvin Redefinition and its Impact on Temperature Traceability

Graham Machin FREng, FRS

National Physical Laboratory, Hampton Road, Middlesex, UK, graham.machin@npl.co.uk

The international system of units (the SI) had its origins in the metric measurement system, established at the time of the French revolution. In the beginning the metric system was only used in France and consisted only of the metre and the kilogram. A great step forward for measurement took place in 1875 with the signing of the metre convention which laid the groundwork of the globalisation of the metric units, and out of which evolved the international system of units (the SI). From those beginnings the SI has grown into the global phenomenon it is today covering the measurements required to facilitate over 99% of all global economic activity. The SI is a coherent unit system comprised of seven base units consisting of mass, length, time, electric current, temperature, amount of substance and luminous intensity.

It might be surprising but the unit of temperature the kelvin was only defined in 1954, perhaps even more so because the foundational ideas of absolute temperature arose mainly from the work of Lord Kelvin (then William Thomson) in the late 1840s to mid-1850s. Kelvin was a person of precocious intellect who became Professor of Natural Philosophy at Glasgow University at the age of 24, a position he held for 53 years, becoming one of, if not, the most influential scientists of the age. As early as 1854 he posited that the absolute temperature scale, later called the kelvin in his honour, could be derived from one fixed-point a dream realised 100 years later 1954.

In this talk Professor Machin will introduce the SI system of units. He will then trace the evolution of the temperature unit, from its empirical origins in the 17th and 18th centuries, to the work of Lord Kelvin in the 19th Century, to the advent of defined temperature scales in 1927, the introduction of the SI unit of temperature, the kelvin, in 1954, up to present day when the kelvin was redefined in May 2019, in terms of a fixed value of the Boltzmann constant, k [1,2]. In the latter part of his talk, the speaker will discuss the implications of the redefined kelvin and how this could profoundly impact the provision of temperature traceability to end users in industry and elsewhere in the decades to come [3, 4].

References

[1] G. Machin “The Kelvin redefined”, Meas. Sci. Technol. 29 022001 (11pp) (2018) https://doi.org/10.1088/1361-6501/aa9ddb

[2] Machin, G., “Evolution of temperature measurement: beginnings, progress and prospects”, HAPP Conference on “Physics and the Science of Living Things” J. Phys.: Conf. Ser. 2877 012112 (2024) DOI 10.1088/1742-6596/2877/1/012112

[3] G. Machin, M. Sadli, J. Engert., A. Kirste, J. Pearce, R. Gavioso “Progress with realizing the redefined kelvin”, Proceedings of the 10th International Temperature Symposium, AIP Conf. Proc. **3230**, 020001 (2024) https://doi.org/10.1063/5.0234456

[4] G. Machin, C. Gaiser, P.M.C. Rourke “The redefined kelvin – progress and prospects”, Phil Trans Roy. Soc. A **384**: 20240463.https://doi.org/10.1098/rsta.2024.0463 (Jan 2026)

Graham Machin

Graham is a NPL Senior Fellow, has >35 years' thermometry research experience, published >290 papers and given numerous international keynote/plenary talks including the "James Schooley Invited Plenary Lecture" at the 10th International Temperature Symposium. He holds visiting/honorary professorships at Birmingham, Glasgow and Strathclyde Universities. He represents the UK on the Consultative Committee of Thermometry (CCT), was chair of the Euramet Technical Committee for Thermometry (2014-2018) and President of the Institute of Measurement and Control (2018-2019). He has been given numerous awards for his work including elected Fellow of the Royal Academy of Engineering (2019), awarded the InstMC Harold Hartley medal for "outstanding contributions to the technology of measurement and control" (2021), elected Honorary InstMC Fellow (2024) and Fellow of the Royal Society (2025). He has wide ranging research interests in thermometry e.g. future kelvin, driftless practical thermometry, clinical thermometry, photonic thermometry and leads NPL's metrology activity for nuclear decommissioning.

2. KEYNOTE: Lifetime-based Phosphor Thermometry for Global Aerothermal Measurement in Thermal Protection Research

Di Peng

School of Mechanical Engineering, Shanghai Jiao Tong University, Shanghai, China,200240
idgnep8651@sjtu.edu.cn

Reliable global measurement of surface temperature and heat flux is critical for thermal protection research. However, the relevant techniques face challenges of complex geometries, limited optical access, and strong radiative interference in harsh environments. This talk presents the development and application of lifetime-based phosphor thermometry (PT), achieving robust, high-resolution, and globally resolved diagnostics under progressively more demanding conditions.

The method is built on gated lifetime imaging using Mg_4FGeO_6:Mn phosphor. Instead of resolving the entire phosphorescence decay with high-speed imaging, the gated strategies extract temperature-sensitive lifetime information from a small number of precisely timed images. This improves signal-to-noise ratio at elevated temperatures, reduces data volume, and enables high-resolution full-field temperature mapping with low-frame-rate cameras. Background radiation correction is readily incorporated, evolving from background subtraction for steady radiation to Reynolds-decomposition-based correction for strong and fluctuating radiation.

Two representative applications demonstrate the capability of this technique. For film-cooled turbine blades, phosphor coating serves simultaneously as a temperature sensor and a simulated thermal barrier coating. Combined with focal-sweep imaging and three-dimensional remapping, the PT captures blade surface temperature distributions and enables quantitative evaluation of the film cooling effectiveness under simulated engine conditions. For hypersonic thermal protection, the method is implemented in a Mach-10 rarefied tunnel to obtain global temperature histories and reconstruct high-resolution heat-flux distributions on HB-2 models, revealing fine aerothermal features associated with shock-boundary-layer interaction, shock–shock interaction, and three-dimensional fin effects.

Overall, this work establishes an integrated diagnostic framework that advances lifetime-based phosphor thermometry from controlled laboratory measurements to realistic and extreme thermal environments, providing a powerful tool for thermal protection system research.

References:

[1] Peng, D., Liu, Y. *, Zhao, X., Kim, K.C., 2016, “Comparison of Lifetime-Based Methods for Two-Dimensional Phosphor Thermometry in High-Temperature Environment,” Measurement Science and Technology, vol. 27, no. 9, 095201.

[2] Cai, T., Peng, D., Liu, Y.*, Zhao, X., Kim K.C., 2017, “A novel lifetime-based phosphor thermography using three-gate scheme and a low frame-rate camera,” Experimental Thermal and Fluid Science, vol.80, pp.53-60.

[3] Shao, H., Zhang, X., Peng, D., Liu, Y., Zhou, W.*, Chen, W., He, Y., Zeng, F. 2022, “Novel focal sweep strategy for optical aerothermal measurements of film-cooled gas turbine blades with highly inclined viewing angle,” ASME Journal of Turbomachinery, vol.144, no.3, 031008.

[4] Zhou, W. Shao, H., Zhang, X., Peng, D., Liu, Y., Li, Y., 2023, “Novel Strategy for Thermal Evaluation of Film-Cooled Blades Using Thermographic Phosphors at Simulated Engine Conditions,” ASME Journal of Turbomachinery, vol.145, no.9, 091009.

[5]Cheng, W., Li, Y., Liu, X., Liu, Y., Peng, D.*, 2023, “Lifetime-based phosphor thermometry for global heat flux measurement in a hypersonic rarefied tunnel under strong background radiation,” Experimental Thermal and Fluid Science, vol.142, 110821.

Di Peng

Di Peng received his Ph.D. in aerospace engineering from The Ohio State University in 2014. He joined School of Mechanical Engineering, Shanghai Jiao Tong University in 2015, and has served as a full professor since 2021. His main research interest is development and application of advanced aerodynamic measurement techniques, including pressure-sensitive paint (PSP), temperature-sensitive paint (TSP) and phosphor thermometry. He has over 100 journal publications and received the Chinese National Science Fund for Excellent Young Scholars. He currently serves as Associate Editor for Experiments in Fluids.

3. Comparing Environmental Barrier Surface Temperature Mapping with either a Y_2SIO_5:Er or Sc_2SiO_5:Er Temperature Sensing Layer

Jeffrey I. Eldridge[a], Michael J. Presby[a], Kang N. Lee[a*], John A. Setlock[b*]

[a]*NASA Glenn Research Center, Cleveland, OH, USA, jeffrey_eldridge@att.net*
[b]University of Toledo, Toledo, OH, USA
**retired*

Phosphor thermometry offers significant advantages for gas turbine engine environments, including insensitivity to emissivity uncertainties, rejection of reflected radiation, and limited interference from fluctuating flame chemiluminescence. However, the background thermal radiation and materials compatibility make the implementation of phosphor thermometry much more challenging with the ongoing transition to higher gas turbine engine temperatures. Currently, the lower-weight, higher-temperature capability SiC/SiC ceramic matrix composite (CMC) components that can support these temperatures are protected by environmental barrier coatings (EBCs) that prevent the unacceptable CMC recession that would otherwise occur in the water vapor-containing turbine engine environment [1-2]. Therefore, the surface phosphor temperature sensing layer must not only exhibit good temperature sensing performance in the presence of intense background radiation up to surface temperatures above 1500 °C, but must also be compatible with the EBC rare earth disilicate ($RE_2Si_2O_7$) topcoat and account for the likely slow transition of the EBC topcoat surface to the rare earth monosilicate (RE_2SiO_5).

Y_2SiO_5:Er has previously been shown to exhibit enhanced relative temperature sensitivity above 1300 °C and strong suppression of interference by background thermal radiation in the 1300 to 1560 °C range [3]. Based on this potential, a 10 μm thick Y_2SiO_5:Er(0.8%) sensor layer was deposited using a slurry process [4] via spin coating onto an EBC-coated SiC disk that had a current generation EBC top coat composition of the rare earth disilicate $Sc_2Si_2O_7$. The slurry contained a minor mullite sintering aid addition to promote coating densification. For potentially needed improved materials sensor layer/EBC compatibility, a second specimen was prepared by depositing a 22 μm thick Sc_2SiO_5:Er(0.8%) sensing layer using the same coating process but without any sintering aid addition. Testing was also performed on standalone sintered disks of both the Y_2SiO_5:Er(0.8%) and Sc_2SiO_5:Er(0.8%) compositions prepared without sintering aids.

Luminescence decay curves over a range of temperatures were acquired by mounting the specimen inside a furnace with an optical window through which a pulsed 522 nm excitation could be transmitted and luminescence emission collected and detected by a photomultiplier tube (PMT) after bandpass filtering centered at 542 nm. Decay times were determined by fitting a single exponential to the data with intensity threshold crossings at 60% and 2% of the initial intensity selected as the start and end of the fitting window, respectively. The decay times determined in this manner are plotted as a function of temperature in Figure 1. The temperature dependence of decay times is fit to a dual effective phonon energy multiphonon emission model

[3] based on a transition from nonradiative multiphonon emission of a small number of large energy phonons to emission of a large number of small energy phonons at high temperatures.

Luminescence lifetime imaging-based temperature maps were obtained using an intensified CCD camera to generate an image stack where each image in the stack was acquired at an incremental increase in delay after a beam-expanded 522 nm excitation pulse. Decay times were determined from the decay curve generated by each pixel in the stack using the same procedure as for the PMT-acquired spot temperature measurements. Furnace calibration measurements were used to convert decay times to temperature at each pixel. Temperature maps acquired in this manner are displayed in Figure 2 along with maps of deviation of pixel temperature from the area-averaged mean temperature. The standard deviation of the pixel temperature values over each temperature map area are shown below the temperature maps.

Despite better relative temperature sensitivity above 1200 °C exhibited by Y_2SiO_5:Er compared to Sc_2SiO_5:Er standalone disks, the better compatibility of the Sc_2SiO_5:Er sensing layer with the underlying EBC enabled surface temperature measurements up to 1535 °C compared to only up to 1382 °C for the Y_2SiO_5:Er sensing layer. Furthermore, because of its more uniform temperature sensing response, the Sc_2SiO_5:Er sensing layer produced without sintering aids showed better relative temperature precision (0.04% at 1535 °C) than could be obtained by the Y_2SiO_5:Er sensing layers produced with sintering aids.

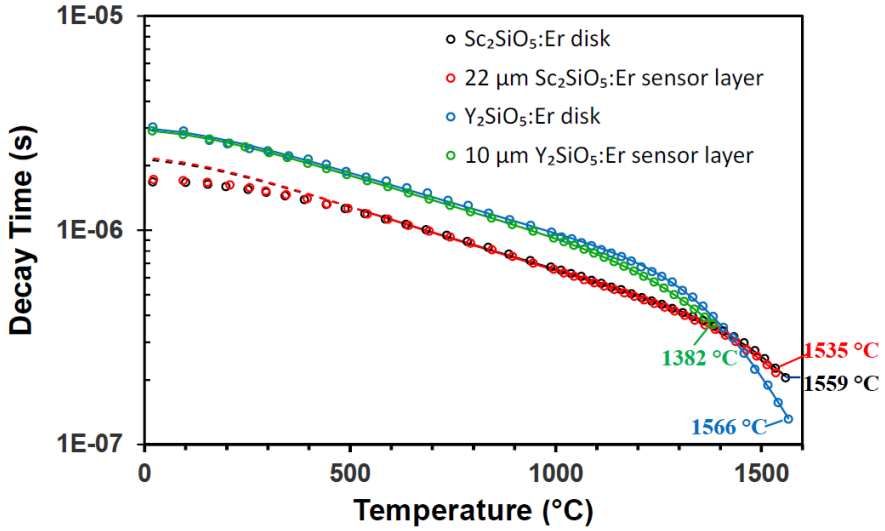

Figure 1. Temperature dependence of luminescence emission decay times for (1) 2.4 mm thick Sc_2SiO_5:Er disk, (2) 22 µm thick Sc_2SiO_5:Er sensor layer on EBC, (3) 2.4 mm thick Y_2SiO_5:Er disk, and (4) 10 µm thick Y_2SiO_5:Er sensor layer on EBC. Upper measurement limit noted for each.

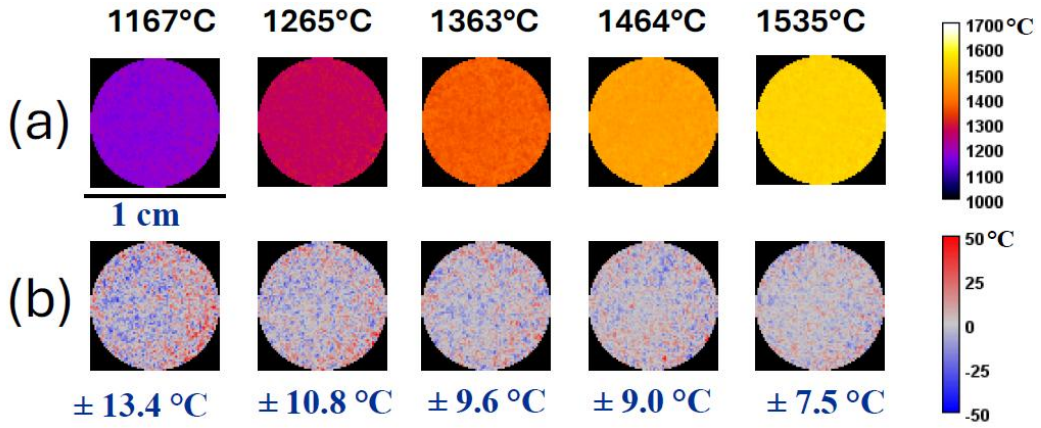

Figure 2. (a) Luminescence lifetime imaging-based temperature maps of 22 μm thick Sc_2SiO_5:Er sensor layer on EBC inside furnace at various specimen thermocouple temperatures. (b) Maps of deviation of pixel temperature from temperature mean (T-Tm).

[1] K.N. Lee, D. Zhu, R.S. Lima, J. Therm. Spray Tech., 30 (2021) 40-58. [2] B.J. Harder, E.J. Gildersleeve, J. Therm. Spray Tech., 35 (2026) 3–19.
[3] J.I. Eldridge, J.A. Setlock, K.N. Lee, AIP Conference Proceedings, vol. 3230 (2024) 120002(pp. 1-9).
[4] K.N. Lee et al., J. Eur. Ceram. Soc., 41 (2021) 1639-1653.

4. Laser-Induced Phosphorescence Thermometry for Dynamic Temperature Measurement of a Film-Cooled Aero-Engine Model Combustor Liner at Elevated Pressure

Yu Huang[a], Xiaoqi Wang[a], Jiacheng Lyu[c], Siyu Liu[a], Wubin Weng[a, b], Yong He[a, b], Zhihua Wang[a,b]

[a]State Key Laboratory of Clean Energy Utilization, Zhejiang University, Hangzhou 310027, China
[b]Qingshanhu Energy Research Center, Zhejiang University, Hangzhou 311300, China
[c]School of Aeronautics and Astronautics, Zhejiang University, Hangzhou 310027, China

Precise liner temperature distribution of aero-engine combustors is essential for cooling design, combustion evaluation, risk identification, and life prediction. Laser-induced phosphorescence (LIP) thermometry is a promising technique for wall temperature measurement in extreme combustion environments. However, existing studies mostly focus on atmospheric pressure or steady-state conditions, whereas dynamic temperature field measurements in high-pressure combustors remain extremely scarce. In this work, LIP thermometry based on the phosphorescence intensity ratio was applied to the film-cooled liner of an aero-engine high-pressure three-sector swirl model combustor (Fig. 1). Four representative engine operating conditions were simulated over 1–5 atm (Table 1), and dynamic measurements of the transient liner temperature field were performed under RP-3 aviation kerosene swirl flame impingement. YAG:Dy was selected as the thermographic phosphor. Based on its emission spectral characterization (Fig. 2), the wavelength bands centered at 458 nm and 492 nm were chosen for ratiometric thermometry. This study successfully acquired continuous dynamic combustor liner temperature fields for the four conditions, covering the entire 300-second process from ignition to near thermal steady state. Quantitative analysis of the dynamic average liner temperature (Fig. 3) showed that, compared with condition 1, increasing the air preheat temperature by 100 K in condition 2 led to a markedly higher dynamic liner heating rate, and the steady-state average liner temperature rose by approximately 180 K. A comparison among conditions 2, 3, and 4 revealed that under the synergistic effect of increasing pressure and decreasing fuel–air ratio, the dynamic liner heating rate increased sharply, whereas the steady-state average temperature decreased gradually. By further integrating the temperature field distribution characteristics (Fig. 4) with the OH^* chemiluminescence signals (Fig. 5) and flame structure observations (Fig. 6), the correspondence among the swirling flame structure, the thermal impingement regions, and the high-temperature zones on the liner was established. This validated the reasonableness of the measured liner temperature fields and revealed the mechanism by which the flame structure regulates the transient liner heating process and the steady-state temperature distribution. This study not only extends the technical boundaries of LIP technology in extreme high-temperature and high-pressure combustion environments, but also provides a key theoretical basis and technical support for dynamic liner temperature measurement and cooling structure optimization in real aero-engine combustors.

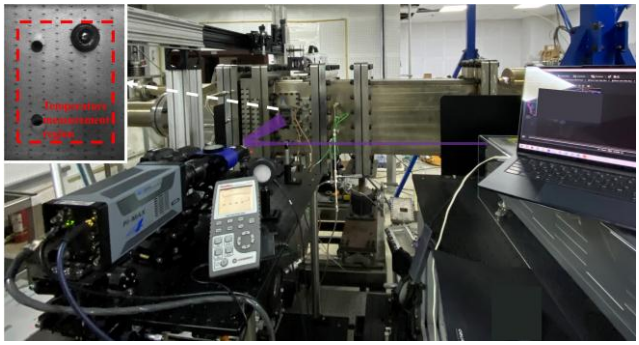

Figure 1 LIP Thermometry System for Film-Cooled Liner of Aero-Engine Model Combustor

Table 1 Experimental Conditions

Conditions	Air			Fuel	Fuel-air mass ratio
	Pressure (atm)	Temperature (K)	mass flow rate (kg/s)	Pressure (MPa)	
1	1	500	0.15	0.7	0.024
2	1	600	0.15	0.7	0.024
3	3	600	0.3	0.8	0.016
4	5	600	0.5	0.9	0.01

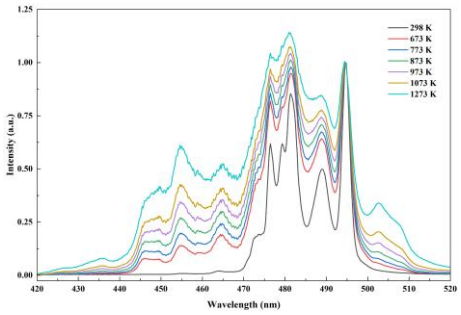

Figure 2 Phosphorescence Spectra of YAG:Dy at Different Temperatures

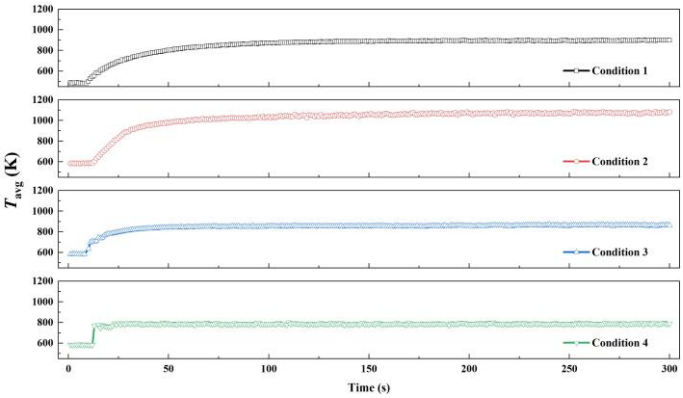

Figure 3 Dynamic Changes of Liner Average Temperature under Different Conditions

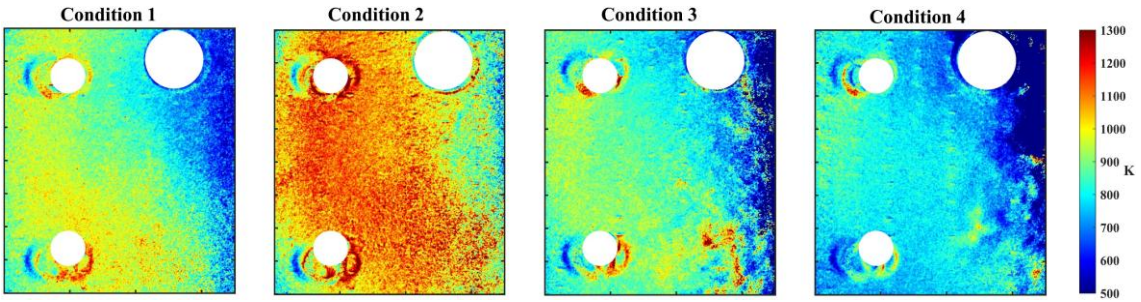

Figure 4 Transient Liner Temperature Fields under Different Conditions (Approaching Steady State)

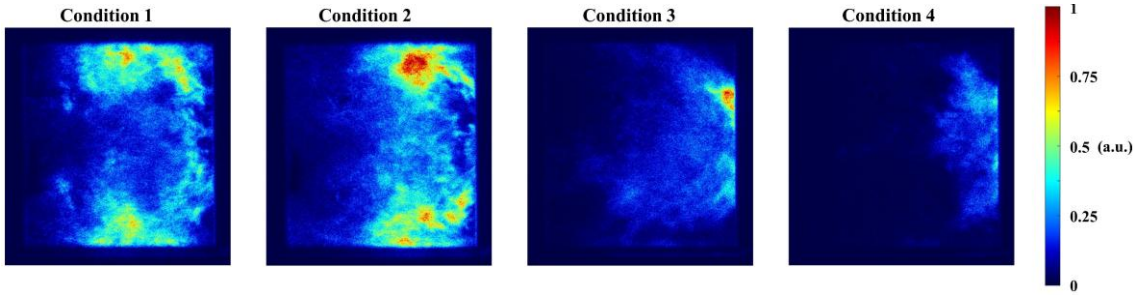

Figure 5 Transient OH* Chemiluminescence Signals under Different Conditions

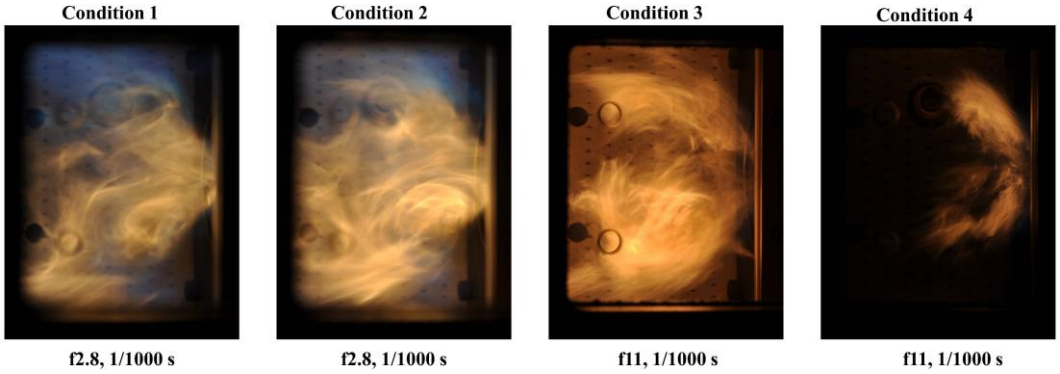

Figure 6 Transient Flame Images under Different Conditions

5. Dual-Gate Aerosol Phosphor Thermometry for Low Temperature Combustion Applications

Erick Johnson[a], Dustin Witkowski[b] David Rothamer[c]

[a]1500 Engineering Drive, Madison, Wisconsin, USA, ebjohnson4@wisc.edu[a]
[b]dwitkowski@wisc.edu, [c]rothamer@wisc.edu

1. Introduction and background

This work introduces dual-gate aerosol phosphor thermometry (DGAPT), a new approach to achieve high-precision gas temperature measurements at conditions relevant to ignition in IC engines. The DGAPT approach, illustrated in Figure 1, has been demonstrated previously for surface and liquid temperature measurements [1,2]. DGAPT offers several benefits relative to other aerosol phosphor thermometry (APT) approaches such as scattering-referenced APT (SRAPT), which has been demonstrated up to 1400 K [3]. Like SRAPT, DGAPT uses the phosphor's temperature sensitive luminescence intensity for thermometry. However, instead of relying on a laser scattering reference signal, DGAPT captures images in two temporal windows during the emission decay. The image ratio is highly temperature dependent when thermal quenching is occurring. For a single exponential temporal decay, the DGAPT ratio can be written as $R_{DGAPT} = S_{frame,1}/S_{frame,2} \sim \left(\exp\left(t_{f1}/\tau\right) - 1\right)$, where $S_{frame,1}$ and $S_{frame,2}$ are the signals for the two cameras, t_{f1} is the first gate end time, and τ is the temperature-dependent emission lifetime. With calibration, the ratio can be used to directly determine temperature. The DGAPT ratio should be independent of particle size and laser fluence, offering improvements, compared to SRAPT, in bias and precision for the harsh conditions found in IC engines.

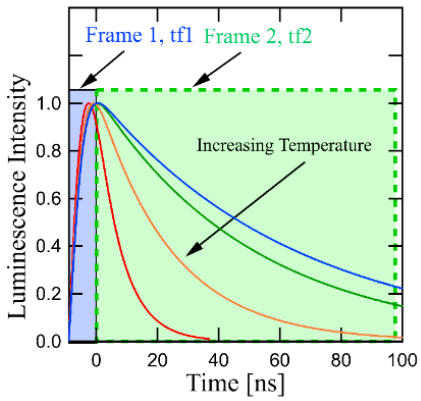

Figure 1: Illustration of DGAPT approach. Camera 1 measures luminescence signal from start of emission until time t_{fl} and camera 2 measures the remaining luminescence signal.

2.Experimental Setup

Experiments were conducted in a seeded air jet at temperatures ranging from 300 K to 1000 K to evaluate the influence of seeding density, laser fluence, and camera gate timing on DGAPT performance. Ce:LuAG phosphor particles (PhosphorTech Corporation) were seeded into a 19-mm diameter air jet using an aerosol generator (TSI, Model 3400A). The seeded air was heated using a 6-kW inline air heater (Tutco SUREHEAT F038825). Excitation was provided by the third harmonic (355 nm) of a flashlamp-pumped Nd:YAG laser operating at 10 Hz. The beam was formed into a sheet using a cylindrical (Thorlabs f =-75mm LK4385-UV) and spherical

lens (Lattice Electro Optics UF-PX-50.8-F-1000-266-355). The sheet was approximately 0.3-mm wide and 4-cm tall at the imaging location. Luminescence was measured using two intensified CCD cameras (PI-Max 4 1024i) viewing the same region through a 50/50 pellicle beamsplitter. Both cameras were equipped with a 550-nm bandpass filter (Semrock FF015333/150-50). Camera 1 acquired the initial luminescence decay, while camera 2 acquired the remaining decay over approximately 200 ns. During post processing, image pairs were software registered, background subtracted, and flat-field corrected before ratio formation. Final ratio images were software binned to yield an object plane pixel size of 570 μm. At each temperature, a Type K thermocouple, with an estimated uncertainty of $\pm$ 25 K above 700 K, was used to determine temperature for the ratio versus temperature calibration.

3. Selected Results

Figure 2(a) compares the room temperature DGAPT ratios as a function of laser fluence with those obtained for SRAPT from 20 to 110 mJ/cm² at different first gate end times (t_{f1}) of 0, 5, and 30 ns measured relative to the temporal location of the peak of the emission. In contrast to the SRAPT ratio, which changes by roughly a factor of 3, DGAPT shows no significant fluence dependence, avoiding biases due to non-uniform laser fluence in engine environments. Figure 2(b) shows a single-shot temperature image at 900 K. At each temperature, 100 single-shot images were acquired. For each image, an 80-pixel interrogation region in the center of the jet was used to calculate the single-shot precision. The results at 900 K are shown in Figure 2(c). The average measured precision is 9 K, a substantial improvement relative to SRAPT [3]. This is attributed to DGAPT not relying on a scattering reference, which leads to added noise for SRAPT when imaging particles with non-uniform size distributions [3].

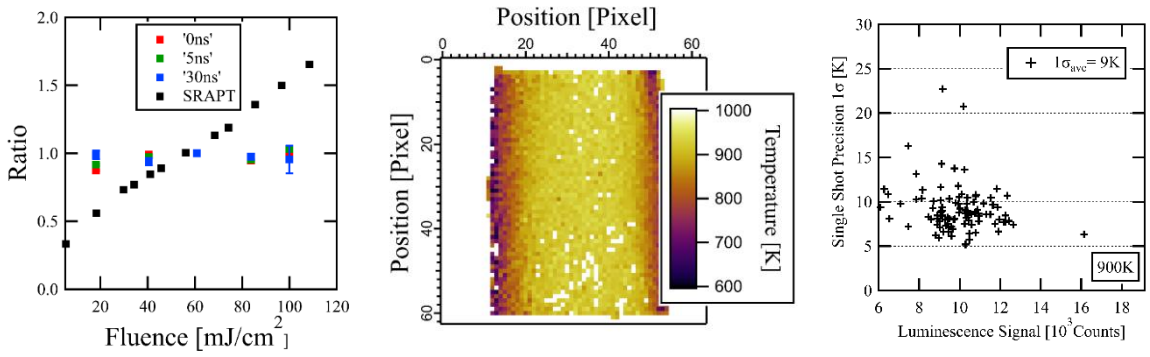

(a) (b) (c)

Figure 2: (a) DGAPT ratio vs. fluence for different first gate end times of 0, 5, and 30 ns compared to SRAPT, (b) Single-shot temperature image at 900 K, and (c) Temperature precision vs. luminescence signal for each single-shot image at 900 K

4.Conclusions

Dual-Gate Aerosol Phosphor Thermometry (DGAPT) was evaluated for spatially-resolved temperature measurements in a heated air jet at temperatures up to 1000 K. DGAPT exhibited no statistically relevant dependence on laser fluence, in contrast to SRAPT. Spatially-resolved temperature fields were obtained at 900 K with single-shot precision of 9 K, demonstrating DGAPT's potential for studying ignition processes in IC engines.

5. Acknowledgements

Research was sponsored in part by the Army Research Laboratory and was accomplished under Cooperative Agreement Number W911NF-20-2-0181. The views and conclusions contained in this document are those of the authors and should not be interpreted as representing the official policies, either expressed or implied, of the Army Research Laboratory or the U.S. Government. The U.S. Government is authorized to reproduce and distribute reprints for Government purposes notwithstanding any copyright notation herein.

6. References

[1] Anthony O Ojo, David Escofet-Martin, and Brian Peterson. High-precision 2D surface phosphor thermometry at kHz-rates during flame-wall interaction in narrow passages. *Proceedings of the Combustion Institute*, 39(1):1455–1463, 2023.

[2] Christopher Abram, Irin Wilson Panjikkaran, Simon Nnalue Ogugua, and Benoit Fond. ScVo4: Bi3+ thermographic phosphor particles for fluid temperature imaging with sub-° C precision. *Optics Letters*, 45(14):3893–3896, 2020

[3] Joshua M Herzog, Dustin Witkowski, and David A Rothamer. Combustion-relevant aerosol phosphor thermometry imaging using Ce, Pr: LuAG, Ce: GdPO4, and Ce: CSSO. *Proceedings of the Combustion Institute*, 38(1):1617–1625, 2021.

6. Measuring Particle Surface Temperature in Non-Premixed Packed-Bed Combustion via Lifetime-Based Phosphor Thermometry

Mohammad Rashik Niaz[1]*, Hassan Khodsiani[1a], Frank Beyrau[1]

[1] Otto von Guericke University Magdeburg, Universitätsplatz 2, 39106 Magdeburg, Germany, **mohammad.niaz@ovgu.de.*

[a] *Now with: Everllence SE, Stadtbachstraße 1, 86153 Augsburg, Germany.*

Validation of packed-bed combustion simulations encompassing heat transfer, flame quenching, particle temperatures, and compositional changes in the gas phase is hampered by a lack of experimental data. This study aims to address that gap by providing spatially resolved particle surface temperature measurements for numerical model development.

In addition to chemiluminescence imaging used to extract the position and structure of the non-premixed CH4/air flame illustrated in Fig. 1(b), we employ lifetime-based phosphor thermometry, which provides a minimally invasive method for obtaining the surface temperature distribution of particles exposed to the flame. This technique has previously been employed to investigate particle temperatures in premixed CH4/air flames [1]. To enable optical access, a model packed bed of cylindrical particles is placed on top of a rectangular slit burner. The burner generates a structurally uniform non-premixed methane/air co-flow flame along the length of the cylindrical particles, thereby enabling a two-dimensional approximation of the system (Fig 1(a)). Three cylindrical particles were coated along their midsection with a thin circumferential strip of YAG:Cr3+ phosphor with HPC binder. The phosphor coatings were excited using a 532nm pulsed laser, and the phosphorescence was captured using a highspeed camera. The camera was fitted with a filter to remove laser, flame chemiluminescence emission and blackbody radiation from the phosphor emission. The background-subtracted images were used to estimate the spatially resolved phosphorescence decay time constant, and subsequently converted to temperature using calibration data. Fig. 1(c) shows the circumferential surface temperature distribution of the three particles over θ = ±30°, with mean temperatures ranging from 455°C to 568°C, resulting from their respective positions within the packed bed.

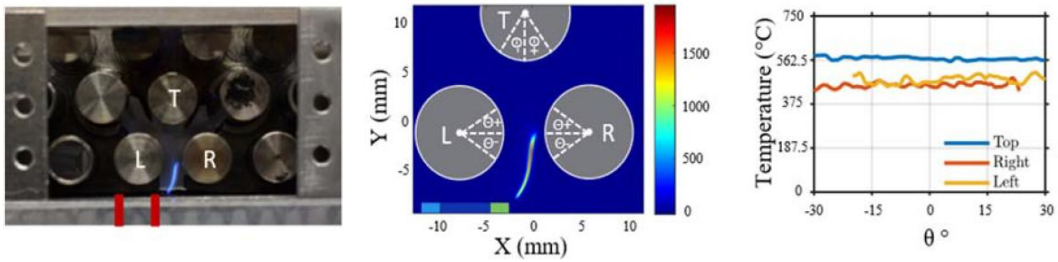

Fig 1: (a) Packed bed consisting of cylindrical particles, with the fuel outlet positioned below the left particle (indicated by red bars) to generate a non-premixed flame within the interstitial space between the three particles. (b) CH chemiluminescence image of the flame acquired using a telecentric lens, indicating the angular positions used for temperature measurements. (c) Temperature distribution of the three particles at different angular positions.

Reference to a journal publication:

[1] M. Khodsiani, F. Beyrau, B. Fond, in: LACSEA 2024 Optica Sensing Congress, Optica, Toulouse, France, Jul. 2024.

7. KEYNOTE: Operational Phosphor Thermography for Hypersonic Wind Tunnel Global Aeroheating Measurements

Casey J. Broslawski[a], Shann J. Rufer[a], Michelle L. Mason[a], Brian R. Hollis[a], Kevin E. Hollingsworth[b], Joe Rodriguez[b], Julia M. Davis[b]

[a]*NASA Langley Research Center, 1 NASA Dr., Hampton, USA,*
[b]*Amentum Technology, Inc., 600 William Northern Blvd., Tullahoma, USA*
Corresponding author contact: casey.j.broslawski@nasa.gov

The Aerothermodynamics Branch was established at NASA Langley Research Center (LaRC) to provide high-fidelity computational and experimental simulation analysis and flight test expertise capabilities in support of the design, development, mission operations, and post-flight reconstruction for access-to-space, planetary entry, and hypersonic flight vehicles. The organization maintains institutional knowledge of and synergy between computational, experimental, and flight disciplines to provide a comprehensive understanding of both slender and blunt body aerodynamics to its customers in government, private industry, and academia. Its portfolio of work includes fundamental and applied research as well as tool development.

The majority of the Branch's hypersonic ground testing occurs in the Langley Aerothermodynamics Laboratory's cold-flow, blowdown wind tunnels: the 31-Inch Mach 10 Air Tunnel and the 20-Inch Mach 6 Air Tunnel [1]. Expertise in a growing suite of diagnostics is provided to customers and implemented as appropriate for each test [2]. Because of the high enthalpies inherent to the speed regime, aeroheating is of perennial interest to researchers studying hypersonic flows and thermal protection systems. Even measurements in cold-flow facilities provide meaningful fluid mechanics and aeroheating data.

Up to the 1990s, the primary technique to measure wall heating was discrete thin-film gauges. Producing an instrumented model was complicated and expensive, and data were limited by the number of sensors which could physically fit on the test article and the channels available in the data acquisition system. At the time, researchers at NASA LaRC began studying the application of a two-color relative-intensity phosphor thermography technique for heat transfer measurements [3 – 5]. This optical technique allowed for a global temperature measurement on the entire test article, increasing the number of data points delivered to the customer by two orders of magnitude. The researchers' concurrent advancements in slip casting [6] and data reduction software [7] meant models could be fabricated, coated, and tested to deliver better data to customers faster and cheaper than the state-of-the-art. While progress has continued over the years (e.g. - the data reduction code was upgraded [8]), the core of the technique has remained largely consistent. To date this patented, two-color phosphor thermography technique has become the foundation of the Aerothermodynamics Branch's experimental aeroheating capability and thus the primary diagnostic tool tested in the LAL facilities.

Each batch of phosphor is produced at NASA LaRC. When excited by ultraviolet (UV) light, broadband "green" signal is produced by ZnCdS: Ag, Ni and a comparatively narrow "red"

light by La2O2S: 1% Eu [6]. Emission from both bands decreases with increasing temperature, but the green signal more so such that it nearly vanishes by 170°C. This range is suitable for the stagnation temperature limit in the 20-Inch Mach 6 Air Tunnel and regions aft of stagnation in the 31-Inch Mach 10 Air Tunnel. The pigments are suspended in a colloidal silica binder and sprayed onto fused silica models to a prescribed thickness by a skilled technician. This application technique allows data to be collected on complex vehicle geometries.

Because the ratio of red and green emission depends on temperature, through careful calibration one can determine the model surface temperature and thus calculate the heat transfer to the model from the flow. A camera system calibration is conducted using an integrating sphere to quantify each detectors' response to a light of known intensity. A three-channel camera is used to enable full control of the red and green sensitivity. Repeated temperature calibrations are conducted in an oven with a thin ceramic plate exposed to a UV light of varying intensity. One can use the system and temperature calibrations to create a look-up-table for temperature as a function of each pixel's red and green response for any UV light intensity. Finally, corrections are made to account for the transmission loss through the tunnel's window. The calibrations are confirmed using heating measurements taken on a canonical hemisphere tested in the 20-Inch Mach 6 Air Tunnel, with additional corrections to achieve the proper normalized stagnation heat flux applied as necessary [9]. Each phosphor batch lasts approximately six months before replacement is recommended to ensure accurate results.

Test articles are produced using a patented slip casting process described in Ref. [6]. Computer models of the test articles are 3-D printed and used to make a mold. A ceramic slurry is poured into the mold and allowed to set until a 6-mm-thick shell is produced, at which point the shell is fired at ~1175°C to densify. The cavity is sealed with a room-temperature vulcanizing rubber, a sting is installed, and then the model is backfilled with a hydraulically-setting magnesia ceramic. Finished products are inspected and fiducial markings are applied by a quality assurance technician.

The calculation of heat transfer is complicated by the injection process. The model heats as it passes through the tunnel's boundary layer flow and into the test core. To correct for this, pre-run data are collected and a step approximation [5, 8] accounts for the lost data. Heat transfer is calculated assuming 1-D conduction into an isothermal wall with constant thermal properties. More recently, a so-called patch-integral method has been developed [10] to replace the step function. This more modern code includes several other improvements, such as inclusion of temperature time history and temperature-dependent thermal properties. Data are traditionally reported as Fay-Riddell normalized values [9], and a temperature-dependent uncertainty as low as 10% is applied [5]. Heating data can be 3-D mapped to computational surfaces if desired.

NASA LaRC's phosphor thermography technique plays a critical, high-profile role in rapidly responding to the Agency's research needs. This diagnostic tool was used to determine the cause of the SSO Colombia disaster and recertify the vehicle for flight. Phosphor thermography contributed to the ground testing for the slender-body BOLT and inflatable heat shield LOFTID

flight tests. Most recently, it was used to quantify the impact of the anomaly observed on the Orion heat shield during the Artemis I mission. These examples are explored in the presentation.

References:

[1] K. T. Berger, K. E. Hollingsworth, S. A. Wright, S. J. Rufer. AIAA SciTech Forum. AIAA 2015-1337 (2015).
[2] M. L. Mason, S. J. Rufer, B. R. Hollis, S. A. Berry, G. M. Buck, V. R. Lessard, F. D. Turbeville, M. N. Rhode, N. S. Rodrigues, B. F. Bathel, and A. N. Leidy. AIAA Aviation Forum and Ascend. AIAA 2024-4111 (2024).
[3] G. M. Buck. 29th Aerospace Sciences Meeting. AIAA-1991-64 (1991).
[4] N. R. Merski. NASA technical Memorandum. NASA-TM-104123 (1991).
[5] N. R. Merski. Journal of Spacecraft and Rockets. 36(2) (1999) 160-170.
[6] G. M. Buck. 38th Aerospace Sciences Meeting & Exhibit. A00-16667 (2000).
[7] N. R. Merski. 36th AIAA Aerospace Sciences Meeting and Exhibit. AIAA 1998-712 (1998).
[8] M. L. Mason and S. J. Rufer. 32nd AIAA Aerodynamic Measurement Technology and Ground Testing Conference. AIAA-2016-4322 (2016).
[9] J. A. Fay and F. R. Riddell. Journal of Aerospace Sciences 25(2) (1958) 73-85.
[10] J. S. Cheatwood. Virginia Polytechnic Institute and State University. Master's Thesis (2022).

Casey Browlaski

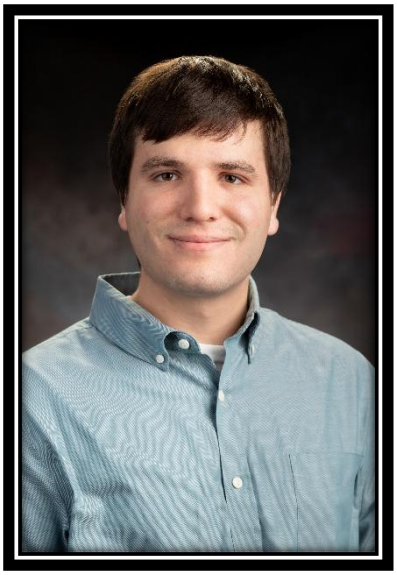

Casey Broslawski is a research aerospace engineer with the Aerothermodynamics Branch at NASA Langley Research Center. As an experimentalist he primarily works in the Center's blowdown hypersonic wind tunnels studying aeroheating and flow physics. He has led wind tunnel test campaigns for government, industry, and academic partners. His responsibilities include the maintenance and development of advanced diagnostic capabilities, most notably the so-called standard two-color phosphor thermography technique. His current research interests include novel materials for the application of phosphor thermography, plume-surface interaction, and hypersonic fluid-thermal-structure interaction. He received a PhD from Texas A&M University in 2022 and is a Young Professional Member of the American Institute of Aeronautics and Astronautics.

8. Towards Full-Surface Thermal Mapping Using Imaging of Thermal History Coatings

Carl Parsons[ab], S. Hochgreb[a], S. Karagiannopoulos[b] , S Araguas Rodriguez[b], J.P. Feist[b]

[a]*Reacting Flows, Department of Engineering, University of Cambridge, UK*
[b]*Sensor Coating Systems Ltd., londoneast-uk, Yewtree Avenue, Dagenham East, UK*

The transition towards net-zero energy systems and higher efficiency aero and gas turbine engines is driving operation at increasingly high firing temperatures. These conditions introduce increased thermal stress and reduce component lifetimes. Consequently, precise surface temperature measurements are required to support component design, validate models, improve understanding of cooling mechanisms, and identify hot spots and thermal gradients. This work investigates the instrumentation used for thermographic phosphor measurements and explores the development of imaging-based readout for Thermal History Coatings (THCs). THCs are a class of thermographic phosphor coatings that record the maximum temperature exposure experienced by a component, hence retaining a temperature memory. Unlike conventional thermographic phosphors that measure instantaneous surface temperature during excitation, THCs undergo permanent temperature-dependent changes that allow the peak temperature reached by a component to be determined after operation through luminescence measurements referenced to calibration data [1].

This paper will review how current THC measurements are typically performed using single-point optical probing, where a laser excites a small region of the coating on a component and the emitted luminescence is collected using a fibre-optic system and a photodetector. While this approach provides high measurement fidelity, mapping large components requires sequential measurement of many points [2], often of the order of several thousand of points.

This work discusses the challenges on how existing phosphor instrumentation can be adapted for imaging-based readout of THCs. Aspects to be considered are sensitivity, spatial resolution and mode-of-detection to achieve rapid, spatially resolved temperature mapping into sub-millimetre spatial accuracy of complex turbine components.

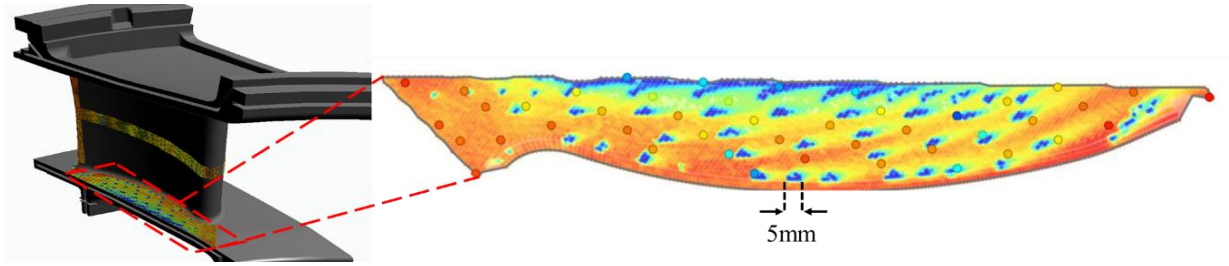

Figure 7-Temperature distribution measured from a THC on the pressure-side platform of a nozzle guide vane, highlighting a ~5 mm thermal gradient [2].

[1] Araguas Rodriguez, S, Bouten, T, Parsa, E, Ishaque, I, Parsons, C, Krsic, G, Counte, J, Axelsson, L, Karagiannopoulos, S, & Feist, J. "Utilising Thermal History Coatings for the Assessment of Hydrogen Fuel on Combustor Temperatures." Proceedings of the ASME Turbo Expo 2025: Turbomachinery Technical Conference and Exposition. Volume 5

[2] Hickey, J, Lee, J, Counte, J, Rai, K, Lee, K, Mun, Y, Araguas Rodriguez, S, Karagiannopoulos, S, Hong, G, & Feist, JP. "Unique High-Resolution Temperature Mapping of Stage 1 Turbine Vane in a Long-Term Engine Test." Proceedings of the ASME Turbo Expo 2024: Turbomachinery Technical Conference and Exposition. Volume 13

9. Phosphor Thermometry of Composites Under Flame Impingement

Maria Lora Veneracion[ab], Benoît Fond[a], François Hild[b]

[a]DAAA, ONERA, Institut Polytechnique de Paris, 92190, Meudon, France, benoit.fond@onera.fr
[b]Université Paris-Saclay, CentraleSupélec, ENS Paris-Saclay, CNRS, LMPS – Laboratoire de Mécanique Paris-Saclay, Gif-sur-Yvette, France, francois.hild@ens-paris-saclay.fr

Composite materials are desirable for building lightweight aerospace structures because of their high strength-to-weight ratio, however their structural integrity is compromised in the event of a fire. Their increasing use in the aerospace sector thus renders composite-flame interactions a topic of interest for civil aviation safety. Models have been developed to better understand their behaviour in combustion environments, however their validation still requires empirical data. The thermomechanical response of composites is governed by temperature-dependent processes, and the parameters on the face of the material exposed to the flame is key to the closure of heat and mass transfer models.

The overall objective of this study is to develop a method for simultaneously measuring surface temperature and deformation of a carbon fibre-reinforced polymer (CFRP) composite during flame impingement. Embedded sensors are intrusive and provide only local or area-averaged information. Infrared (IR) thermography is non-contact, yet typically applied to the back face of the material to avoid complications related to emissivity changes during degradation as well as interference from strong flame radiation in the IR range. [1] To circumvent these issues, the proposed system exploits phosphor thermometry (PT) and couples it with digital image correlation (DIC) in order to obtain full-field measurements. [2]

The PT system developed is based on lifetime imaging using a high-speed camera. The phosphor, YAG:Cr^{3+}, was selected because it can be excited by green light, which minimizes UV-excitable fluorescence from the polymer. Furthermore, its lifetime can easily be resolved with a high-speed camera and varies between 2.16 ms at 20°C and 0.15 ms at 400°C, with a temperature sensitivity ranging from 3.6 down to 0.5 %/K. It is applied onto a CFRP plate using an airbrush and a ceramic binder. A photograph of this CFRP sample is shown in Fig. 1a, where the horizontal structures are oriented in the direction of the fibres. The surface is illuminated using an expanded beam from a nanosecond pulsed laser at 532 nm. The luminescence is detected using a Phantom v2640 equipped with an 85 mm f/1.4 lens with a frame rate of 4800 fps. Prior to measurements, lifetime was calibrated against temperature using an aluminium block with an embedded thermocouple, placed on a heating plate.

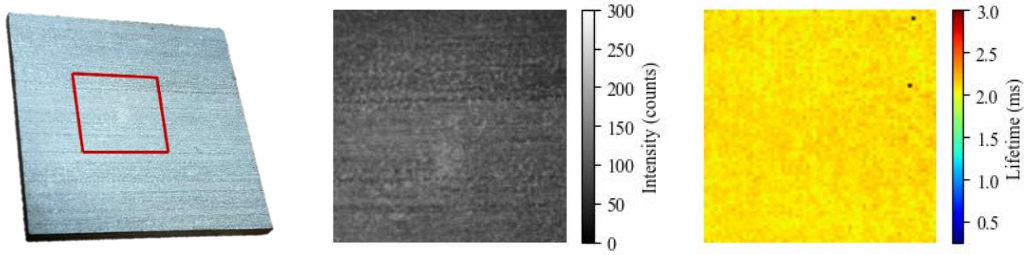

(a) (b) (c)

Figure 1. (a) An oblique view of the painted composite plate with the region of interest (ROI) enclosed in red; (b) intensity distribution of the ROI in the initial decay frame; (c) ROI lifetime map at room temperature

A room temperature lifetime image is shown in Fig. 1c. Despite strong inhomogeneity in the particle distribution (Fig. 1b), causing 20% variation in intensity, the measured lifetime map is rather homogeneous with a pixel-to-pixel standard deviation of 0.059 ms or 2.33 K.

The setup for the flame impingement experiment, in which a flame from a propane-butane blowtorch is directed towards the composite surface, is shown in Fig. 2a. In a first test, the flame is placed in the optical path of the camera without impinging on the sample, to identify which optical filter would minimize the impact of the flame emissions on the lifetime measurements while maintaining a sufficient signal level. Decay time traces are reconstructed pixelwise from the evolution of the grey levels across sequential images, with Fig. 2b showing averaged decay curves in the same ROI using 600 nm long-pass (LP) and 650 nm bandpass (BP) filters. Lifetime calculations are done by fitting a subset of data points into an exponential function. An iterative algorithm [3] is used to determine this subset which can be seen in red in Fig. 2b. When using the long-pass filter, flame emissions induce oscillations that strongly distort the decay curve and make lifetime extraction inaccurate, as can be seen in the curves. On the other hand, the bandpass filter is able to suppress the interference from the water vapour emission lines, and the flame in this test case appears to have minimal impact on the lifetime and thus the temperature calculations – an average change of 1K is seen across the entire plate. The bandpass filter was therefore deemed more suitable for the PT system.

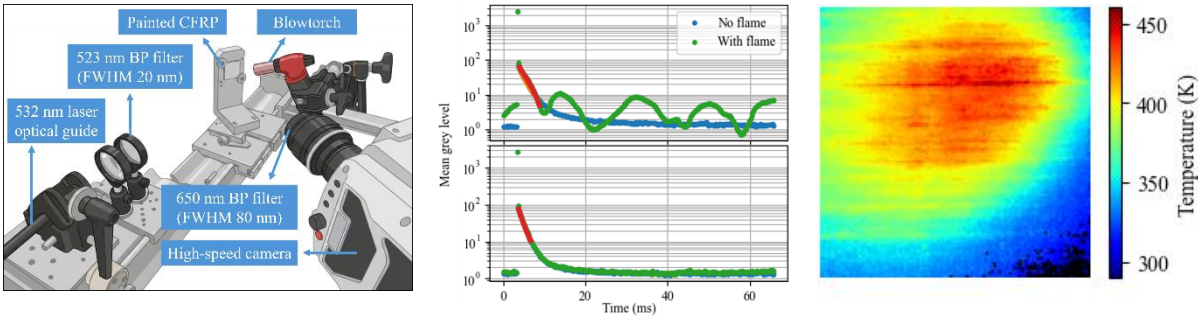

(a) (b) (c)

Figure 2. (a) Flame impingement experimental setup; (b) luminescence decay curves of the composite at room temperature with exponential fits (red lines), recorded with and without the flame in the field of view using a 600 nm long-pass filter (top) and a 650 nm bandpass filter (bottom); (c) temperature map of the exposed face of the plate during flame impingement

The temperature field obtained from the luminescence decay following a single excitation pulse during flame impingement is shown in Fig. 2c, with the highest temperatures observed near the point of impingement. Striated thermal structures are visible, seemingly corresponding to the orientation of the carbon fibres which are more conductive relative to the polymer matrix, and which results in anisotropy in the composite thermal conductivity.

These preliminary results show that PT can be used for front-face temperature mapping of composites exposed to a flame. The observed thermal anisotropy confirms the method's capability to capture material-specific behaviours in such conditions, underlining its relevance for understanding composite-flame interactions. Future work will focus on coupling this PT system with DIC to enable simultaneous full-field temperature and deformation measurements.

References :

[1] G. Leplat, Y. Le Sant, P. Reulet, T. Batmalle, Fire Mater. 45 (2020) 435–447.

[2] E. Jones, A. Jones, C. Winters, Strain 58 (2022).

[3] J. Brübach, J. Janicka, A. Dreizler, Opt. Lasers Eng. 47 (2009) 75–79.

10. Full-Field Luminescent Intensity Ratio Thermography Through Motion – Uncertainty and New Methods

Jeffrey M. Wagner[a,b], , Caroline Winters[b,c], Ryan B. Berke[a], Elizabeth M.C. Jones[d]

[a]*Utah State University, Old Main Hill, Logan, UT, USA, jeffrey.wagner@usu.edu*
[b]*Sandia National Laboratories (SNL), Albuquerque, NM, USA*
[c]*National Physical Laboratory (NPL), London, UK*
[d]*University of Illinois, Urbana-Champaign, IL, USA*

Luminescent intensity ratio (LIR) is a popular technique that obtains an optical temperature signal from thermographic phosphor luminescence by taking the ratio of the emitted intensity between two distinct spectral bands. The LIR technique is of great interest to the field of experimental solid mechanics as it has been demonstrated to provide full-field temperature in the visible spectrum with minimal adjustments to the standard, two-camera stereo digital image correlation (DIC) measurement which is already routinely implemented to measure full-field strain. Combining thermographic phosphors with digital image correlation (TP+DIC) can provide the full-field strain and temperature necessary to quantify thermomechanical material behavior [1]. However, the LIR method has previously been shown to be sensitive to experimental geometry, causing apparent temperature changes during material motion that are non-physical [2]. This research aims to address this limitation of LIR to ensure that researchers can reliably apply TP+DIC towards complex thermomechanical experiments that may involve curved surfaces, significant out-of-plane deformation, or large displacements.

To address this concern, LIR is first derived in radiometric terms and novel LIR formulations are proposed that utilize the geometric measurements of DIC to supplement the phosphor thermography. This results in four different methods of assessing LIR—the two traditional per-pixel methods (the raw signal and the derived averaged signal) and the two novel per-feature methods (the raw signal and the derived non-Lambertian signal)—as shown in Figure 1.

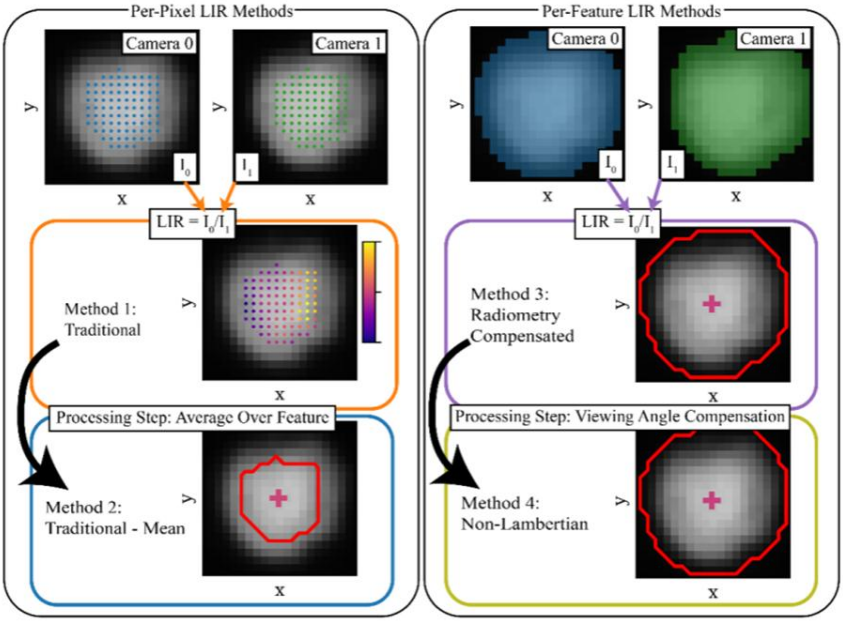

Figure 1: Visual Illustration of all Four LIR Methods Evaluated in This Work.

To compare these four LIR methods to one another, a phosphor coupon was made consisting of Mg3F2GeO4:Mn (MFG) deposited in binder onto a stainless-steel substrate. Two cameras were placed in a stereo-vision configuration and filtered to the appropriate 630 and 660 nm spectral emission bands of MFG to perform the LIR method. With the coupon mounted on a heater and a stimulating ultra-violet LED fixed on the specimen mount, a series of three experiments were performed to assess the sensitivity of all LIR methods to motion.

First, angular sensitivity was assessed by rotating the specimen at room temperature and measuring any change in the observed LIR of each method. This resulted in measured angular dependent emission (i.e. non-Lambertian emission) of the phosphor test article and justified the use of the non-Lambertian LIR model. Next, nine different temperature calibrations were taken throughout the focal volume of the experiment and the sensitivity of LIR-to-temperature was assessed for all methods. These repeat temperature calibrations confirm the reported temperature sensitivity of per-pixel LIR methods in existing literature, but illustrate that per-feature formulations can dramatically reduce sensitivity to position over the entire temperature range. Finally, the test article was translated randomly throughout the focal volume of the experiment at two isothermal temperatures (47°C and 131°C), probing the complex interplay between varying viewing angle and position in space. As shown in Figure 2, this final experiment illustrates that for both temperature trials the temperature calibration prediction interval of the per-feature LIR methods provides excellent agreement with the observed temperature variation at all positions in space while the per-pixel LIR methods show strong sensitivity to position. These experiments illustrate the benefit of moving from per-pixel to per-feature LIR methods that eliminate the sensitivity of LIR to motion and provide reliable uncertainty quantification through the temperature calibration process.

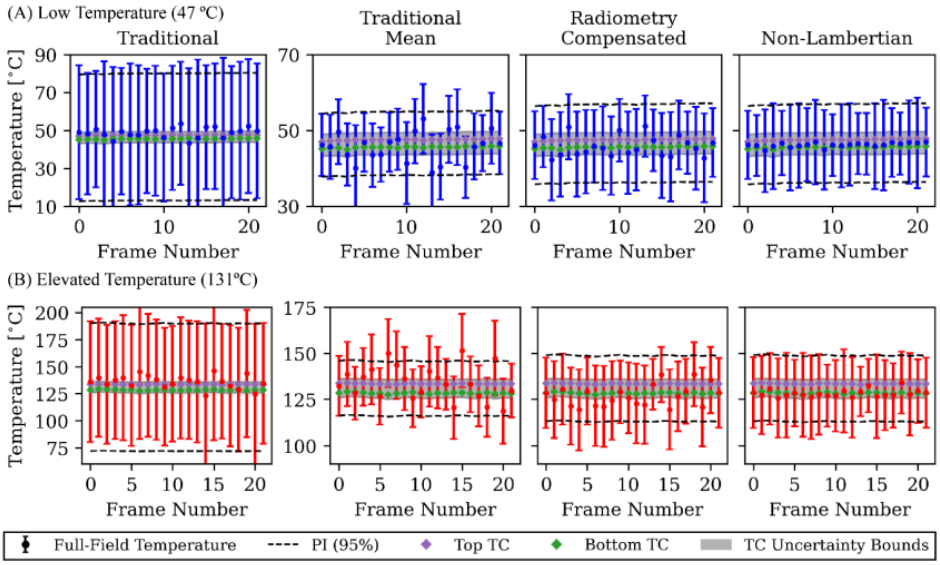

Figure 2: Results of Translating Isothermal Specimen to Various Locations in Space

[1] E. M. C. Jones, A. R. Jones, C. Winters, *Strain*, vol. 58 (2022).
[2] N. Fuhrmann, J. Brübach, A. Dreizler, *Proceedings of the Combustion Institute*, vol. 34 (2013).

SNL is managed and operated by NTESS under DOE NNSA contract DE-NA0003525.

11. Dynamic Simultaneous Measurement of Three-Dimensional Temperature and Deformation in High-Temperature Aerothermoelastic Response using Lifetime-Based Phosphor Thermometry

Ruiyu Fu[a,b], Di Peng[a,b], Yingzheng Liu[a,b], Tao Cai[a,b]

[a]School of Mechanical Engineering, Shanghai Jiao Tong University, Shanghai 200240, People's Republic of China
[b]Gas Turbine Research Institute, Shanghai Jiao Tong University, Shanghai 200240, People's Republic of China

In fields such as aerospace and energy systems, there is an urgent demand for high-precision, spatiotemporally resolved, and simultaneous three-dimensional (3D) temperature-deformation measurement techniques to characterize the thermoelastic deformation and thermodynamic behavior of critical components—such as hypersonic vehicle wings and rotating turbine blades—under extreme thermo-mechanical coupling conditions. Conventional phosphor thermometry based on intensity ratio can be applied to moving surfaces; however, the measurement inherently suffers from angular dependence due to the blue-shift effect of optical filters under oblique incidence [1]. Furthermore, dynamic variations of the viewing angle between the measured point and the detector during motion exacerbate spatial non-uniformity and introduce systematic errors in the temperature measurements.

In contrast, the lifetime-based phosphor thermometry, owing to its intrinsic self-referencing characteristic, offers higher accuracy and greater robustness against angular interference in static measurements [2]. Nevertheless, in dynamic scenarios, the pixel position corresponding to a given object point continuously shifts during the phosphorescence decay process. This leads to spatial misalignment of the extracted phosphorescence time-series signals and severe distortion in the decay curve fitting, constituting a critical technical bottleneck that limits the practical application of the lifetime-based method in dynamic measurements.

To address these challenges, this study proposes a dynamic 3D temperature-deformation simultaneous measurement method for moving surfaces by integrating lifetime-based phosphor thermometry (PT) with digital image correlation (DIC). To enable accurate determination of the phosphorescent lifetime on moving surfaces, a DIC-assisted phosphor intensity tracking algorithm is developed. As shown in Fig.1(a), the algorithm performs sub-pixel trajectory tracking and phosphor intensity reconstruction for speckle feature points throughout the phosphorescent decay- image sequence, thereby enabling accurate recovery of the true decay curve.

Experimentally, a combined screen-printing and spraying process is employed to fabricate a $Mg_4FGeO_6:Mn^{4+}$ (MFG) coating that features both high-contrast speckle characteristics and stable phosphorescence emission. As shown in Fig.1(b), a measurement system is established utilizing 395 nm pulsed ultraviolet excitation and simultaneous acquisition with two high-speed cameras. Through cross-correlation matching of the phosphorescence signals recorded by the dual cameras, the dynamic three-dimensional point cloud and full-field deformation of the measured surface are reconstructed based on the principle of binocular stereo vision. Furthermore, the two-dimensional temperature distribution obtained from the lifetime method

is mapped pixel by pixel onto the dynamic 3D coordinates, ultimately achieving spatiotemporally simultaneous reconstruction of the temperature and deformation fields.

Validation experiments involving a thin iron sheet subjected to hot jet impingement, forming a typical high-temperature aerothermoelastic response environment. As shown in Fig. 2, the high-frequency vibration behavior and the dynamic evolution of the non-uniform surface temperature under transient thermal loading were successfully captured. The results demonstrate that the developed phosphor intensity tracking algorithm effectively suppresses the influence caused by pixel drift on lifetime calculation, enabling accurate and simultaneous measurement of surface temperature and deformation during motion.

Overall, this study demonstrates that the proposed method overcomes the limitations of the lifetime-based phosphor thermometry in dynamic motion scenarios and achieves full-field, high-precision, spatiotemporally simultaneous measurement of 3D temperature and deformation on moving surfaces. It provides a robust diagnostic tool for investigating thermo-mechanical coupling mechanisms in dynamically loaded components under extreme conditions, as well as for performance optimization and reliability assessment of advanced equipment.

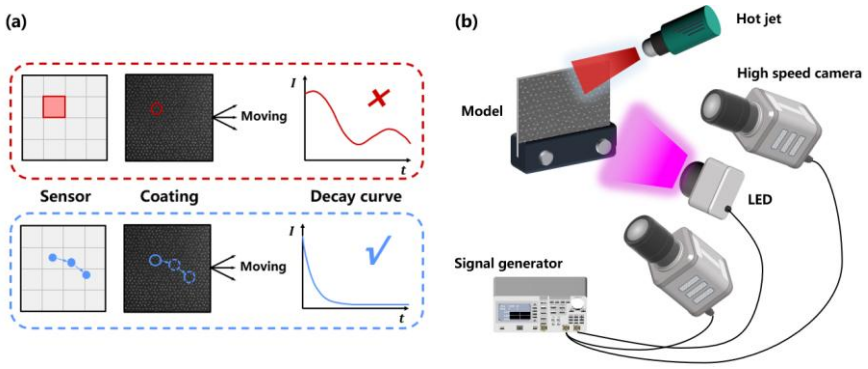

Figure 1. (a) schematic diagram of phosphor intensity tracking and (b) experimental setup of hot jet impingement.

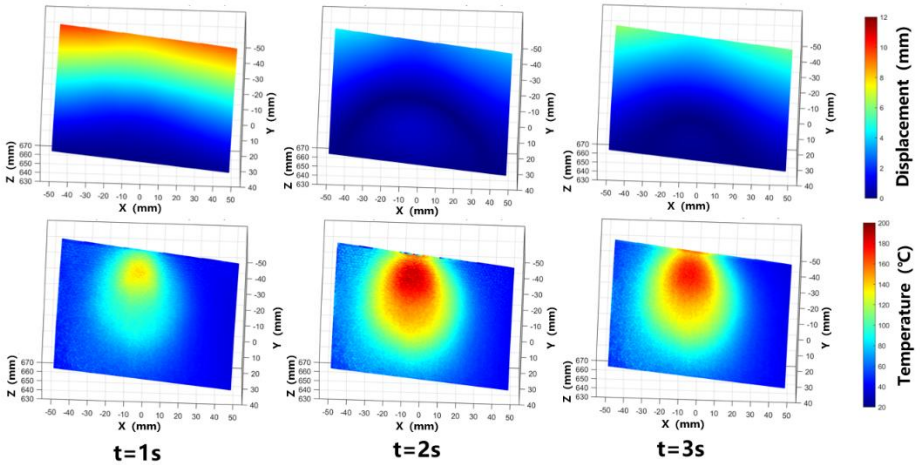

Figure 2. Time-resolved deformation and temperature distribution of the iron sheet under hot jet impingement.

Reference:

[1] E.M.C. Jones, A.R. Jones, K.N.G. Hoffmeister, et al., Meas. Sci. Technol. 33 (2022) 085201.

[2] N. Fuhrmann, J. Brübach, A. Dreizler, Proc. Combust. Inst. 34 (2013) 3611–361

12. 808 Nm Near Infrared Excited Ho3+ and Tm3+ Based Metal-Organic Frameworks for Luminescent Thermometry and Photothermal Conversion

Helene Serier-Brault,[a] Albenc Nexha,[b] Dasheng Lu,[c] Maria Cinta Pujol,[b] Jaume Massons,[b] Patricia Haro Gonzales,[d] Joan Josep Carvajal[b]

[a] *Nantes Univ., CNRS, Institut des Matériaux de Nantes Jean Rouxel, Nantes 44000, France. helene.brault@cnrs-imn.fr*
[b]*Univ. Rovira i Virgili, Dept. Química Física i Inorgànica, Campus Sescelades, E-43007, Tarragona, Spain.*
[c]*College of Rare Earths, Jiangxi University of Science and Technology, Ganzhou, 341000, PR China*
[d]*Nanomaterials for Bioimaging Group, Facultad de Ciencias, Universidad Autónoma de Madrid, Madrid 28049, Spain.*

Lanthanide-based metal–organic frameworks (MOFs) are promising hybrid materials combining the optical properties of lanthanide ions with the structural versatility and porosity of MOF architectures. In this work, Ho^{3+}/Tm^{3+}-doped MOFs based on 1,3-benzenedicarboxylic acid were investigated as multifunctional materials for luminescent thermometry and photothermal conversion under 808 nm near-infrared excitation**.** The materials were synthesized by a precipitation method and characterized using X-ray diffraction, Raman spectroscopy, FT-IR, SEM, and elemental analyses, confirming the formation of crystalline frameworks with homogeneous lanthanide distribution. Upon 808 nm excitation, the MOFs exhibit upconversion luminescence with characteristic emission bands attributed to Ho^{3+} (green at ~550 nm and red at ~650 nm) and Tm^{3+} (deep red at ~700 nm). In this system, Tm^{3+} ions act as sensitizers, absorbing the excitation energy and partially transferring it to Ho^{3+} ions through energy transfer processes. The temperature dependence of the emission intensities was investigated between 293 and 333 K**,** revealing a gradual thermal quenching of the luminescence. The intensity ratio between the Ho^{3+} emission at 550 nm and the Tm^{3+} emission at 700 nm provides the best thermometric parameter, reaching a maximum relative thermal sensitivity of 7.3 % K^{-1} at 333 K and a temperature resolution of 0.068 K. These performances are significantly higher than those reported for many lanthanide-doped inorganic hosts and previously reported MOF-based thermometers. In addition, the materials exhibit efficient photothermal behavior under continuous 808 nm laser irradiation due to non-radiative relaxation processes of Tm^{3+} ions. Temperature increases up to ~311 K were observed, with photothermal conversion efficiencies reaching 56 %, depending on the Tm^{3+} concentration. These results demonstrate that Ho^{3+}/Tm^{3+}-doped MOFs represent a promising multifunctional platform capable of simultaneous heat generation and temperature sensing, with potential applications in catalysis, biomedicine, and energy conversion technologies.

13. Europium-Doped Terbium-1,3,5-Benzenetricarboxylate MOF for Measuring Temperature in the 20–80 K Range in a Micro Tensile-Testing Set-Up

Antoine Lamothe[a], Thierry Sentenac[a], Damien Texier[a], Étienne Copin[a]

[a]*Univ Toulouse, IMT Mines Albi, INSA Toulouse, ISAE-SUPAERO, CNRS, ICA, Albi, France.*

Hydrogen is a promising energy carrier for the decarbonization of industry and transport. In the aeronautical industry, choice is to store hydrogen in its liquid form, hence at 20 K (−252.85 °C), which allows for safer and denser storage. Studying the thermomechanical behavior of materials from ambient to cryogenic temperatures is therefore a major challenge to ensure the integrity of future hydrogen fuel tanks. Indeed, certain thermomechanical configurations can lead to premature material damage. For this purpose, an experimental cryogenic tensile test set-up is being developed at the Clement Ader Institute (Figure 1). With a capacity to reach temperatures below 20 K and optical access to the sample, it aims to provide a research tool for the characterization, identification and classification of the thermal and mechanical response of metallic materials at the microscopic scale and for the 20–80 K temperature range. Since standard IR thermography is made inoperative at such temperatures and contact probes only provide point-wise information, phosphor thermometry is selected to develop a technique for simultaneous full-field temperature and strain measurement. Indeed, high spatial resolution at the microscale is required to resolve early indicators of premature damage such as dislocation movements, slip bands, etc. [1].

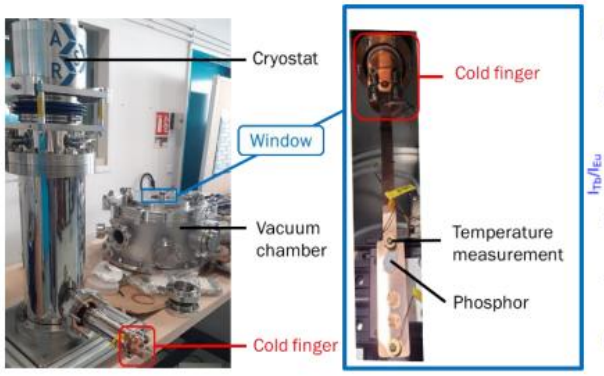

Figure 1. Cryogenic experimental set-up used to obtain calibration curves. It can be modified to accept a micro tensile-testing machine.

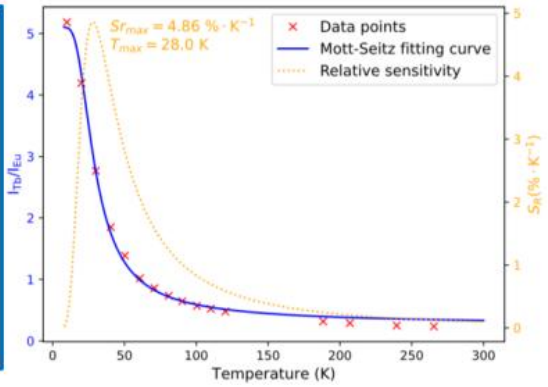

Figure 2. Temperature dependence of the Luminescence Intensity Ratio I_{Tb}/I_{Eu} (red crosses: experimental data; blue solid line: Mott-Seitz fit; R2 = 0.997) and relative sensitivity (orange dashed line)

A first step aimed at identifying, developing and studying a phosphor with high sensitivity to temperature in the studied range (20–80 K). It also needed to be compatible with the functionalization of metallic surfaces in the form of a random speckle pattern with a suitable spatial resolution to perform Digital Image Correlation (DIC) at the microscale. Based on literature, Europium-doped Terbium-1,3,5-benzenetricarboxylate (referred as Tb-btc) Metal Organic Framework (MOF) was selected for its good sensitivity in the 10–100 K temperature

range [2]. Moreover, the ability of its ligand to selectively bond on gold layers functionalized with thiols, as reported by Ameloot et al. [3], should ensure the quality of the phosphor coatings at the microscopic scale. As a simpler alternative to the hydrothermal route commonly used for the synthesis of MOF, Tb-btc was synthesized using the precipitation method in a mixture of ethanol and water described by Liu et al [4]. Scanning Electron Microscopy (SEM), Energy Dispersive Spectroscopy (EDS), X-ray diffraction (XRD), and Thermogravimetric Analysis (TGA) confirmed that the needle-shaped particles obtained correspond to the expected Europium doped [Tb(btc)(H_2O)$_6$] structure reported in the literature, with the appropriate composition. The room temperature photoluminescence emissions of the powder exhibited the typical Tb^{3+} and Eu^{3+} f-f lines around 490 nm (Tb: $^5D4 \rightarrow {}^7F6$), 540 nm (Tb: $^5D4 \rightarrow {}^7F5$), 580 nm (Eu: $^5D0 \rightarrow {}^7F1$) and 615 nm (Eu: $^5D0 \rightarrow {}^7F2$) when excited at 365 nm.

To investigate the temperature sensitivity of Tb-btc, the calibration curve was determined using the cryogenic set-up of the ICA. Small deposits of Tb-btc embedded in a commercial binder (HPC, ZYP Coatings) were made on a cold finger next to a temperature measurement point (silicon diode: Figure 1). The deposits were positioned directly beneath a 7 mm thick BK7 optical window and approximately 30 mm away from the collecting optical fiber. Through the window, the sample was excited with a 365 nm fiber-coupled UV LED (Thorlabs), and photoluminescence spectra from 8 K to ambient were recorded with a fiber-coupled spectrometer (Ocean Optics). The emission from Tb3+ luminescent centers showed strong sensitivity to temperature between 8 K and 120 K, resulting from the restricted Tb-to-Eu energy transfer when at very low temperature [5]. Figure 2 highlights the calibration curve based on the intensity ratio between the peaks located around 545 nm and 620 nm (LIR=I545/I620 respectively of Tb^{3+} and Eu^{3+}). The resulting curve is accurately fitted by a Mott-Seitz model commonly used to describe the behavior of such MOFs. A strong decrease in the ratio with increasing temperatures is highlighted, resulting from the reactivation of energy transfers, until saturation. The relative sensitivity is also plotted with a maximal value of 4.8 %·K^{-1} at 28 K. Even though this maximal sensitivity is lower than the 16.1 %·K^{-1} obtained by Amiaud et al. with {[$Tb_{1.8}Eu_{0.2}$(H_2Btec)(Btec)(H_2O)2]·$_4H_2O$}n [6], it remains greater than 1 %·K^{-1} over the whole temperature range studied (20–80 K).

Despite its lower maximum sensitivity to temperature, Tb-btc was chosen for its ability to precipitate directly onto metallic surfaces, which enables coatings with good adhesion. Preliminary studies of Tb-btc coatings on aluminum substrate sputtered with a 75 nm thick gold layer are underway at the ICA. Such speckles show promising results, thanks to the adhesion of 1.0 µm long and 0.3 µm wide luminescent Tb-btc crystals on the gold surface, suggesting the possibility of accurate full-field temperature and deformation measurement at the microscopic scale.

[1] J. C. Stinville, M. P. Echlin, D. Texier, F. Bridier, P. Bocher and T. M. Pollock, *Experimental Mechanics,* vol. 56, p. 197–216, February 2016.

[2] X. Zhou, L. Chen, Z. Feng, S. Jiang, J. Lin, Y. Pang, L. Li et G. Xiang, *Inorganica Chimica Acta,* vol. 469, p. 576–582, January 2018.

[3] R. Ameloot, E. Gobechiya, H. Uji-i, J. A. Martens, J. Hofkens, L. Alaerts, B. F. Sels et D. E. De Vos, *Advanced Materials,* vol. 22, p. 2685–2688, June 2010.

[4] K. Liu, H. You, Y. Zheng, G. Jia, Y. Song, Y. Huang, M. Yang, J. Jia, N. Guo and H. Zhang, *Journal of Materials Chemistry,* vol. 20, p. 3272–3279, April 2010.

[5] V. Trannoy, A. N. Carneiro Neto, C. D. S. Brites, L. D. Carlos and H. Serier-Brault, *Advanced Optical Materials,* vol. 9, p. 2001938, 2021.

[6] T. Amiaud, V. Jubera et H. Serier-Brault, *Journal of Materials Chemistry C,* vol. 11, p. 10951–10956, 2023.

14. Distributed Photonic Molecular Logic in Lanthanide-Bearing MOFS via Multi-Channel Emission

Zoé Languénou-Coat,[a,b] Hélène Serier-Brault,[a] Carlos D.S. Brites[b*]

[a] Nantes Université, CNRS, Institut des Matériaux de Nantes Jean Rouxel, IMN, F-44000 Nantes, France

[b] Phantom-g, CICECO – Aveiro Institute of Materials, Department of Physics, University of Aveiro, 3810-193 – Aveiro, Portugal, carlosbrites@ua.pt

Silicon-based technologies are approaching their physical and practical limits as chip miniaturization continues and the demand for computational power increases. Computational and materials research is therefore being pursued to bridge the growing gap between technological potential and current capabilities. Among the emerging alternatives, molecular computing is a promising approach, enabling computational tasks at the microscopic scale in challenging environments.[1]

Metal–organic frameworks (MOFs) based on trivalent lanthanide ions (Ln^{3+}) are ideally suited for information processing because their optical properties, modulated by light excitation and temperature, can be exploited. Eu^{3+} and Tb^{3+} act as luminescent optically active centers in molecular logic systems and emit over a broad wavelength range spanning the UV–Vis–NIR spectral regions, with characteristic narrow line-like emission bands (<10 nm) and long-lived excited-state lifetimes (>1 μs). Furthermore, the tunability of MOFs enables precise control over the local environment surrounding Ln^{3+} ions, thereby influencing their luminescent behavior and responsiveness to external stimuli. Consequently, Eu^{3+}/Tb^{3+} mixed MOFs are highly attractive for the development of molecular logic gates, using excitation wavelength and temperature as logical inputs.

By precisely tuning the relative composition of Gd^{3+}, Tb^{3+}, and Eu^{3+} within a structurally invariant framework, the optical response can be encoded at the material level, resulting in modular platforms for distributed multi-channel photonic logic. The photonic input is provided by the excitation wavelength, while spectrally resolved Tb^{3+} and Eu^{3+} emissions serve as multiple output channels. Finally, we introduce temperature as an independent control input, enabling dynamically reconfigurable logic. These results establish a distributed approach to molecular logic in which functionality is governed by material composition, providing a scalable pathway toward parallel and adaptive photonic computing.

Reference

[1] C.D.S. Brites, Mater. Horiz. 12 (2025) 4016–4026.

15. A Study of Surface Temperature Measurements: Transient Heating and Cooling of Oak Discs using Phosphor Thermometry

Si Shi[a]; Anthony O. Ojo[b]; Rory M. Hadden[c]

[a]University of Edinburgh, Kings Buildings, UK, sshi2@ed.ac.uk
[b]University of Edinburgh, Kings Buildings, UK, anthony.ojo@ed.ac.uk
[c]*University of Edinburgh, Kings Buildings, UK, rory.hadden@ed.ac.uk*

The role of firebrands in the spread of wildfires and impacts on the wildland–urban interface fire are well documented. Firebrands produced from a variety of fuel sources (e.g., trees, burning structures) can be lofted in air and transported elsewhere, potentially resulting in a secondary ignition upon landing. Knowledge of the surface temperature of these materials helps to understand their heat transfer and burning behaviours during transport in air.

In this work, transient surface temperature of a proposed firebrand surrogate is measured using 2D phosphor thermometry in a wind tunnel. Using a blower and an air heater, oak discs (12 mm in diameter and 4 mm in thickness) coated with the phosphor Mg_4FGeO_6:Mn (MFG) were exposed to the hot air flow after which the heater is turned off for the disc to undergo cooling. For each test, a type K miniature thermocouple (TC) was adhered in the centre of the disc's back, and the acquired temperature readings are compared to the results of the phosphor thermometry approach. This study aims to assess the feasibility of applying this technique on wood in a non-reactive setting, which offers insights for future work of measuring surface temperatures on burning wood. Compared to other single point methods, the spatial temperature variations provided by the 2D measurements is of particular merits, as the burning characteristics across the wood surface can be largely different. Importantly, this investigation also explores the development of phosphor thermometry using a low-cost setting, as LED is used as the light source. The general schematic of the setup is shown in Figure 1.

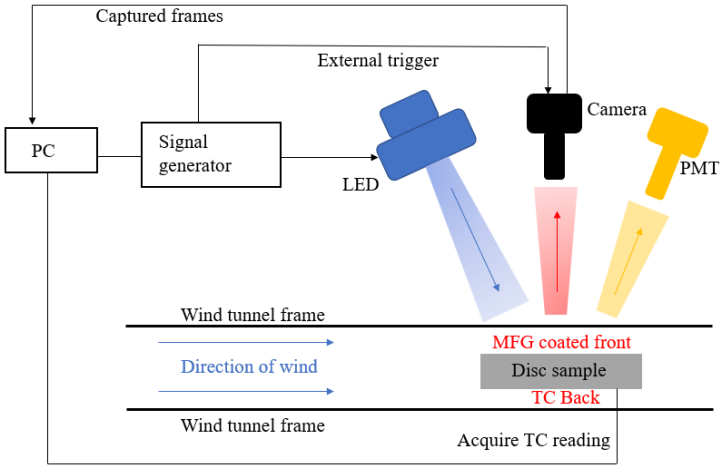

Figure 1 Experimental setup.

The method described by Cai et al. [1] was adopted, using a camera (125 Hz) fitted with a 650 ± 22.5 nm bandpass filter. The first frame (F1) was captured when the LED light is fully on. With an interframe time of 1 ms, the second frame (F2) was captured right after the excitation light ends and a background (BG) signal was obtained at the end of decay. Calibration of

intensity ratio R ($R = \frac{F1-BG}{F2-BG}$) as a function of temperature was carried out on an MFG-coated stainless-steel plate equipped with a K-type thermocouple.

Surface temperature measurements were conducted on different disc samples, subject to a variety of wind speed and air heater power. For each test, temperature data from four concentric of rings were extracted across the disc surface. This allows the spatial variations to be determined with the designated pixel radius set to be 5, 10, 15, and 20 (Figure 2). In consideration of the wind effect, a full ring was further divided into sections of upstream and downstream, and a mean temperature was obtained for each half.

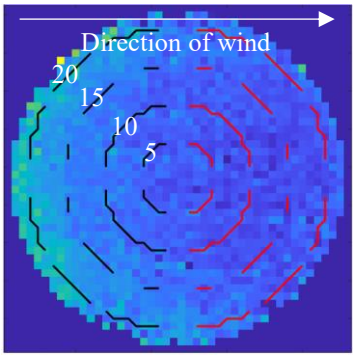

Figure 2 Example of upstream (black) and downstream (red) half rings.

From the analysis, temperatures at the most inner (R = 5) and most outer ring (R = 20) are a reasonable representation for the general spatial differences across the disc surface. An example of results for temperature and uncertainty is shown in Figure 3. During heating, clear spatial variations can be observed, as temperatures of the most outer edge at upstream are consistently higher than the results of other locations by about 10-15 ℃. The temperature differences between sections are comparatively less discernible in the cooling period. Temperature uncertainty increase during heating and decrease at a slower rate during cooling, suggesting an uneven cooling process across the wood surface.

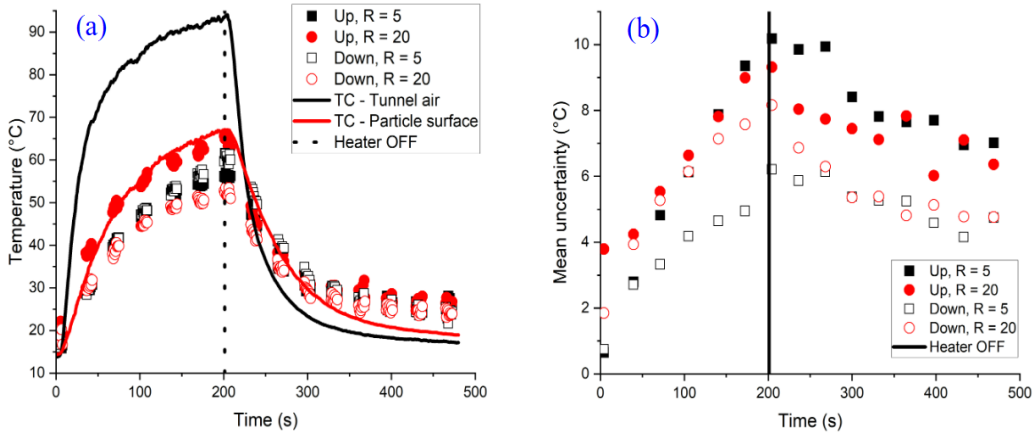

Figure 3 Example of results at the condition of wind speed of 1 m/s and low air heater level: (a) temperature results; (b) uncertainty results.

In conclusions, for a given condition, the temperatures at the upstream R = 20 consistently provide the highest values across the disc surface during heating, and results from this location are the closest to the thermocouple readings with the discrepancy being generally under 5 ℃. The degree of spatial differences varies, as values in some cases are relatively uniform while for some conditions, result at the hottest location can be up to 15 ℃ higher than the

temperatures at the coolest location. In addition, most uncertainty demonstrates that it reaches the highest level at around 10 ℃ towards the end of heating. The technique proves to be promising on the wood in this non-reactive study, hence can be considered for the potential application of wood burning.

References

[1] T. Cai, D. Peng, Y. Z. Liu, X. F. Zhao, K. C.Kim, Exp. Th

16. Combining of Fringe Projection (FP) 3D Reconstruction and Laser-Induced Phosphorescence (LIP) Thermometry for Application Of 3D Surface Temperature Measurement

Yidian Yang[a], Wubin Weng[a, b], Yan Dai[a], Qingchi Chen[a], Siyu Liu[a], Shixing Wang[a, b], Yong He[a, b], Zhihua Wang[a, b]

[a]State Key Laboratory of Clean Energy Utilization, Zhejiang University, Hangzhou 310027, China
[b]Qingshanhu Energy Research Center, Zhejiang University, Hangzhou, 311300, P. R. China

Hot-section components in aero-engines and gas turbines typically feature complex geometric configurations and operate under extremely high temperatures and severe thermal cycling, which can easily induce high-temperature ablation and creep deformation. To optimize structural design and enhance equipment performance, simultaneous measurement and accurate mapping of the three-dimensional (3D) surface topography and wall temperature field of hot-section components are urgently required. To address this need, this paper proposes a 3D wall temperature field measurement method that integrates fringe projection (FP) 3D reconstruction with laser-induced phosphorescence (LIP) thermometry (the experimental setup is shown in Fig. 1). In the experiment, periodic laser (λ=355 nm) fringes were generated by interference using a Diffractive Optical Element (DOE) and spatial filtering, and were then projected onto the surface of a 3D object coated with $BaMgAl_{10}O_{17}$:Eu (BAM) phosphor and heated by a hot-air gun. A dual-wavelength imaging system equipped with a telecentric lens was used to capture phosphorescent fringe signals at two spectral bands centered at 400 nm and 455 nm at an oblique angle (Fig. 2). By demodulating the phase change of the fringes induced by surface irregularities of the 3D object, 3D reconstruction was achieved. Experimental results show that the root-mean-square error (RMSE) of the 3D reconstruction reaches 0.142 mm (Fig. 3). Meanwhile, the phosphorescent fringe image was divided horizontally into multiple subregions, and Fourier transform, bandpass filtering, and inverse Fourier transform were sequentially applied to each subregion to accurately extract the amplitude distribution of the fringe signals (Fig. 4). The amplitude ratio of the two spectral bands was obtained and can be used to calculate the temperature field with a calibration curve. As the heating power of the hot-air gun increased from 1000 W to 2000 W, the average phosphorescence intensity ratio $\overline{\left(I_{400}/I_{455}\right)}$ increased from 0.4166 to 0.5447 (Fig. 5) indicating the temperature increasing. This study verified the feasibility of using phosphorescent fringe signals for 3D reconstruction and intensity-ratio thermometry, and provided a solid technical foundation for 3D temperature field measurement on complex geometric structures.

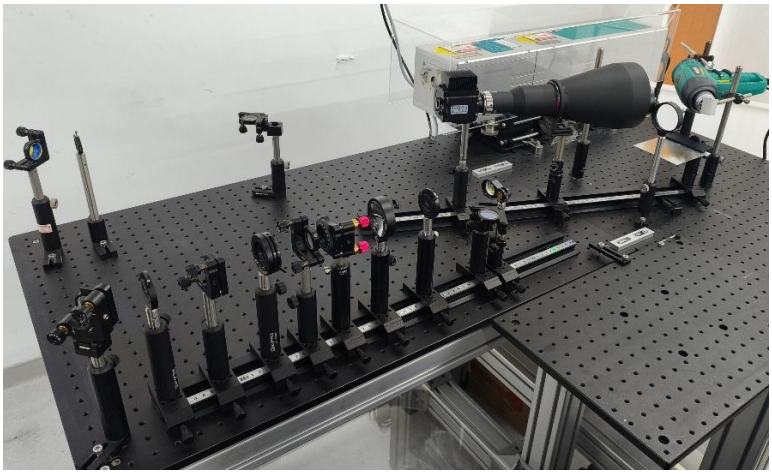

Fig. 1 Experimental setup

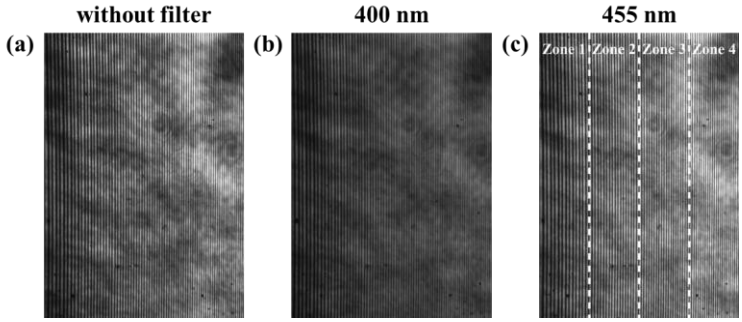

Fig. 2 Fringe patterns on the surface of the 3D object captured by the camera without a filter, and with 400 nm and 455 nm bandpass filters, when the heating power P = 1000 W

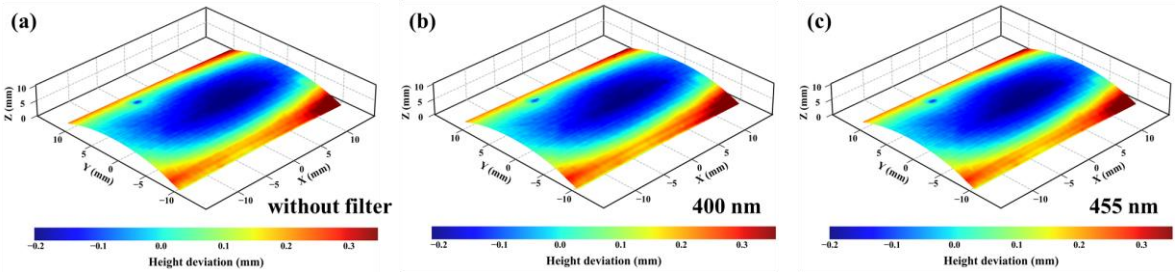

Fig. 3 Deviation values of the normal height from 3D reconstruction performed on each of the three fringe patterns when the heating power P = 1000 W

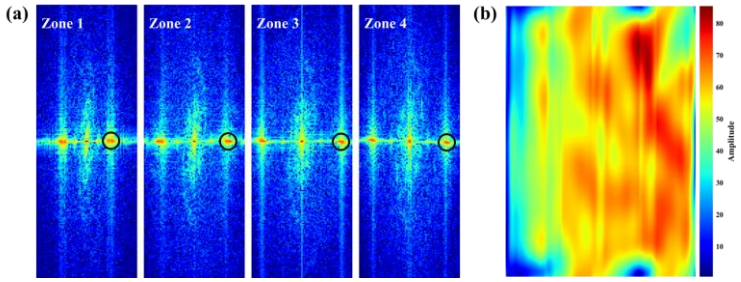

Fig. 4 Frequency spectrum obtained by Fourier transform of the phosphorescent fringe pattern at 455 nm(a); Fringe amplitude map obtained by inverse Fourier transform after filtering(b)

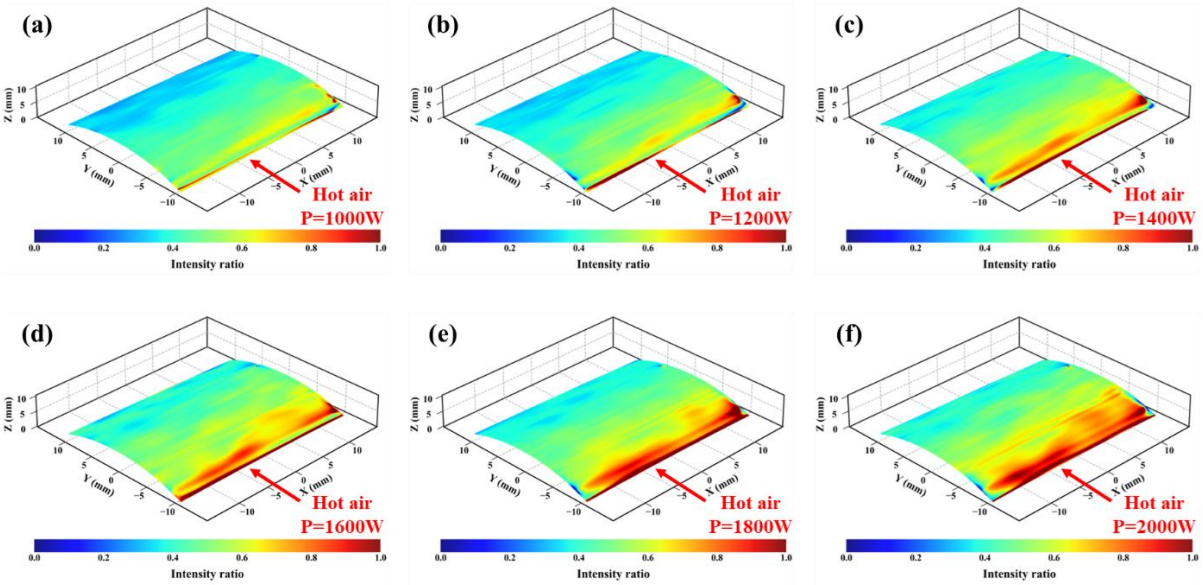

Fig. 5 Ratio of the amplitudes of the phosphorescent fringe signals at 400 nm and 455 nm on the surface of the 3D object under different heating powers of the hot-air gun

17. Exploitation of Multi-Phase Spectral Emissions for Offline Industrial Temperature by Thermal History Coatings up to 1600 °C

Abbi L Mullins, Joseph Counte, Silvia Araguas Rodriguez, Solon Karagiannopolous, Jöerg Feist
Sensor coating systems, londoneast-uk, Yewtree avenue, London, RM107FN
a.mullins@sensorcoatings.com

Higher gas turbine efficiency can be linked to increasing turbine inlet temperature, with current in-engine component surface temperature reaching to ~1600 °C. Such temperatures require innovations including active cooling and thermal barrier coating (TBC) to protect metallic sections from failure due to melting, thermal gradients, and thermal cycling. Measuring the temperatures of such surfaces is therefore of import for validation of cooling design, identifying hot spots that can reduce part lifetime, and to further push innovation for increasing efficiency. Whilst several temperature sensing technologies exist in the gas turbine industry, these can often only give singular temperature datapoints for one location, require invasive contact with the desired surface, or require line of sight not typically available in an in-engine test.
Thermal History Coating (THC) has been demonstrated for off-line temperature evaluation of historic maximum temperatures as a 3D temperature map. THCs, based on the luminescence of rare-earth ions doped into oxide ceramic host materials, are sprayed by atmospheric plasma spray (APS) onto a component as a thin coating. An irreversible change in the ceramics crystallinity as temperature increases affects the local environment of the luminescent ions, thus affecting their luminescent parameters including spectral emission. Changes to emission parameter with temperature such as peak intensities, width, and position allow for calibration of the spectral parameter to a series of set temperatures which can then be used for on-component temperature determination.

This work will provide a basic understanding of the fundamental mechanisms behind changes in rare-earth doped oxide host materials emission spectra relating to both composition and temperature effects, how a range of luminescence parameters can be used for temperature calibration, and the equipment required for measurement of off-line thermometry.

THC is further demonstrated for two industrial in-engine testcases: Enriching fuel with hydrogen in a combustor, and a Stage 1 turbine blade.[1,2] Results led to the combustor showing increased local temperature with hydrogen addition and thus identified the need for improved cooling.[1] The stage 1 blade thermal mapping showed great comparison to the customers own heat transfer codes, thus validating its usage as a credible temperature measurement technique for in-engine testing.[2]

THCs have shown great potential for model and component validation alongside cooling design evaluations including for applications within the power, aerospace, and automotive industry, providing advantages such as thin and non-destructive application, requiring non-invasive evaluation post-operation, and ability for temperature data to be digitised as a 3D temperature. map.

18. Surface Temperature Imaging During Flame Spread Over PMMA Using Phosphor Thermometry

Anthony O. Ojo[a], David Morrisset[b], Abhijit Padhiary[c], Rory M. Hadden[d], Brian Peterson[e]

[a] *IMT, University of Edinburgh, UK, anthony.ojo@ed.ac.uk*
[b] *School of Civil Engineering, University of Queensland, Australia, d.morrisset@uq.edu.au*
[c] *IMT, University of Edinburgh, UK, abncsu@gmail.com*
[d] *IIE, University of Edinburgh, UK, rory.hadden@ed.ac.uk*
[e] *IMT, University of Edinburgh, UK, brian.peterson@ed.ac.uk*

To accurately understand how heat transfer affects flame spread over solid fuels, it is crucial to know the surface temperature ($T_{surface}$) both ahead of, and underneath the flame sheet[1]. Phosphor thermometry (PT) has recently advanced such knowledge by enabling two-dimensional (2-D) $T_{surface}$ measurements during flame spread over polymethyl methacrylate (PMMA)[2]. There, $T_{surface}$ measurements from PT were combined with flame position measurements during flame spread. The findings provided insight into temperature distributions in the preheated zone ahead of the flame and in the burning (pyrolysis) area beneath it. In the region ahead of the flame front, $T_{surface}$ data from PT matched thermocouple (TC) measurements. However, as pyrolysis occurs, PMMA surface regression led to the detachment of the TC and its exposure to elevated gas-phase temperatures, thus preventing accurate $T_{surface}$ measurements. Though PT could provide $T_{surface}$ measurements on the burning surface under the flame, its measurement accuracy there still needs assessment. Such assessment is necessary as the burning PMMA surface not only exhibits a unique fluorescence signature, it also undergoes thermal decomposition, which affects phosphorescence signals levels. This study assesses the accuracy of 2-D $T_{surface}$ measurements in the burning region during downward flame spread over PMMA.

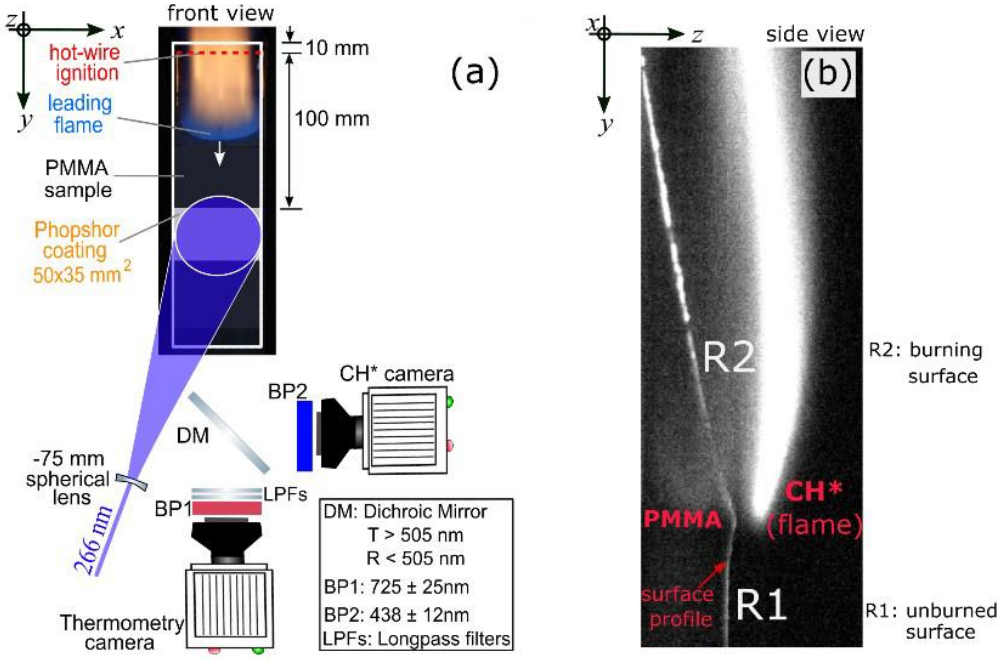

Figure 1: (a) Experimental setup of flame spread configuration with optical diagnostics layout, (b) instantaneous side-view image of the flame and PMMA surface profile.

In this work, pulsed 266 nm laser light is used to excite a 2 μm thick phosphor ($Gd_3Ga_5O_{12}$:Cr,Ce) coating applied on a PMMA surface, with two different setups implemented for thermometry. The first setup, shown in Fig.1(a), measured 2-D $T_{surface}$ distributions using an intensity ratio approach that exploits the intensities of images captured by a CMOS camera during individual phosphorescence decay. The second setup featured measurements of $T_{surface}$ at a single location (0-D) on the coating using a photomultiplier tube (PMT) to detect phosphorescence decay signals. Chemiluminescence (CH*) imaging, performed simultaneously with $T_{surface}$ measurements, tracks the flame progression during flame spread.

The results show that 2-D $T_{surface}$ measurements, especially from the burning surface, can be impacted by fluorescence and loss of PMMA material accompanying thermal decomposition. While a time-gating strategy can be implemented to avoid the short-lived fluorescence signals, the loss of PMMA material under the flame was unavoidable (Fig. 1(b)), leading to reduced phosphor particles on the burning surface. Figure 2(a) shows that during flame spread, phosphorescence signal levels under the flame decreases and deviated significantly from expected intensity levels observed during temperature calibration. Such variations in signal levels induced the non-linear response of the CMOS camera, thus necessitating the implementation of mitigation strategies for accurate $T_{surface}$ measurements.
0-D $T_{surface}$ measurements using a PMT which has better linearity response showed that, without addressing fluorescence and camera non-linearity effects, inaccuracies of 2-D $T_{surface}$ measurements can be as high as 120°C. To address these issues, mitigation strategies, involving time-gating and isolation of images prone to non-linearities, were implemented; thereby improving the accuracy of 2-D $T_{surface}$ measurements on the burning surface as shown in Fig. 2(b). In Fig. 2(c), an instantaneous spatially-resolved $T_{surface}$ distribution on PMMA is shown relative to the flame position, highlighting that the burning surface under the flame is at near constant temperature of ~ 400 ºC.

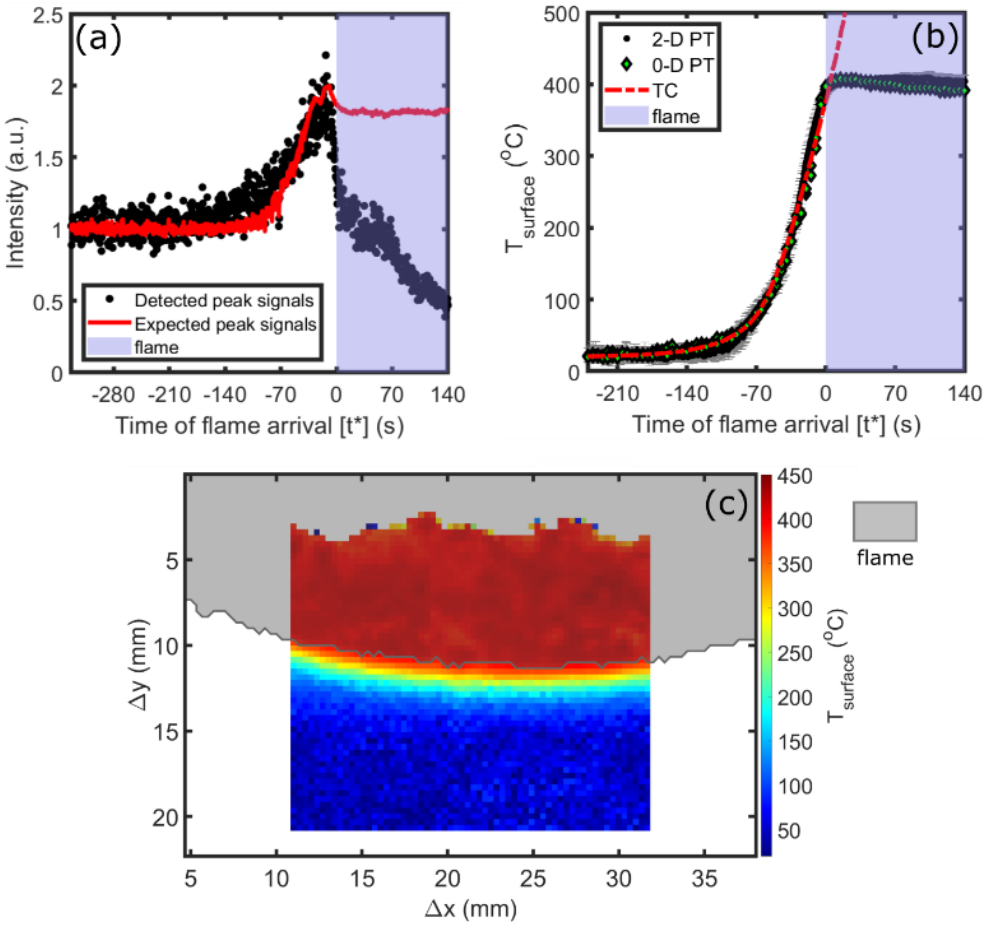

Figure 2: (a) Evolution of detected peak intensity during flame spread relative to the expected peak intensity evolution computed based on calibration data, (b) Temporal evolution of $T_{surface}$ measured using a thermocouple (TC), 0-D PT and 2-D PT, (c) Instantaneous $T_{surface}$ map measured using PT, together with the flame region (indicated by the CH* signal) overlaid as a gray shaded area.

Findings from this work provides insight into the uncertainties and their mitigation strategies when implementing surface PT in flame spread environments or in solid-fuel research. This work also finds use in other applications, where the conditions during PT calibration may be different in the environment in which PT measurements is to be implemented.

References:

[1] A. C. Fernandez-Pello, T. Hirano. *Combust. Sci. Technol.* 32 (1983) 1–31.

[2] J. Burnford, D. Morrisset, A. O. Ojo, R.M Hadden, A. Law, B. Peterson B, *Fuel*. 365 (2024) 131201.

19. Progress Towards Thermographic Shake-The-Box for Simultaneous 3D Temperature and Velocity Measurements in Flows

Moritz Stelter[a], Benoît Fond[b], Frank Beyrau[a]

[a]Otto von Guericke University Magdeburg, Universitätsplatz 2, Magdeburg, Germany, moritz.stelter@ovgu.de

[b]Department of Aerodynamics, Aeroelasticity and Acoustics (DAAA), ONERA, the French Aerospace Lab, Paris-Saclay University, Meudon, France

Volumetric thermometry and velocimetry are helpful tools for the investigation of turbulent, intrinsically three-dimensional (3D) flows. While various flow velocimetry techniques are established, isolated measurements of flow velocity cannot provide all necessary information to fully understand non-isothermal flows. Instead, simultaneous knowledge of the temperature distribution is needed. One approach to obtain simultaneous, instantaneous and discrete 3D temperature and velocity information in transparent turbulent flows relies on the integration of phosphor thermometry with volumetric flow velocimetry. Here, we present our latest progress towards thermographic Shake-The-Box, based on an earlier implementation in [1].

3D flow velocimetry often uses micron-sized tracer particles, which are assumed to follow the flow truthfully. Pulsed light illuminates the particles, and cameras record their Mie scattering from multiple angles. From these recordings, tomographic reconstruction or triangulation determines particle 3D positions, allowing shot-to-shot displacement and velocity calculations. Shake-The-Box [2] was adapted for this work to provide velocities from individual particles. To also measure temperature, ZnO thermographic phosphor particles were selected as tracers, and the velocimetry system was extended with a phosphor thermometry setup: a pulsed UV laser excites luminescence and two cameras capture spectrally separated images of it for ratiometric temperature measurements. Recording Mie scattering and luminescence simultaneously enables combined 3D velocity and temperature results using the same tracers.

In recent work, we focused on improving the processing of recorded image data to increase the number of combined temperature and velocity samples obtained. This involved tuning camera calibration, 3D position triangulation, 3D particle tracking, and enhancing luminescence particle image segmentation by exploring eight methods for temperature extraction. Reprocessing the same raw data as in [1] with these improvements doubled the number of samples from 3100 to 6950 shown in fig. 1 without compromising precision, demonstrating the significant impact of data processing on the final results.

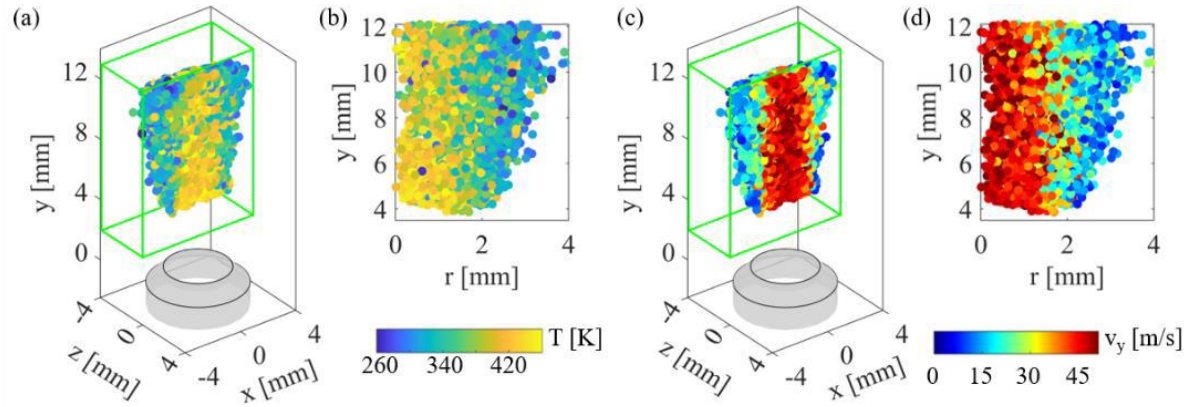

Figure 1: Cumulative temperature (a,b) and velocity (c,d) results obtained in a heated gas jet. Particles are false-colored to indicate their temperature or velocity and ploted in cut-open 3D (a,c) and height above nozzle versus distance from the jet axis plots (b,d). Adapted from [3] (CC-BY 4.0).

[1] M. Stelter, F. J.W.A. Martins, F. Beyrau, B. Fond, Meas Sci Technol 34 (2023) 074008.
[2] M. Novara, D. Schanz, A. Schröder, Exp Fluids 64 (2023) 93.
[3] M. Stelter, Three-dimensional thermometry and velocimetry in fluid flows using thermographic phosphor tracer particles, PhD thesis, Otto von Guericke University Magdeburg, 2025.

20. A Network-Enabled Particle Identification and Joint Position-Intensity Reconstruction Method for 3D Simultaneous Temperature-Velocity Measurement in Fluids

Di Luan[a, b], Cameron Tropea[c], Di Peng[a, b], Yingzheng Liu[a, b], Tao Cai[a, b]

[a] Key Lab of Education Ministry for Energy Machinery and Engineering, School of Mechanical Engineering, Shanghai Jiao Tong University, Shanghai 200240, People's Republic of China

[b] Gas Turbine Research Institute, Shanghai Jiao Tong University, Shanghai 200240, People's Republic of China

[c] Fachgebiet Stroemungslehre und Aerodynamik, Technische Universitaet Darmstadt, Peter-Grünberg-Straße 10, 64287 Darmstadt, Germany

Over the past few decades, significant progress has been made in understanding heat and mass transfer in fluids through the development of simultaneous temperature-velocity measurement techniques based on thermosensitive phosphorescent particles [1]. For a comprehensive analysis of flow structures involving heat transfer, it is essential to perform measurements in three-dimensional (**3D**) space rather than being limited to two-dimensional (**2D**) planes. In this context, velocity measurements are typically conducted using Particle Image Velocimetry (**PIV**) or Particle Tracking Velocimetry (**PTV**) techniques [2, 3, 4]. However, for temperature measurements, accurately tracking the intensity decay of moving particles in 3D space remains a significant challenge. As a result, most studies employ the intensity ratio method instead of the lifetime method to determine the temperature of phosphorescent particles [5]. Despite this limitation, the phosphorescent decay lifetime method inherently offers higher measurement accuracy than the ratiometric method due to its self-referencing nature [6]. Therefore, developing methodologies that enable the application of phosphorescence lifetime thermometry in 3D simultaneous temperature-velocity measurement in fluids is of great importance.

A network-enabled particle identification and joint position-intensity reconstruction method is proposed in this research, which enables the application of the lifetime method to phosphorescent particles in 3D measurement. By integrating this method with PTV, simultaneous 3D measurement of temperature and velocity fields in fluids is achieved. In the proposed system, phosphorescent particles are excited by 395nm UV light, and particle images within the measurement volume are captured by high-speed cameras arranged at different viewing angles. For particle identification, a neural network model is developed based on the imaging characteristics of spherical, uniformly luminescent particles. This model allows accurate extraction of both particle positions and phosphorescent intensities from each frame in a single camera view.

Furthermore, the relationship between the normalized particle intensity in the image and the particle position relative to the camera is established using the point light source - small aperture camera model. By combining this with the Shake-The-Box (**STB**) algorithm for cross-frame particle matching, the trajectory and intensity decay sequences of particles moving in3D

space can be reconstructed. This enables simultaneous measurement of both velocity and temperature fields. In experimental conditions, the proposed method achieves a temporal resolution of 0.1 s and a spatial resolution of 100 μm within a measurement area over 2×10^5 cubic millimeters.

The effectiveness of this method was verified by measurement of a central high-temperature injection flow in a large cavity. In the experiment, fluid at room temperature (25 ℃) was contained in an octagonal cylinder with an inner diameter of 200 mm, the injection orifice with a diameter of 6 mm was positioned along the axis of the cylinder. Initially the injection orifice was 2 mm below the free liquid surface, and the high-temperature fluid (180 ℃) was injected into the room-temperature fluid at an adjustable uniform speed of 10~100 mm/s. Four high-speed cameras were arranged in a 90° azimuth sector in front of the cylinder to capture images of the measurement area, which were synchronized with the UV excitation light sequence.

As shown in **Figure 1**, the proposed method successfully achieved simultaneous measurement of temperature and velocity within a 35×80×80 mm volume. The injection jet and surrounding vortex ring structure were effectively captured, and the temperature and velocity distribution in the flow were presented in color-code scatter plots. These results demonstrate the feasibility of the method in engineering applications and its strong potential for future application.

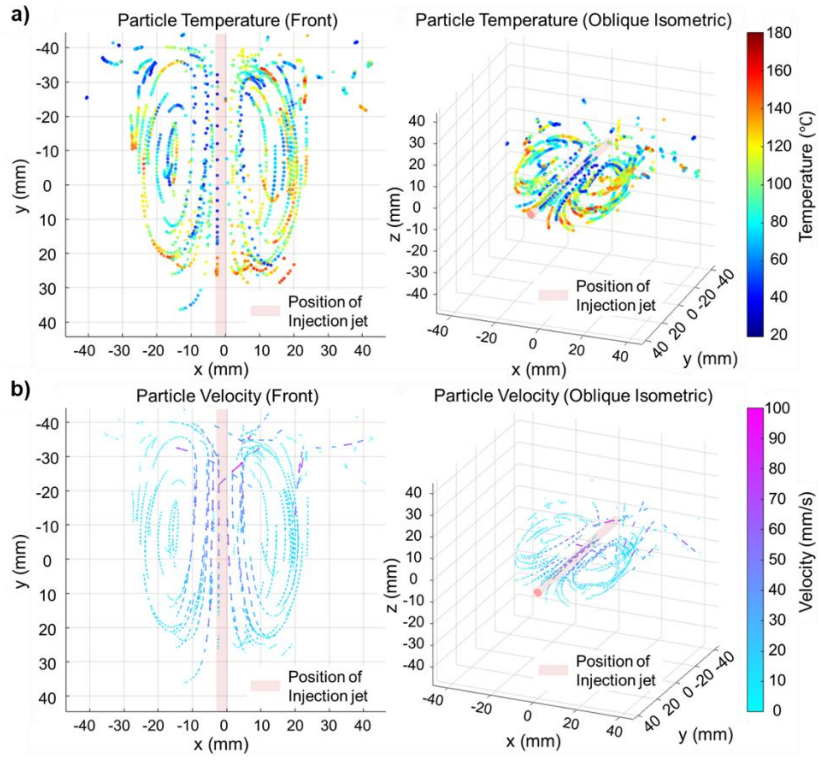

Figure 1 a) The particle temperature distribution; b) The particle velocity distribution

References

[1] Abram C, Fond B, Beyrau F (2018) Temperature measurement techniques for gas and liquid flows using thermographic phosphor tracer particles[J]. Progress in energy and combustion science 64: 93-156.

[2] Abram C, Fond B, Beyrau F (2015) High-precision flow temperature imaging using ZnO thermographic phosphor tracer particles[J]. Optics express 23(15): 19453-19468.

[3] Massing J, Kähler CJ, Cierpka C (2018) A volumetric temperature and velocity measurement technique for microfluidics based on luminescence lifetime imaging[J]. Experiments in Fluids 59: 1-13.
[4] Cai T, Han J, Kim M et al (2022) Adaptive window technique for lifetime-based temperature and velocity simultaneous measurement using thermographic particle tracking velocimetry with a single camera[J]. Experiments in Fluids 63(10): 157.
[5] Stelter M, Martins FJWA, Beyrau F et al (2023) Thermographic 3D particle tracking velocimetry for turbulent gas flows[J]. Measurement Science and Technology 34(7): 074008.
[6] Fuhrmann N, Brübach J, Dreizler A (2013) Phosphor thermometry: A comparison of the luminescence lifetime and the intensity-ratio approach[J]. Proceedings of th

21. Film Cooling Flow Analysis Using ZnO Phosphor Thermometry – Spectral Intensity Ratio Method

Arunprasath Subramanian[a], Gildas Lalizel[a], Patrick Berterretche[a], Eva Dorignac[a]

[a]*Institut P', CNRS , ISAE-ENSMA, Université de Poitiers,1 av Clément Ader, 86360 Chasseneuil du Poitou, France*
gildas.lalizel@ensma.fr

In this work, ZnO phosphor thermometry was successfully implemented to study film cooling configurations in the commissioned BATH test bench. The aim of the study was to show the effectiveness of the phosphor thermometry as a viable option to study 2D flow structures in temperature dependent flows with practical applications like gas turbines.
A cold jet seeded with ZnO particles was injected in a main seeded crossflow at 150°C with a blowing ratio M=3. This blowing ratio was used due to the better visualization possible due to high penetration of the injected cold jet. High resolution 2-D temperature contour results were obtained through a series of experiments for two test cases using the spectral intensity ratio method. A single hole case and an auxiliary hole system case were analyzed in this study.
Through the ZnO phosphor thermometry, it was possible to show that the auxiliary hole system has very favorable flow characteristics as compared to the single hole case, as the cold injected jet stays closer to the wall. Additionally, the injected jet in the auxiliary hole case has a greater lateral spread (Y/D>0.8) than that of the single hole case (Y/D ~ 0.4). The possibility of identifying key coherent structures like the jet-shear layer vortices show the fidelity of the phosphor thermometry technique providing useful insights in improving film cooling methods.

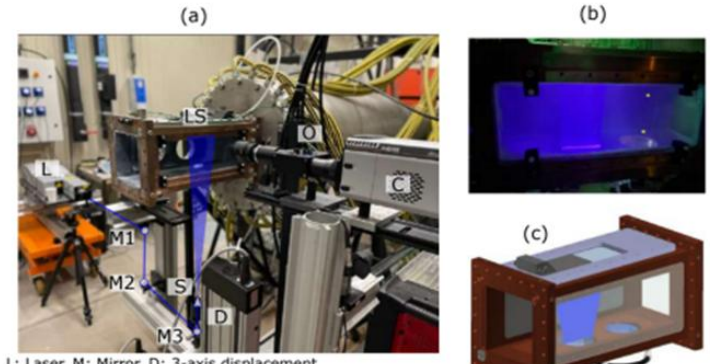

Fig. 1. Experimental setup of the film cooling study applying ZnO Phosphor thermometry

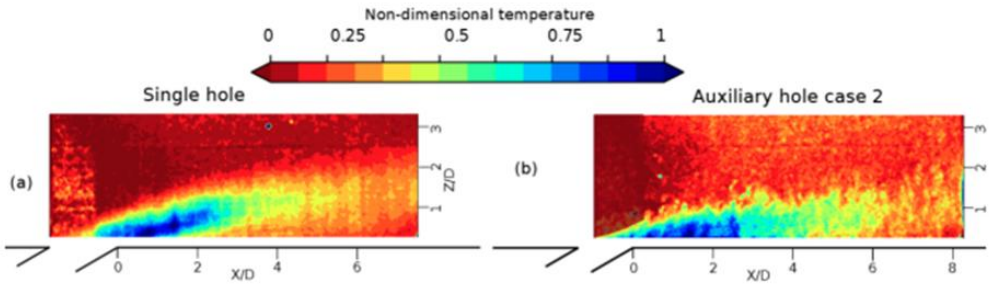

Fig. 2. Time averaged 2-D temperature flow field of 2 film cooling cases

Day 2 – Thursday 25/06/2026
Sessions 5, 6, 7A, and 7B

22. KEYNOTE: An Introduction to Primary Thermometry

Robin Underwood

National Physical Laboratory, Teddington, UK, TW11 0LW, robin.underwood@npl.co.uk

All calibrated temperature measurements can be traced back to the unit of thermodynamic temperature, the kelvin, defined as a base unit in the International System of Units (SI). Even so, it is extremely rare to find a measurement that directly utilises the kelvin definition. Instead, almost all temperature measurements are referenced to the International Temperature Scale of 1990 (ITS-90), a practical scale based on fixed points and interpolating instruments designed to approximate thermodynamic temperature. Industrial thermometers are calibrated by comparison with 'standard' thermometers calibrated according to the ITS-90.

Primary thermometers use the fundamental physics of temperature to realise the kelvin from its SI definition. The ITS-90, and hence all traceable temperature measurements worldwide, was built on the results of primary thermometry experiments.

Post-1990, primary thermometers continue to probe the small discrepancies between the ITS-90 and true thermodynamic temperature. Furthermore, recent updates to the BIPM-published Mise en pratique – effectively the 'user manual' for the definition of the kelvin – allow users the option of direct traceability to the kelvin, bypassing the ITS-90. It is anticipated that over the next few decades this route will become more widely adopted by National Measurement Institutes, perhaps one day surpassing the ITS-90 as the preferred traceability route.

This talk will give a brief explanation of the foremost methods of primary thermometry: acoustic gas thermometry (AGT), Johnson noise thermometry, radiometric thermometry, polarising gas thermometry and Doppler broadening thermometry. Special attention will be given to AGT, as this is the main area of research at NPL. Recent results will be highlighted, and plans for future research will be discussed.

Robin Underwood

Dr Robin Underwood is a Senior Scientist in the Temperature and Humidity Group at NPL. He has worked in radiation thermometry and on acoustic gas thermometry (AGT) measurements of T-T90 and the Boltzmann Constant. His current work is focussed on developing primary AGT for direct realisations of the kelvin. He also works on applications of AGT for air temperature measurement.

23. KEYNOTE: Nanodiamond Quantum Thermometers: Material Development and Applications

Masazumi Fujiwara

Okayama University, 3-1-1, Tsushimanaka, Kita-ku, Okayama 700-8530, Japan
masazumi@okayama-u.ac.jp

Temperature is a fundamental parameter in biological processes, yet conventional thermometry is limited at small scales. Nitrogen-vacancy (NV) center-based fluorescent nanodiamonds are promising quantum thermometers, offering enhanced sensitivity through spin manipulation and enabling localized temperature measurements in complex environments [1]. Over the past decade, their applications have expanded from device thermal analysis to biological systems, alongside advances in material development, while also revealing challenges in measurement accuracy and reliability.

In this talk, I will present our recent efforts in both applications and materials development. We have employed nanodiamonds to probe cellular temperature responses in *Caenorhabditis elegans*. To support such studies, we developed a bio-labeling and imaging platform based on surface-charge-engineered nanodiamonds, enabling stable in vivo retention, low toxicity, and reliable NV spin readout. Combined with artifact-suppressed imaging, this approach allows accurate spin-based measurements in living systems [2,3]. In parallel, we engineered high-quality nanodiamonds with reduced spin impurities, achieving over an order-of-magnitude improvement in spin coherence times and enabling quantum-enhanced temperature measurements with higher sensitivity and lower microwave power [4].

Finally, I will discuss key challenges in nanodiamond thermometry, including calibration accuracy, particle variability, and measurement artifacts, as well as the need for validation and standardization through comparison with established techniques. These efforts are essential for realizing reliable and quantitative applications in materials science and biology.

[1] M. Fujiwara et al., “Diamond quantum thermometry: From foundations to applications”, Nanotechnology **32**, 482002 (2021).
[2] M. Fujiwara et al., “Real-time nanodiamond thermometry probing in-vivo thermogenic responses”, Sci. Adv. **6**, eaba9636 (2020).
[3] K. Kinjo et al., “Surface-charge tailored quantum sensor nanodiamonds for toxicity-free in vivo spin-active fluorescence imaging”, submitted.
[4] K. Oshimi et al., ACS Nano **18**, 35202 (2024).

Masazumi Fujiwara

Masazumi Fujiwara is a Professor in the Department of Chemistry at Okayama University, Japan. His research focuses on nanoscale thermometry using quantum sensing with nanodiamond nitrogen-vacancy (NV) centers, particularly in biological systems. He also develops nanodiamond materials to improve sensing performance. He has received the Masao Horiba Award and the MEXT Excellent Researcher Award.

24. Emissivity Characterisation of Engineering Materials and Thermographic Phosphors Within ThermoSI

Albert Adibekyan[a], Ingmar Mueller[a], Christian Monte[a], Aldo Mendieta[b], Laura Bevilacqua[b], and Gavin Sutton[b]

[a]Physikalisch-Technische Bundesanstalt (PTB), Berlin, Germany, albert.adibekyan@ptb.de
[b]National Physical Laboratory (NPL), Teddington, UK

Reliable, traceable surface temperature measurement is a key enabler for advanced manufacturing, energy-efficient industrial processes and autonomous process control. Conventional surface thermometry, based on contact probes or thermal imaging, often suffers from large and poorly quantified uncertainties due to unknown emissivity and reflected radiation. The ThermoSI project within the European Partnership on Metrology addresses these issues by developing traceable in-situ thermometry solutions, including quantitative thermal imaging supported by thermographic phosphors, practical Johnson noise thermometry and AI-enabled self-validating temperature measurements.

One of the project tasks underpins quantitative thermal imaging by providing traceable emissivity data for key engineering materials and thermographic phosphors. Quantitative use of thermal imagers and phosphor coated reference spots requires knowledge of the spectral, angular and hemispherical emissivity of both the substrate and the phosphor coating over relevant temperature and spectral ranges. However, emissivity is notoriously difficult to measure with sufficiently low uncertainty, and independent methods are needed for validation.

A broad set of industrially relevant materials was investigated, including four representative engineering substrates (steels, aluminum, Inconel and titanium alloys), which served as the basis for a systematic emissivity study. Each material was examined in three configurations: the bare substrate, substrate with binder and substrate with a binder and MFG ($Mg_4GeO_{5.5}F$:Mn) phosphor mix (coating). Emissivity measurements were carried out using the Emissivity Measurement in Air Facility (EMAF) of PTB [1-2] over the temperature range 20 °C to 500 °C. A subset of samples was also measured in vacuum at −40 °C by means of the Reduced Background Calibration Facility 2 (RBCF2) [3]. The measurements include spectral, directional and hemispherical emissivity and were complemented by investigations of sample-to-sample variation as well as coating uniformity across different regions of the surface. In addition, the ageing behavior of the coated samples was studied through repeated thermal cycling (20 °C, 200 °C, 500 °C and back to 20 °C). The resulting emissivity dataset provides a reliable foundation for quantitative thermal imaging and for the use of the phosphor-based thermometry technique in industrial environments. These reference data for key engineering materials, which will be made openly available via the Zenodo repository, represent a crucial resource for improving surface temperature measurements under realistic and demanding operating conditions. They will support the development and validation of reliable non-contact thermometry approaches across a wide range of advanced manufacturing applications.

Acknowledgment

The project 23IND11 ThermoSI has received funding from the European Partnership on Metrology, co-financed from the European Union's Horizon Europe Research and Innovation Programme and by the Participating States.

References

[1] C. Monte, J. Hollandt, High-Temperatures – High-Pressures, 39, 151-164, 2010
[2] C. Monte, J. Hollandt, Metrologia, 47, 172-181, 2010, doi: 10.1088/0026-1394/47/2/S14
[3] A. Adibekyan, et al., Int J Thermophys. 38, 89, 2017, doi:10.1007/s10765-017-2212-z

25. Group V Metalates as High-Temperature Thermosensitive Phosphors

Federico A. Rabuffetti

Department of Chemistry, Wayne State University
5101 Cass Avenue, Detroit, Michigan, USA
far@wayne.edu

Refractory niobates and tantalates are ideal hosts for high-temperature thermosensitive phosphors activated with rare-earths. A distinct feature of these materials is their chemical tunability, which makes them ideal platforms to understand the interplay between crystal structure, electronic structure, and luminescence thermal quenching. This understanding provides the basis to exercise synthetic control over temperature-dependent luminescence and thermometric response.

In this talk I will use group V metalates to illustrate how we are approaching the challenge of establishing a set of crystal-chemical principles that enable the design of high-temperature thermosensitive phosphors. Synthesis, high-end structural analysis, and luminescence studies of dysprosium-doped $Ba_3MgTa_2O_9$ and Y_3NbO_7 will be described to demonstrate how chemical substitutions may be used to rationally tune structural and electronic features governing thermal quenching. From a luminescence thermometry standpoint, I will show that both phosphors are capable of temperature sensing up to 1200 °C, thus expanding the compositional library of high temperature thermosensitive phosphors [1,2].

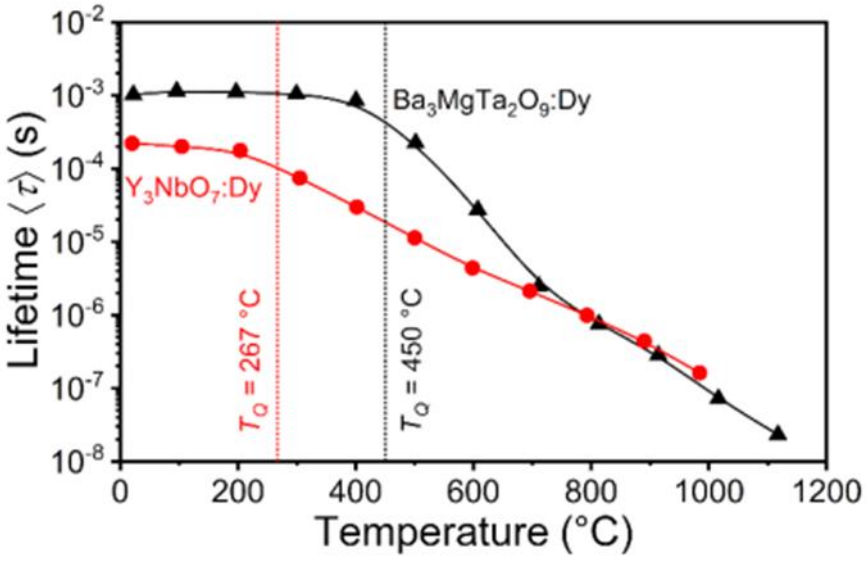

Lifetime *vs* temperature curves of thermosensitive phosphors $Ba_3MgTa_2O_9$:Dy and Y_3NbO_7:Dy.

[1] M.R. Imer, A. Afugu; Z.-F. Liu; and F.A. Rabuffetti. Luminescence of Triple Perovskite $Ba_3MgTa_2O_9:Dy^{3+}$ Up to 1100 °C. *The Journal of Physical Chemistry C* **2024**, 128, 16628–16639.
[2] M.R. Imer and F.A. Rabuffetti. Luminescence of Y_3NbO_7:Dy Up to 1000 °C. *Journal of Luminescence* **2025**, 278, 121017.

26. Sense and Sensibility in Sensing

Andries Meijerink,[a,c] Freddy Rabouw,[a] Markus Suta,[b] Rik Post,[a] Martine Hoogenraad,[a] Thomas van Swieten,[a] Guitong Zhang,[c] Lizhi Cui,[c] Jiapeng Wu,[c] Yuhua Wang[c]

[a]Debye Institute for Nanomaterials Science, Utrecht University, The Netherlands
[b]Inorganic Photoactive Materials, Heinrich Heine University, Düsseldorf, Germany,
[c]School of Materials and Energy, Lanzhou University, Lanzhou, 730000, China
a.meijerink@uu.nl

The field of luminescence temperature sensing is maturing. There is a strong focus on finding new luminescent materials with high relative sensitivity in different temperature ranges for high precision temperature measurements.[1-3] Many applications of temperature sensing relying on luminescent (nano)crystals are reported, ranging from probing living organisms to catalytic reactors.[2-5] The results are promising but commercial success is lagging behind. One reason is the challenge of universal reproducibility and reliability. This issue was addressed in a workshop '*In luminescence thermometry we trust. Can we?*' organized in the framework of the European NanoTBtech project and also in recent publications.[1,6-9] Many issues remain unresolved and in this presentation we will try to make sense of two specific challenges that are relevant for the most widely applied type of luminescent thermometers, *LIR* (Luminescence Intensity Ratio) thermometers relying on emission from two thermally coupled levels:

What is the onset temperature of Boltzmann equilibrium where reliable temperature sensing starts? How do we sensibly define onset temperature?

What causes variations in ΔE values for coupled levels in the same material measured by different groups/instruments and how does this affect reliability and reproducibility?

Sensible answers will (hopefully) be given and illustrated with experimental results. Finally, a partial solution based on anti-Stokes/Stokes (AS/S) vibronic lines will be presented as an option for calibration-free luminescence thermometry.

In the first part of the presentation the onset temperature for Boltzmann equilibrium will be discussed. In the past we and other groups have reported plots of ln(*LIR*) vs. $1/T$ where at high temperatures a good linear fit is obtained with a slope of $-\Delta E/k_B T$ where k_B is the Boltzmann constant, as illustrated in Figure 1.[10-13] At low temperatures the ln(*LIR*) becomes constant or even increases upon further lowering of the temperature. This is ascribed to non-equilibrium emission from the higher emitting level in competition with non-radiative relaxation to the lower emitting level. For Eu^{3+} and Sm^{2+} this behavior has been well-explained as emission from the higher $^5D_1$ level can be clearly observed.[11,12] However, for two work horse ions for luminescence thermometry, Er^{3+} and Nd^{3+}, similar behavior has been observed and also been explained by non-equilibrium emission from the higher level ($^2H_{11/2}$ for Er^{3+} or $^4F_{5/2}$ for Nd^{3+}) even though this emission could not be observed down to the lowest temperatures. Also, the ln(*LIR*) values reported at low temperatures vary for the same luminescent material. Here careful experiments are conducted showing that the ln(*LIR*) values reported at low temperatures

are too high and are in fact integrated 'intensity' of noise and background signal in the spectral region where emission from the higher energy level is expected. Emission spectra measured over a wide intensity range to detect very weak non-equilibrium emission provide an upper limit of the non-equilibrium emission intensity at 4 K for the $^2H_{11/2}$ emission of Er^{3+} in $NaYF_4$ and Y_2O_2S. This upper limit is much lower than the constant ln(*LIR*) values reported for the low temperature range.[10] We find that for $^2H_{11/2}/^4S_{3/2}$ emission of Er^{3+} and $^4F_{5/2}/^4F_{3/2}$ emission of Nd^{3+} the *LIR* values measured follow Boltzmann equilibrium starting from the lowest temperatures where actual emission lines could be identified above background noise.

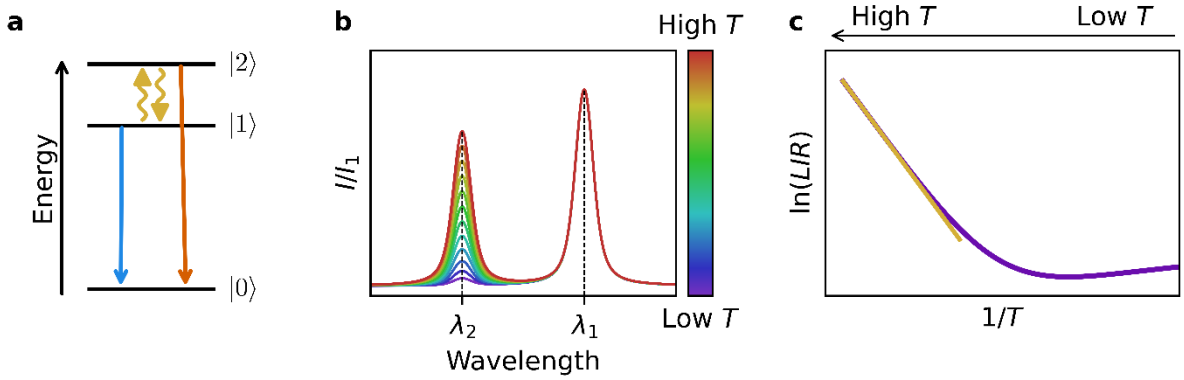

Figure 1 (a) Energy level scheme illustrating emission of two thermally coupled levels (b) Temperature dependent emission spectra for the three-level system and (c) Schematic plot of the ln(*LIR*) vs. 1/*T* with a linear part (Boltzmann equilibrium) and the typically reported deviation at low temperatures.

In the second part of the presentation the calibration curves and fitting parameters of the temperature dependence of the *LIR* will be discussed. For the same ion/host combination large variations in ΔE and pre-factor are reported. For example, for the most widely used luminescent thermometer $NaYF_4:Er^{3+}$ the energy difference between the two emitting states $^4S_{3/2}$ and $^2H_{11/2}$ has been found to be anywhere between 650 cm^{-1} and 800 cm^{-1}.[1,10,14] Fitted values for Er^{3+} and Nd^{3+} in different hosts will be compared with actual ΔE values determined from low temperature excitation and emission spectra. The impact of variations in ΔE on temperature accuracy and factors contributing to these variations (e.g. spectral response/corrections, temperature range used for fitting, deviations from a three level system, (in)accuracy of temperature readings heating stage) will be discussed. A calibration free thermometer will be presented: the anti-Stokes/Stokes vibronic intensity ratio for ν_6 and ν_4 vibronic lines of Mn^{4+} in $K_2SiF_6:Mn^{4+}0.1\%$ follows the theoretically expected $B\cdot\exp(-E_{vib}/k_BT)$ temperature dependence allowing direct determination of temperature from emission spectra using only the energy of the vibration involved (E_{vib}) and a pre-factor B that equals $(\nu_{AS}/\nu_S)^3$. All the challenges and pitfalls presented may make you feel '*The more I know of luminescence thermometry, the more I am convinced that I shall never find a thermometer that I can really trust. I require so much!*' but together we can expect to succeed and resolve all issues as '*to wish is to hope and to hope is to expect*'.

References

[1] C.D.S. Brites, S. Balabhadra, L.D. Carlos, Adv. Opt. Mater. 7 (2019) 1801239.
[2] M. Suta and A. Meijerink, Adv. Theor. Simul. 3 (2020**)** 2000176.
[3] M. Liu, J. Liang and F. Vetrone, Acc. Chem. Res. 57 (2024) 2653−2664.
[4] A. Bednarkiewicz, L. Marciniak, L. D. Carlos and D. Jaque, Nanoscale 12 (2020) 14405-1442.
[5] T. S. Jacobs, T. P. van Swieten, S. J. W. Vonk, I. P. Bosman et al. ACS Nano 17 (2023) 20053-20061.
[6] C. Brites, R. Marin, M. Suta, A. Neto, E. Ximendes, D. Jaque, L.D. Carlos, Adv. Mater. 35 (2023) 2302749.
[7] T. P. van Swieten, A. Meijerink and F. T. Rabouw, ACS Photonics 9 (2022) 1366-1374.
[8] A. Bednarkiewicz, L. Marciniak, L. D. Carlos and D. Jaque, Nanoscale 12 (2020) 14405-14421.
[9] A. D. Pickel, A. Teitelboim, E. M. Chan, N. J. Borys, P. J. Schuck, C. Dames, Nat. Comm. 9 (2018) 4907.
[10] M. Suta, Nanoscale 17 (2025) 7091-7099.
[11] R. G. Geitenbeek, H. W. de Wijn and A. Meijerink, Physical Review Applied 10 (2018) 064006.
[12] L. Cui, Z. Dong, D. Yu, Y. Wang and A. Meijerink, Sci. Adv. 10 (2024) 7737.
[13] T. P. van Swieten, J. M. Steenhoff, A. Vlasblom, R. de Berg, et al. Light: Sci & Appl. 11 (2022) 343.
[14] X.F. Wang, Q. Liu, Y.Y. Bu, C.S. Liu, T. Liu, X.H. Yan, RSC Adv. 5 (2015**)** 86219-8623

27. Thermodynamic and Kinetic Control in Luminescence Thermometry – How to Achieve Ultra-Wide Performance Ranges

B. Bendel,[a] D. Pham Thuy,[a] P. Pandey,[a] M. Suta[a]

[a] Inorganic Photoactive Materials, Institute of Inorganic Chemistry, Heinrich Heine University Düsseldorf, Universitätsstr. 1, 40225 Düsseldorf, Germany, markus.suta@hhu.de

Luminescence thermometry has emerged as a method for non-invasive, remote temperature sensing with spatial resolution at the micrometer scale [1]. It becomes increasingly relevant for e.g., *in situ* monitoring of temperature changes in chemical reactions [2], over *in vivo* bioimaging [3] to investigation of fundamental thermodynamic phenomena at the nanoscale [4]. A particularly simple way of luminescence thermometry employs an ensemble of non-interacting luminescent centers with two thermally coupled and radiatively emitting states, usually from the same electron configuration. The luminescence intensity ratio then follows Boltzmann's law. Trivalent lanthanoids with their narrow-line $4f^n \leftrightarrow 4f^n$ transitions have become particularly interesting in that regard.

Among the different possible emitters, Er^{3+} has become a primary working horse example in that area and seems to manage every application question in mind for that technique. Throughout this talk, we will discuss why that is [5–7] and what are ways to even improve the performance of such a luminescent thermometer on purpose. This will be demonstrated on the examples of Gd^{3+} [8] and Cr^{3+} [9], which shows a dynamic Boltzmann-type working range from below 77 K to over 800 K within one and the same compound. By that targeted approach, it is possible to design luminescent thermometers for various spectral emission ranges with constantly high dynamic working ranges. It will be finally shown what the role of selection rules of nonradiative transitions in the performance of luminescence thermometers is, how to prove and how to change them [10].

References

[1] C. D. S. Brites, R. Marin, M. Suta, A. N. Carneiro Neto, E. Ximendes, D. Jaque, L. D. Carlos, *Adv. Mater*. 2023, *35*, 2302749.

[2] T. Hartman, R. G. Geitenbeek, G. T. Whiting, B. M. Weckhuysen, *Nat. Catal.* 2019, *2*, 986-996.

[3] F. E. Maturi, C. D. S. Brites, E. C. Ximendes *et al.*, *Laser Photon. Rev.* 2021, *15*, 2100301.

[4] a) C. D. S. Brites, X. Xie, M. L. Debasu, X. Qin, R. Chen, W. Huang, J. Rocha, X. Liu, L. D. Carlos, *Nat. Nanotechnol.* 2016, *11*, 851–856 ; b) F. E. Maturi, R. S. R. Filho, C. D. S. Brites, J. Fan, R. He, B. Zhuang, X. Liu, L. D. Carlos, *J. Phys. Chem. Lett.* 2024, *15*, 2606–2615; c) R. S. R. Filho, C. D. S. Brites, L. D. Carlos, *J. Phys. Chem. Lett.* 2025, *16*, 11683-11689.

[5] M. Suta, A. Meijerink, *Adv. Theory Simul*. 2020, *3*, 2000176.

[6] M. Suta, *Nanoscale* 2025, *17*, 7091–7099.

[7] T. P. van Swieten, J. Steenhoff, A. Vlasblom, R. de Berg, S. Mattern, F. T. Rabouw, M. Suta, A. Meijerink, *Light*: *Sci. Appl.* 2022, *11*, 343.

[8] D. Yu, H. Li, D. Zhang, Q. Zhang, A. Meijerink, M. Suta, *Light: Sci. Appl*. 2021, *10*, 236.

[9] a) I. Widmann, G. Kinik, M. Suta, H. Huppertz et al., Adv. Funct. Mater. 2024, 34, 2400054; b) G. Kinik, I. Widmann, B. Bendel, H. Huppertz, A. Meijerink, M. Suta, Light: Sci. Appl. 2025, 14, 388.

[10] a) T. Förster, L. Ceccon, B. Bendel, M. Bettinelli, F. Piccinelli, M. Suta, Mater. Adv. 2026, 7, 2652–2662; b) B. Bendel, D. Pham Thuy, A. Hoffmann, D. Wenzel, S. S. Weber, S. Haibach, L.-W. Sadem, M. Suta in finalization 2026; c) P. Pandey, B. Knies, I. Hartenbach, M. Suta, in finalization 2026; d) B. Bendel, M. Nöchel, J. Salama, M. Suta, in finalization 2026.

28. KEYNOTE: Luminescence Thermometry Beyond the Diffraction Limit

Andrea D. Pickel[a]

[a]Walker Department of Mechanical Engineering, The University of Texas at Austin, 204 E. Dean Keeton Street, Austin, TX, USA, andrea.pickel@austin.utexas.edu

Optical thermometry methods offer the benefit of remotely acquiring the temperature-dependent signal from the far field, but the spatial resolution of conventional optical techniques is inherently diffraction limited. To retain the desirable capability of far-field optical operation while simultaneously achieving spatial resolution below the diffraction limit, alternative strategies must be developed. This talk will introduce two approaches to accessing spatial temperature information at sub-diffraction length scales using far-field optics. The first approach takes advantage of the spectrally narrow and wavelength-tunable emission bands of lanthanide-doped upconverting nanoparticles (UCNPs) [1]. By employing different UCNP species whose temperature-dependent emission signatures are separable in the spectral domain, we can perform temperature measurements at multiple discrete points within a sub-diffraction region. We use a single laser to excite both isolated $NaYF_4$:Yb^{3+},Er^{3+} and $NaYF_4$:Yb^{3+},Tm^{3+} UCNPs and concurrently acquire their temperature-dependent luminescence. We show that the emission spectra and temperature response originating from individual UCNPs of each composition and from tandem pairs consisting of adjacently located UCNPs of both compositions are in strong agreement. As a practical demonstration of this method, we use a tandem pair of UCNPs less than 110 nm apart to resolve a nearly 20 K temperature difference resulting from the sharp temperature gradient generated by a laser-heated Ag nanodisk.

The second approach involves the adaptation of a super-resolution imaging technique known as stimulated emission depletion (STED) for nanothermometry [2]. We show that individual highly Tm-doped $NaYF_4$:Yb^{3+},Tm^{3+} UCNPs enable both thermometry based on temperature-dependent spectral peak intensity ratios and STED imaging. We measure temperature-dependent emission spectra of individual UCNPs and identify a spectral peak intensity ratio that shows sensitive, repeatable temperature dependence with good particle-to-particle uniformity. Using a custom-built STED imaging and spectroscopy system, we also demonstrate single-UCNP spectroscopic depletion. We further show that the sub-120 nm imaging resolution of our system is maintained from room temperature up to 400 K. Using a liquid-air interfacial self-assembly method, we create uniform UCNP monolayers and multilayers that can subsequently be placed on a sample surface. By scanning the surface of a UCNP-coated substrate at different uniform temperatures, we can record temperature-dependent ratios at each pixel and generate temperature maps in both diffraction limited and STED modes. We then perform measurements on a Joule-heated microstructure and show that STED nanothermometry can resolve a temperature gradient that is undetectable with diffraction limited thermometry. Finally, we also apply STED nanothermometry to record the temperature rise resulting from photothermal heating of individual metallic nanocrystals that lack the capability to serve as their own thermometers, further highlighting the broad potential applications of STED nanothermometry.

[1] B. Harrington, Q. Xiao, J. Lin, A. Johnson, and A.D. Pickel, “Sampling Sub-Diffraction Temperature Gradients with Spectrally Orthogonal Nanoparticle Luminescence,” *ACS Photonics* **12,** 6468-6475 (2025).
[2] Z. Ye, B. Harrington, and A.D. Pickel, “Optical Super-Resolution Nanothermometry via Stimulated Emission Depletion Imaging of Upconverting Nanoparticles,” *Science Advances* **10,** eado6268 (2024).

Andrea Pickel

Andrea Pickel is an Assistant Professor in the Walker Department of Mechanical Engineering at The University of Texas at Austin. Her research focuses on harnessing luminescent probes and spectroscopic techniques to develop micro and nanoscale thermal metrology for challenging operating environments. Current applications of interest include device thermal management, catalysis, and crystallization phenomena. Andrea is the recipient of an American Chemical Society Petroleum Research Fund (ACS PRF) Doctoral New Investigator Award (2020), a Furth Fund Award (2021), and an NSF CAREER Award (2022), and she was named a Scialog Fellow for Automating Chemical Laboratories (2024). Her teaching contributions have been recognized with the G. Graydon Curtis ’58 and Jane W. Curtis Award for Non-Tenured Faculty Teaching (2023). Andrea received her Ph.D. in Mechanical Engineering from the University of California, Berkeley in 2019, where she was supported by an NSF Graduate Research Fellowship and a UC Berkeley Chancellor’s Fellowship. She received her B.S. in Mechanical Engineering with University and College Honors from Carnegie Mellon University in 2014. Prior to joining UT Austin in 2026, she was an Assistant Professor at the University of Rochester from 2019–2025.

29. Effect of Motion on Lanthanide Luminescence Intensity Ratios: Implications for Thermal Sensing

Riccardo Speghini, Aya Dannane, Mohammadreza Khodabakhsh, Eva Hemmer

Department of Chemistry and Biomolecular Sciences, University of Ottawa, 10 Marie Curie Street, Ottawa (ON) K1N 6N5, Canada, ehemmer@uottawa.ca

Lanthanide-doped nanoparticles (LnNPs) have shown strong potential as luminescent, ratiometric nanothermometers, for example for temperature sensing in cells, blood vessels, tissues, and microelectronic devices. In contrast, the effect of motion on the luminescence intensity ratio (LIR) of LnNPs has been much less studied. A few reports have shown that motion can influence the green-to-red and blue-to-green LIR of upconverting Ho^{3+} and Tm^{3+}/Tb^{3+} nanoparticles, as well as the near-infrared emission ratio of Tm^{3+}-based nanoparticles.[1–3] This raises the question of how motion and temperature may simultaneously affect the LIR, and therefore how reliable ratiometric nanothermometry is under unknown dynamic conditions.

In this work, we address this question using Er^{3+}/Yb^{3+} co-doped β-$NaGdF_4$ upconverting nanoparticles (UCNPs) in dispersion, where motion is controlled by varying the stirring speed. We find that stirring causes a stronger decrease in the red Er^{3+} emission intensity compared to the green emission. This effect is attributed to changes in the population dynamics of the emitting states under stirring conditions. While this motion-induced change in the LIR could be used for motion sensing, the green-to-red LIR is also known to be temperature dependent. Therefore, careful calibration is required when using this LIR for temperature sensing under unknown motion conditions. By contrast, the green-to-green ratio of Er^{3+}, which is widely used for nanothermometry, appears to be less affected by stirring. However, we find that excluding the frequently observed Er^{3+} green emission band at 557 nm from the LIR calculation is crucial to obtain reliable temperature readings.

This presentation discusses the mechanism behind motion-dependent changes in the LIR, its potential overlap with temperature effects, and possible strategies to improve the robustness of luminescent nanothermometry under dynamic conditions.

Reference:

[1]] L. Zhang, S. Hu, X. Fu, N. Zhang, F. Huang, T. Pang, H. Huang, A. Xie, D. Chen, J. Mater. Chem. C 13 (2025), 10602.

[2] G.Tessitore, S. L. Maurizio, T. Sabri, C.D. Skinner, J. A. Capobianco, Adv. Mater. 32 (2020), 2002266.

[3] Y. E. Serge Correales, M. Khodabakhsh, N. de Melo Costa Serge, R. Gonçalves, E. Hemmer, manuscript under review.

30. Real-Time Intracellular Temperature Imaging and Monitoring. Application to Local Magnetic Hyperthermia Therapy

Rafael Piñol,[a] Carlos D.S. Brites,[b] Yuanyu Gu,[a] Raquel Moreno-Loshuertos,[c] Justyna Zeler,[b] Abelardo Martínez,[d] G. Maurin-Pasturel,[a] Patricio Fernández- Silva,[b] L. Saraiva,[b] A. N. Carneiro Neto,[2] Rafael Cases,[1] Luís D. Carlos,[b*] Angel Millán,[a*]

[1] Institute of Nanoscience and Materials of Aragon, Pedro Cerbuna 12 50009 Zaragoza, Spain, amillan@unizar.es

[b] Phantom-g, CICECO-Aveiro Institute of Materials, Department of Physics, University of Aveiro Campus de Santiago, 3810-193 Aveiro, Portugal, lcarlos@ua.pt

[c] Departamento de Bioquímica, Biología Molecular y Celular, Universidad de Zaragoza, Pedro Cerbuna 12 50009 Zaragoza, Spain, raquelml@unizar.es

[d] Departamento de Electrónica de Potencia. I3A. Universidad de Zaragoza 50018 Zaragoza, Spain

It is well known that lanthanides show unique luminescence emission features, such as narrow emission bands, long lifetimes, large stokes shifts and photostability [1]. As isolated ions they have a low absorption cross-section, but coordinated to organic ligands, which serve as antennas and chemical shields, they can reach high quantum yields [2]. Moreover, lanthanide coordination compounds show a temperature dependence in a wide temperature range, including physiological temperatures, which varies between them. All this, combined with their molecular nature, makes them excellent candidates for ratiometric nanothermometry. Here, we show the high versatility of this thermometric system that can be applied to bulky, layered, surface self-assembled monolayers, and nanoparticles. Finally, we will pay special attention to their performance as intracellular thermometers [3,4].

References

[1] C.D.S. Brites, A. Millán, L.D. Carlos, in: J.C. Bunzli, V. Pecharsk (Eds.), Handbook on the Physics and Chemistry of Rare Earths, vol 49, Elsevier, Amsterdam, 2016, pp 339-427.

[2] G. Maurin-Pasturel, R. Piñol, R. Cases, C. D.S. Brites, L. Saraiva, A. N. Carneiro Neto, I. Ara, L. Falvello, M. Sanjuán, L. D. Carlos, A. Millán, Opt. Mater. 176 (2026) 118113.

[3] R. Piñol, J. Zeler, C. D. S. Brites, *et al.* Nano Lett. 2020, 20, 6466–6472.

[4] Y. Gu, R. Piñol, R. Moreno-Loshuertos, C. D. S. Brites, *et al.* ACS Nano, 17 (2023) 15219–15221.

31. From Brownian Motion to Protein Unfolding: Fluorescent Sensing of EGFP at the Nanoscale

Yongwei Guo[a], Ramon S. Raposo Filho[a], Carlos D. S. Brites[a], Luís D. Carlos[a]

[a] Phantom-g, CICECO–Aveiro Institute of Materials, Physics Department, University of Aveiro, 3810-193, Aveiro, Portugal

Green Fluorescent Protein has emerged as a highly versatile optical sensor since its development and widespread adoption in the 1990s, and it has been extensively utilized in fluorescence labeling, live-cell imaging, and biosensing applications.[1] Here, we propose an enhanced green fluorescent protein (EGFP), without engineering, to enable decoupled pH/temperature readout via multidimensional spectral analysis. We systematically map the spectral responses of EGFP across physiological ranges, identifying the energy of the main emission peak (temperature) and relative intensity (pH) as orthogonal parameters resilient to self-absorption and concentration effects.

Building upon its temperature-dependent fluorescence properties, we further exploit EGFP to investigate protein Brownian motion under varying temperatures. Our results show that the protein Brownian velocity increased linearly with temperature, providing new evidence into thermally driven molecular motion.[2] By analyzing the temperature-dependent fluorescence quenching of EGFP at varying concentrations in H_2O and D_2O revealed that EGFP's thermal unfolding transition occurs at higher temperatures in D_2O (64°C) compared to H_2O (56°C). Additionally, analysis of temperature-dependent Brownian velocity uncovered a crossover temperature between low-density (LD) and high-density (HD) motif fluctuation transitions, which shift from 55°C in H_2O to 65°C in D_2O, corroborating the stabilizing effect of isotope substitution on protein conformation. These results suggest that the persistence of LD motifs governs protein thermal stability, highlighting the critical role of the hydration environment in protein conformational dynamics.[3]

Overall, our work not only establishes EGFP as a practical and multifunctional optical sensor for temperature and pH but also provides new insights into protein–water interactions.

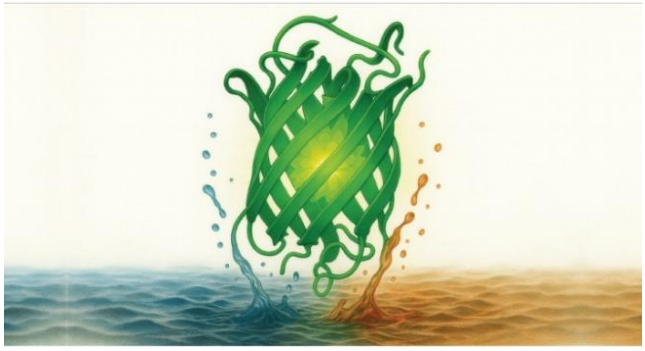

Figure. The density fluctuation of EGFP hydration water.

[1] Richard N. Day, Michael W. Davidson, Chem. Soc. Rev. 38 (2009) 2887–2921.
[2] Yongwei Guo, Fernando E. Maturi,* Carlos D. S. Brites, and Luís D. Carlos*, Adv. Phy. Res. 3 (2024) 2400085-2400092.
[3] Yongwei Guo, Fernando E. Maturi, Ramon S. Raposo Filho, Carlos D. S. Brites*, Luís D. Carlos*, J. Phys. Chem. B, 129 (2025) 12042−12050.

32. Towards a Metrology Framework for Quantum-Based Nanoscale Temperature Sensing

Aldo Mendieta[a], Junqing Jiang[a], Gavin Sutton[a]
[a]National Physical Laboratory, Hampton Rd, Teddington, UK, aldo.mendieta@npl.co.uk

Temperature plays an important role in healthcare and biology, influencing physical, chemical, and biological processes. Conventional thermometry techniques, such a contact probes or thermal imagers, struggle to measure local transient temperatures at the cellular level, requiring more precise, non-invasive and faster responding thermometers.

Nitrogen–vacancy (NV) centers in diamonds are point defects whose electronic spin properties are extremely sensitive to temperature changes[1], making them powerful probes for nanoscale thermometry. Because NV spins can be initialized and read out with light, NV diamonds enable non-invasive, high-spatial-resolution temperature sensing while remaining stable in complex environments such as biological cells. Yet, despite strong laboratory progress, the field still lacks the metrological foundations needed for real-world deployment

However, issues like biased sensing [2] (i.e. viscosity, magnetic field influence or PH levels influence in the luminescence priorities), lack of standardised calibration mechanisms and accurate uncertainty determination remain. This work aims to address these challenges, exploring all-optical approaches to improve temperature sensitivity and seeking to build a metrology framework focused on improving the reliability and traceability of temperature measurements at the nanoscale using NV diamonds with a target temperature sensing resolution of 0.1 °C and 1 °C uncertainty.

The objectives of this work are a) to investigate all optical approaches, particularly focusing on a ratiometric approach, for improved temperature sensitivity of NV nanodiamonds and b) explore the challenges associated with the use of thermal microscopy stages for calibration of these nanothermometers. This work seeks to establish a set of tools that lay the groundwork for advanced metrology in nanoscale NV diamonds-based thermometry, with a particular focus on applications in biology.

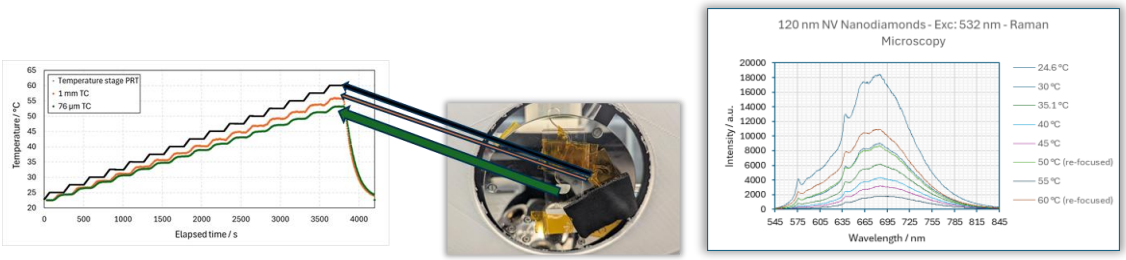

Figure 1. Left. Temperature offset at different positions near the NV diamonds sample in a microscopy stage. Right. Luminescence spectra at different temperature point for 120 nm NV diamonds

References:

1. Fujiwara, M. and Y. Shikano, *Diamond quantum thermometry: from foundations to applications.* Nanotechnology, 2021. **32**(48).
2. Kucsko, G., et al., *Nanometre-scale thermometry in a living cell.* Nature, 2013. **500**(7460): p. 54-58.

33. Fibre Optic Thermometry using Fibre Bragg Grating (FBG) and Luminescent Techniques – Making Better Informed Choices

Xin Lu[1], Marcus Schukar[1], Tong Sun[2] Guillaume Failleau[3], Stephan Krenek[4] and Kenneth T. V. Grattan[2], k.t.v.grattan@city.ac.uk

[1] Bundesanstalt für Materialforschung und -prüfung (BAM), Unter den Eichen 87, 12205 Berlin, Germany
[2] City St. George's, University of London, Northampton Square, London, EC1V 0HB, UK
[3] Laboratoire National de métrologie et d'Essais (LNE), 29 avenue Roger Hennequin, 78197 Trappes, France
[4] Physikalisch-Technische Bundesanstalt (PTB) Abbestraβe 2–12, 10587 Berlin, Germany

Fibre optic thermometry has revolutionized thermal sensing in environments where traditional electronic sensors – such as thermocouples or Resistance Temperature Detectors (RTDs) – fail due to electromagnetic interference (EMI), high voltages or corrosive atmospheres, for example. They were amongst the first fibre optic sensors to be developed, using a range of different (and often simplistic techniques), usually operating over limited temperature ranges.

Providing industry with a better understanding of the optimum way of making choices in thermometry is vitally important today. Over the years, it has become clear that amongst the various optical methods for point and quasi-distributed sensing, **Fibre Bragg Gratings (FBG)** and **Luminescent (Fluorescence) decay** techniques are the two most prominent, each offering distinct physical mechanisms and operational advantages. However, for the instrumentation engineer – and the scientist in industry – a key question is, given this choice, which is the best to use for any particular application? Examining the key characteristics of each of these and comparing and contrasting underpinning mechanisms, as well as areas where they have been and are being used, provides a basis for a more informed decisions. This study has arisen from work done across Europe as measurement and control of temperature plays a key role in achieving the European Green Deal for optimizing low-carbon energy systems.

Fibre Bragg Grating-based (FBG) Thermometry is based on the thermal expansion of the silica and the thermo-optic effect (the change in refractive index with temperature). As temperature increases, the physical grating period expands and the refractive index shifts, causing a linear shift in the reflected Bragg wavelength. Key advantages include:
Multiplexing capability: An important strength of FBGs is the ability to write multiple gratings with different Bragg wavelengths on a single fibre network – allowing an easy approach to quasi-distributed sensing, where many temperature points can be monitored.
Digital Accuracy: Because the information is encoded in the wavelength (an absolute parameter), the system is immune to fibre bending effects e.g. signal intensity fluctuations.
Speed: FBGs offer high-speed response times, suitable for dynamic thermal events.

Luminescent (Fluorescence)-based Thermometry utilizes the temperature-dependent optical properties of specific materials (often rare-earth doped phosphors or crystals) attached

to the tip of a fibre. There are two primary methods by which the sensors are calibrated – relying on measurements that are intensity-based and lifetime-based. The **fluorescence lifetime** technique is generally seen as the industry standard (the **fluorescence intensity ratio** technique is also used), where a pulse of light excites the phosphor, and the sensor measures the rate at which the resulting luminescence decays. Key advantages of the use of the technique include:

Complete Dielectric Isolation: Luminescent probes are often entirely non-metallic and extremely small, making them the 'gold standard' for medical applications (like MRI or RF ablation) and microwave processing.

Point Sensing Excellence: While not as easily multiplexed in large numbers, such as FBGs, they are exceptionally stable for single-point measurements in high-intensity electromagnetic fields.

Point Accuracy: They are less sensitive to mechanical strain than FBGs, which can sometimes provide false temperature readings if the fibre is stretched [3].

As temperature rises, non-radiative relaxation processes become more dominant, causing the luminescence to decay more rapidly, which can affect the intensity of the light received.

Making an informed choice of the right sensor for the application in mind requires a focus on a number of key issues, with particular regard to the following:

Temperature range to be measured: both FBG-based and luminescent sensors experience different physical effects which can affect the temperature range (both upper and lower, into the cryogenic as required) and careful consideration of these is necessary when selecting the appropriate sensor system for a particular application.

Number of sensors to be deployed – and whether in point sensing or quasi-distributed mode: different luminescent media can be multiplexed along a single sensor and excited from the same source but the limitation to this becomes apparent when more than ten such sensors are used – an issue not usually experienced with FBG-based sensors.

Time response needed from the sensor system: for the FBG-based system is this usually determined by the response time of the interrogation system (and thus the sweep rate of the interrogator) – usually <5kHz. For the luminescent thermometer, in principle nanosecond excitation and emission could allow multi-MHz response with high power laser excitation.

Sensitivity to Strain: FBGs are inherently sensitive to both temperature and mechanical strain, so to measure pure temperature, the FBG must be 'strain-isolated' in a specialized housing. Luminescent sensors, conversely, are largely unaffected by physical fibre stress, making them easier to package for simple temperature probes, although strain effects in such sensors have been reported.

Instrumentation cost: Luminescent systems generally require less expensive interrogation hardware for single-point monitoring. However, as the number of sensing points increases, the cost-per-point of an FBG system drops significantly due to its multiplexing capabilities.

Effect of temperature change on the sensor signal-to-noise ratio: For luminescent sensors, as the temperature rises, non-radiative relaxation processes become more dominant, causing the luminescence to decay more rapidly. This can affect the intensity of the light received from the sensor and thus the signal-to-noise ratio in the measurement.

Combined FBG and luminescent thermometry and fibre laser thermometry

Experimenters have constructed fibre-optic sensors to measure temperature and strain by combining the properties of Fibre Bragg Gratings with the fluorescent lifetimes of various doped fibres and these show some advantages which can be considered for any particular application. Further, fibre lasers can combine luminescent material (which lase) with both FBG and chirped FBG-based mirrors and these have been demonstrated as sensors, taking advantage of calibrating the narrow band wavelength of the laser itself against the measurand.

Acknowledgement

The project 22IEM07 INFOTherm has received funding from the European Partnership on Metrology, co-financed from the European Union's Horizon Europe Research and Innovation Programme and by the Participating States.

34. PHOSTECH: Development of a Practical Hand-Held Phosphor Thermometer

Gavin Sutton, Aldo Mendieta, Phil Cooper, Carter Wong, Matthew Stewart

National Physical Laboratory, Teddington, UK, TW11 0LW, gavin.sutton@npl.co.uk

Many manufacturing processes—such as welding and forging—require accurate, non-contact measurement of high-temperature surfaces to ensure product quality. Infrared thermometers are commonly used but can suffer from inaccuracies caused by poor knowledge of surface emissivity and reflected background radiation. To compensate, operators often run processes at higher-than-optimal temperatures, resulting in increased energy consumption and negative impacts on quality and sustainability.

PHOSTECH, a cutting-edge technology developed by NPL, overcomes these limitations by delivering accurate non-contact surface temperature measurements based on the intensity ratio (IR) method using the ubiquitous phosphor Mg_4FGeO_6:Mn (MFG). PHOSTECH was funded through a Government Office for Technology Transfer (GOTT) grant [1]. These awards aim to identify, develop, and transfer valuable public-sector innovations and intellectual property into real-world use, delivering economic and societal benefit. Following on from an initial smaller GOTT grant to assess the market need and identify key stakeholders, NPL were awarded a larger grant to develop a practical phosphor thermometer and test it in industrial environments. To our knowledge, this is the first example of a practical (hand-held) instrument that can operate independently of computer control.

a) b)

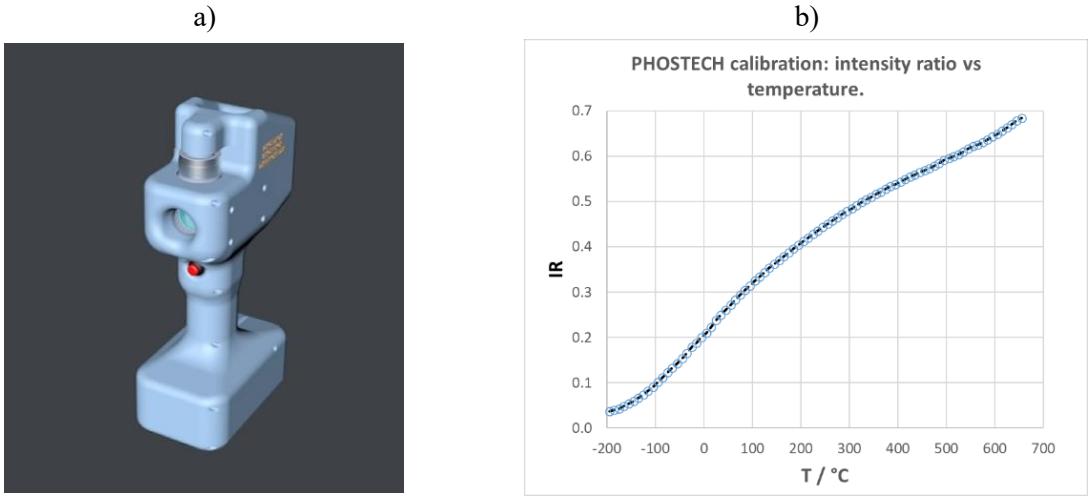

Figure 1 The PHOSTECH practical phosphor thermometer: a) design sketch, b) IR vs T calibration.

In this presentation, we describe the instrument design, phosphor coating optimisation, and instrument performance, present examples of industrial testing, and discuss the next steps towards commercialisation.

[1] https://www.gov.uk/government/organisations/government-office-for-technology-transfer.

35. Fiber-Coupled Phosphor Thermometry for applications in gas turbine combustion

Patrick Nau

German Aerospace Center (DLR), Institute of Combustion Technology, Pfaffenwaldring 38-40, 70569 Stuttgart, Germany, patrick.nau@dlr.de

The transition toward sustainable energy systems has intensified interest in hydrogen-fueled gas turbines. Due to significantly different combustion characteristics between hydrogen and conventional fuels such as methane, modern gas turbine combustors must operate under fuel-flexible conditions. A key parameter for optimizing performance, efficiency, and component lifetime is the accurate knowledge of wall temperature distributions. However, temperature measurements in technically relevant combustor environments are challenging due to limited optical access.

The limited optical access in technically relevant combustors often requires optical probes with an endoscope or flexible probes using fiber optics. Phosphor thermometry has proven to be a reliable non-intrusive technique for surface temperature measurements. While fiber-coupled configurations have been successfully applied for point measurements in gas turbines, the extension to two-dimensional (2D) imaging under realistic conditions has remained largely unexplored. This work presents the demonstration of a fully fiber-coupled phosphor thermometry imaging system applied to a model gas turbine combustor, enabling spatially resolved wall temperature measurements under methane and hydrogen combustion.

Different approaches to perform 2D measurements will be discussed. In this work an approach based on the temperature-dependent phosphorescence decay of thermographic phosphor was used. In contrast to intensity-based techniques, which are susceptible to systematic errors such as misalignment and wavelength-dependent attenuation, a time-resolved method is employed. This approach evaluates the phosphorescence decay time (lifetime, τ), providing high sensitivity and robustness, as it is independent of absolute signal intensity. In addition, it provides a large dynamic range, which was necessary for the intended application.

Experiments were conducted in an atmospheric jet-stabilized combustor operated at a constant global equivalence ratio ($\Phi = 0.74$) and thermal power of 10 kW. Fuel compositions were pure methane, pure hydrogen and a methane-hydrogen mixture. Both premixed and non-premixed configurations were investigated. The combustor featured quartz walls coated with the phosphor $GdAlO_3$:Cr, which is suitable for temperature measurements in the range of approximately 400–1100 °C.

The optical setup utilized a pulsed Nd:YAG laser (532 nm) coupled into a fiber bundle for excitation. The emitted phosphorescence signal was collected via an imaging fiber bundle and recorded using a high-speed camera operating at frame rates up to 500 kHz. This configuration enabled fully fiber-based excitation and detection, overcoming limitations related to optical

accessibility in large-scale combustion systems. The achieved spatial resolution was approximately 1.7 mm per pixel over an area of about 55 × 55 mm².

Data processing involved averaging multiple laser shots to improve signal-to-noise ratio, followed by pixel-wise evaluation of phosphorescence decay curves. Background correction was performed to account for camera-induced signal offsets. Decay times were extracted using non-linear least-squares fitting, with adaptive fitting windows depending on temperature. A pixel-wise calibration approach was implemented to compensate for non-linear detector behavior, resulting in accurate temperature reconstruction across the full field of view. The achieved precision ranged from approximately 0.2% to 2% (2–12 K). Four temperature maps were overlapped to cover the complete length of the combustor window. The measurements demonstrated good consistency across overlapping regions, confirming the reliability of the imaging approach.

The resulting 2D temperature maps revealed clear dependencies of wall temperature distributions on fuel composition and mixing configuration. Increasing hydrogen content led to higher wall temperatures and shorter flame lift-off heights, which were directly reflected in the measured temperature fields, particularly near the jet region. In contrast, regions dominated by recirculated exhaust gases showed weaker sensitivity to fuel variation.

Limitations were observed at the lower and upper bounds of the measurable temperature range (<400 °C and >1100 °C), as well as for very high temperatures where the decay rates exceeded the temporal resolution of the camera. Extending the measurable range would require alternative phosphors or detection systems with higher frame rates.

In conclusion, this study demonstrates that fully fiber-coupled phosphor thermometry imaging is a viable and powerful tool for spatially resolved temperature measurements in gas turbine combustors under realistic operating conditions. The technique provides high accuracy, robustness against systematic errors, and compatibility with restricted optical access. The obtained temperature maps offer valuable experimental data for validating and improving numerical combustion models, and supporting the development of gas turbine technologies.

36. From Bulk to Micro-Scale: Instrumentation Workflows for Phosphor Thermometry

Anna Gakamsky[*], Georgios E.Arnaoutakis[#], Stuart Thomson[*]

[*] Edinburgh Instrument, 2 Bain Square, Livingston, UK

[#] School of Engineering, Hellenic Mediterranean University, Heraklion, Crete, Greece

Phosphor thermometry relies on reproducible temperature-dependent changes in luminescence spectra and decay kinetics, which place strong demands on measurement methodology and instrumentation. We present an instrumentation-focused workflow for phosphor thermometry development based on photo- and thermo-luminescence spectroscopy, extending established bulk measurements to micro-scale characterisation.

Temperature-dependent photoluminescence measurements are used to quantify spectral redistribution, thermal quenching, and lifetime evolution as thermometric readout parameters, while complementary thermoluminescence measurements provide insight into trap populations and thermal stability limits relevant for calibration. Time-resolved methods spanning nanosecond to millisecond regimes enable lifetime-based thermometry that is robust against optical losses and excitation fluctuations.

Micro-luminescence spectroscopy combined with a temperature stage enables spatially localised thermometric characterisation of individual phosphor particles, making it possible to evaluate scale-dependent effects beyond ensemble-averaged bulk measurements.

Finally, we demonstrate how the described temperature-dependent photoluminescence and lifetime measurements can be automated and customised using new instrumentation-level software tools (FluoAuto and FluoAPI), enabling reproducible, high-throughput thermometric characterisation.

This talk will illustrate how integrated instrumentation and controlled data acquisition strategies underpin reliable phosphor thermometry development across length scales.

Day 3 – Friday 26/06/2026
Sessions 8 and 9

37. KEYNOTE: Exploiting Off-line Thermographic Phosphors for Thermal Mapping of Industrial Turbomachinery

Silvia Araguas Rodriguez

Sensor Coating Systems, londoneast-uk, The Cube, Yew Tree Ave, Dagenham RM10 7FN, s.araguas@sensorcoatings.com

Accurate temperature measurement in industrial turbomachinery remains a significant engineering challenge due to extreme operating environments, limited optical access, rotating components, and the difficulty of instrumenting highly stressed hardware. Nevertheless, reliable thermal data is essential for validating thermal models, assessing cooling performance, improving efficiency, and supporting component life prediction in modern high-temperature systems. Conventional sensing approaches are often unable to provide the spatial resolution or survivability required in these environments, driving continued interest in non-contact optical measurement techniques such as thermographic phosphors.

Over recent decades, considerable effort has been devoted to the development of real-time, or on-line, phosphor thermometry methods, with notable success in laboratory and research applications where optical access and instrumentation constraints can be carefully controlled. However, some industrial applications continue to present practical limitations that restrict the deployment of on-line diagnostics. These challenging scenarios have highlighted the growing importance of off-line thermographic phosphors Thermal History Coatings & Paints which enable post-exposure thermal mapping through analysis of cumulative thermal exposure post-operation.

This keynote presents a retrospective perspective on the evolution of off-line thermographic phosphor techniques, focusing on their strengths as practical solutions for industrial thermal mapping in harsh and inaccessible environments. By capturing high resolution thermal maps, these coatings provide a robust means of assessing temperature distributions in hard-to-reach regions, rotating components, and other areas where conventional instrumentation or real-time optical interrogation is impractical.

The presentation will review key developments in coating materials, phosphor systems, calibration methodologies, and interrogation techniques that have enabled wider industrial adoption. A range of applications across aerospace propulsion, industrial gas turbines and power generation will be discussed, highlighting how differing operational challenges have shaped the implementation of thermal history technologies in each case.

Finally, the talk will consider the future direction of off-line thermographic phosphors, including advances in measurement methodologies, material systems and accuracy, as well as implementation into other applications such as maintenance, overhaul and repair. As industrial demands continue to grow, off-line thermographic phosphors are increasingly moving from specialist research tools towards practical, deployable technologies for real-world thermal assessment.

Silvia Araguas-Rodriguez

Dr Silvia Araguás Rodríguez is Technical Director at Sensor Coating Systems, where she focuses on the development and industrial implementation of novel thermal history technologies, including thermal history coatings for high-temperature measurement in harsh environments. She has contributed to the advancement and deployment of these technologies across aerospace propulsion and industrial gas turbines, bridging the gap between materials development and practical industrial diagnostics.

Her broader research interests include luminescent materials, functional coatings, and the synthesis of nanomaterials for sensing applications. She holds a PhD in Materials Engineering from Imperial College London and an MSc in Nanotechnology from University College London.

38. Photoluminescent Sensor for Thermal History Diagnostic in the 500-1000°C Range

Lisa Guibbert[a,b, c], Étienne Copin[b], Sandrine Duluard[a], Philippe Brevet[c], Thierry Sentena[c,b], Florence Ansart[a]

[a] Univ. Toulouse, Toulouse INP, CNRS, CIRIMAT, Toulouse, France, sandrine.duluard@utoulouse.fr
[b] Univ Toulouse,IMT Mines Albi, INSA Toulouse, ISAE-SUPAERO, CNRS, ICA, Albi, France, etienne.copin@mines-albi.fr
[c] Safran Helicopter Engines, Avenue Joseph Szydlowski, Bordes, France, philippe.brevet@safrangroup.com

The measurement of temperature in helicopter engines is a major challenge for component dimensioning and certification. Conventional measurement methods currently used on turbomachine have significant limitations: thermochromic paints provide limited thermal resolution, whereas measurements with thermocouples or infrared thermometry are not suitable to obtain temperature maps on moving parts or hard-to-reach areas, and have low spatial resolution [1,2]. In response to these constraints, Safran Helicopter Engines is turning to an approach based on the use of photoluminescent coatings sensitive to thermal history.

These coatings contain phosphors whose optical emissions, triggered by laser or LED excitation, depend on the maximum equivalent temperature reached during a past thermal event, as a result of thermo-activated physico-chemical and/or microstructural transformations. Spectral or temporal analysis of room-temperature fluorescence emissions from coated parts after an engine test run can be used to derive maps correlating the detected signal with the maximum temperatures experienced during the test [3].

In this work, Eu-doped Y_2O_3 phosphors were developed to record thermal history in the 500–1000 °C range. These phosphors are synthesized via low-temperature soft-chemistry routes. Laboratory synthesis is compared to large-scale industrial production. The influence of short-duration (< 20 min) thermal treatment at different temperatures is studied in terms of structural, morphological and photoluminescence properties to investigate thermal history sensitivity.

TGA/ATD analyses showed that a transition occurs around 550 °C, where precursor materials transform into the final lattice expected for the phosphor. Microstructural characterizations by XRD revealed a continuous increase in crystallinity and crystallite size with the annealing temperature. Together, these structural modifications led to a significant evolution of the photoluminescence response in this temperature range.

As illustrated in Figure 1 (left), all samples show photoluminescence emissions in the red region (≈ 612 nm), which increases with temperature from 500 °C to 1000 °C. To calibrate the response of the material to thermal history, a Luminescence Intensity Ratio (LIR) approach was selected, using specific spectral bands of the activator that show distinct sensitivities to the

changes induced by thermal exposure. As shown in Figure 1 (right), the LIR increases continuously with treatment temperature from 500 °C to 1000 °C. Results follow the same trend between laboratory and industrial powders, confirming the success of the scale-up and the reliability of the LIR method chosen.

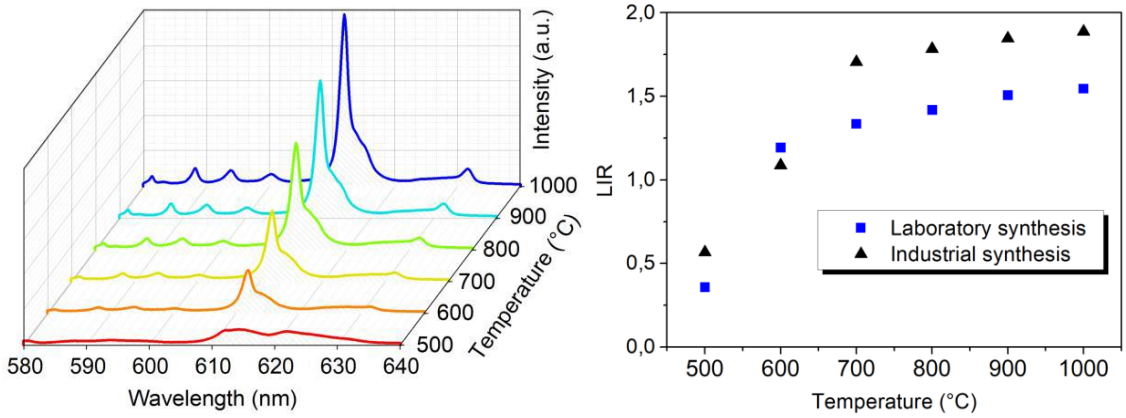

Figure 1: Room temperature emission spectra (left) and LIR (right) of $Y_2O_3:Eu^{3+}$ powders annealed at different temperatures from 500°C to 1000°C (duration <20 min).

To assess the practical application of the phosphor, various coating formulations were developed by dispersing the industrial powder into either commercial or laboratory-synthesized binders. These formulations were deposited onto typical metallic substrates used in helicopter engines and then calcined in a furnace under the same conditions as the powders (< 20 min in the 500–1000 °C range). To simulate real engine thermal cycles with improved control, additional samples were exposed to high temperatures using an infrared (IR) heating bench developed in the laboratory. The ratiometric response of the coatings is currently under investigation.

[1] A.H. Khalid, K. Kontis, Sensors 8 (2008) 5673-5744.
[2] A. Rabhiou, J. Feist, A. Kempf, S. Sinner, A. Heyes, Sensors and Actuators A. 169 (2011) 18-26.
[3] E.B. Copin, X. Massol, S.Amiel, T. Sentenac, Y. Le Maoult, P. Lours, Smart Mater. Struct. 26 (2017).

39. Surface Thermometry of Extruded Plastics During Immersion Cooling

Moritz Stelter[a], Sandra Gottwals[a], Stefan Bergmann[b], Gunar Boye[a], Frank Beyrau[a]

[a]Otto von Guericke University Magdeburg, Universitätsplatz 2, Magdeburg, Germany, moritz.stelter@ovgu.de
[b]Ematik GmbH, Otto-Lilienthal-Straße 7, 39120 Magdeburg

Plastics are a class of very versatile materials that are used in various applications. One way to produce plastic parts is extrusion. In commonly used screw extruders, plastic pellets serve as raw material. They are molten within the extruder by combined electric heating and shear forces-induced friction caused by the rotation of an extruder screw. The liquified plastic is then pressed through a die at the extruder outlet to create parts with defined profiles. To maintain correct dimensions, the part has to be cooled below its melting point after leaving the die.

To better understand this cooling process, surface temperature measurements of the moving plastic part are needed. As water sprays and baths are widely used for cooling in extrusion processes, remote thermometry techniques such as infrared thermography cannot be used.

In this work, we show that phosphor thermometry can be used to measure the surface temperature of a moving plastic part during immersion cooling. A sketch of the extrusion line is shown in Figure 1. To enable surface thermometry, Mg3.5FGeO5:Mn particles are mixed with the raw plastic pellets before extrusion. This way, the phosphor is integrated directly into the finished part during extrusion. Then, a blue LED is used to excite luminescence emissions from the embedded phosphor particles which is detected using a photodiode read by an oscilloscope for lifetime-based phosphor thermometry.

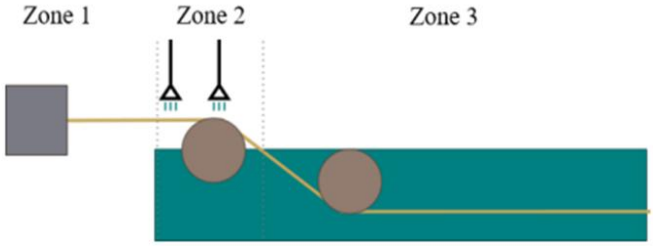

Figure 1: Sketch of the industrial extrusion line with three cooling zones: (Zone 1) Cooling through convection in air once the plastic leaves the extruder, (Zone 2) water spray cooling, and (Zone 3) immersion cooling in a water bath.

Preceding thermometry in the production line of an industrial partner, a temperature calibration was done in lab using two setups. First, to obtain calibration data in the presence of water, an extruded plastic-phosphor tube sample was suspended in a precision thermostat filled with water (cf. sketch in Figure 2a). The water was heated to multiple set temperatures between 22°C and 90°C and calibration data was recorded once thermal equilibrium between water and tube sample was established. While this arrangement is similar to the industrial process, the temperatures in the real process reach up to 200°C at the outlet of the extruder. Hence, our calibration had to be augmented with data for higher temperatures using a second setup. For this, a metal wire was placed within the tube sample to provide electrical heating while the tube

was not submerged within the thermostat but surrounded by air (cf. sketch in Figure 2b). This way, the tube surface temperature could be measured using infrared thermography as reference and the calibration range was extended up to 200°C. As shown in Figure 2c, a continuous calibration curve could be fitted using the unified data from both calibration setups.

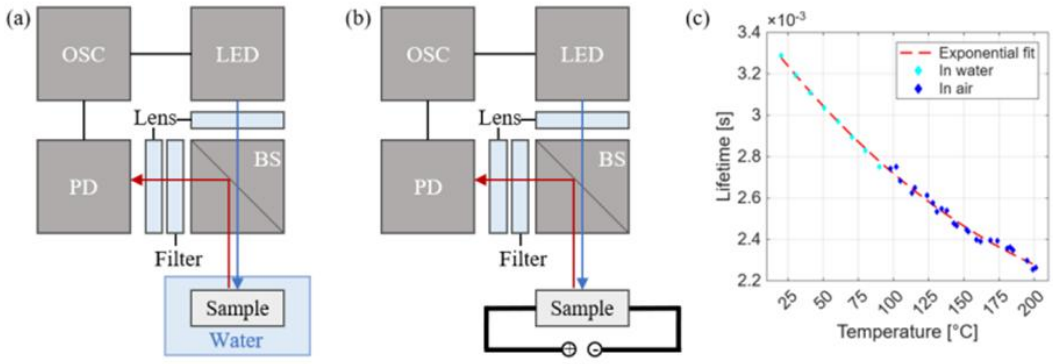

Figure 2: Sketched temperature calibration setups containing an oscilloscope (OCS), a light-emitting diode (LED), a dichroic beamsplitter (BS), and a photodiode (PD). Calibration of plastic-phosphor tube samples were performed submerged in water (a) and in air (b). Calibration curve derived as exponential fit from combined data of both calibration setups(c).

Once the calibration has been successfully completed, initial plastic surface temperature measurements in the industrial production line were conducted. Temperature results are shown in Figure 3 against the normalized distance from the extruder outlet. In the first cooling zone (convection in air), valid surface temperatures could be measured using infrared thermography and no phosphor thermometry was applied. In the second cooling zone (spray cooling), the limitations of both infrared thermography and the current state of the phosphor thermometry implementation are evidenced. For infrared thermography, the measured temperature drops intermittently towards the cooling water temperature, indicating an influence from a water film on the plastic part or water spray within the detection path. Temperatures obtained using phosphor thermometry in this zone show strong scattering and overshoot the temperatures indicated by infrared thermography. Transitioning from the spray cooling to immersion cooling, the temperatures from phosphor thermometry show much better precision and drop continuously towards the cooling water temperature of approximately 25 °C.

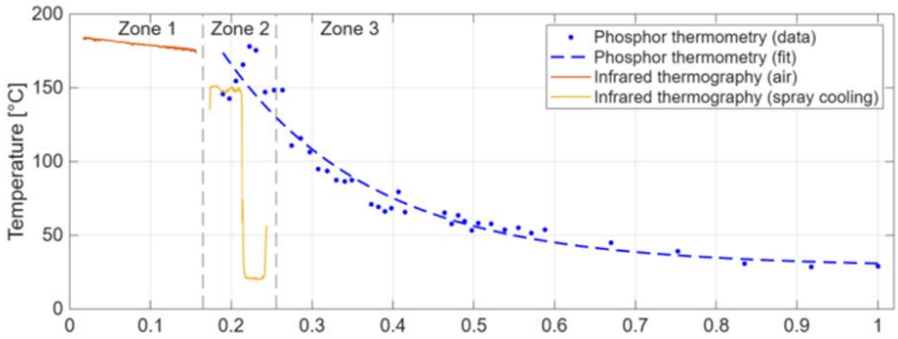

Figure 3: Plastic surface temperatures measured at increasing distances from the extruder outlet using infrared thermography and phosphor thermometry.

The surface temperatures recorded during immersion cooling in a real plastic extrusion process will be used to validate a numerical model which will allow a generalization of these results to other plastic part geometries and cooling conditions. This will allow us to improve the quality of the extruded plastic part by reducing internal stresses and improving dimensional accuracy. At the same time, it will be possible to reduce the size of the cooling bath and the amount of energy needed to maintain a constant temperature for the cooling water, leading to economic and ecologic improvements. As measurements in the spray cooling zone remain challenging, this region will be the focus for further studies.

40. Toward Temperature and Pressure Measurement of Shock Compressed Materials using Phosphor Photoluminescence

Eric R. Westphal[a], Aaron M. Hansen[b], Noelle M. Collins[c], Caroline Winters[d], and Linda E. Hansen[e]

[a]*Ceramics and Materials Physics, Sandia National Laboratories, 1515 Eubank Blvd SE, Albuquerque, NM 87123, USA, erwestp@sandia.gov*
[b]*Solid Dynamics Experiments, Sandia National Laboratories, 1515 Eubank Blvd SE, Albuquerque, NM 87123, USA, amhanse@sandia.gov*
[c]*Non-Destructive Environments and Diagnostics, Sandia National Laboratories, 1515 Eubank Blvd SE, Albuquerque, NM 87123, USA, nmcolli@sandia.gov*
[d]*Fire Science and Technology, Sandia National Laboratories, 1515 Eubank Blvd SE, Albuquerque, NM 87123, USA, cwinte@sandia.gov*
[e]*Phenomenology and Signatures, Sandia National Laboratories, 1515 Eubank Blvd SE, Albuquerque, NM 87123, USA, lehanse@sandia.gov*

Knowledge of both pressure and temperature within shock compressed materials are important state variables but their measurement techniques can be difficult to decouple. This causes conventional measurement techniques for each to be challenging. Pyrometry allows for nonintrusive temperature measurement but can suffer from low sensitivity due to fluctuations in material emissivity and interference from hot gases within the shocked material. This technique also suffers from poor signal-to-noise below 2500 K, making lower temperature measurements difficult. Pressure sensitive paints depend upon oxygen concentration at their interface leading to losses in sensitivity above ~0.42 GPa. This paper explores temperature and pressure sensitive photoluminescence of phosphor materials as an alternative measurement to address these challenges.

Pressure variation of these phosphors was achieved within a diamond anvil (DAC) capable of compressing these materials to ~20 GPa. Y_2O_3:Eu, Y_2O_3:Dy, and YVO_4:Eu powders (Phosphor Technology Ltd) were each loaded individually into the DAC along with a 4:1 mixture of methanol:ethanol that acted as the compressible pressure transmitting medium. Ruby powder was loaded into the DAC alongside each phosphor and the R1 emission line was tracked to monitor sample pressure, which is known to redshift with increasing pressure [1]. A 532 nm diode laser was focused on one of the diamonds of the DAC using a 10x microscope objective and excited both the phosphor and ruby powder. Emission was collected through this objective and directed to an optical fiber connected to an Ocean Optics QEPro spectrometer which recorded emission from each material.

To determine phosphor temperature dependence, phosphor powders were loaded into quartz cuvettes (10 mm path length) and placed within a high temperature furnace (Mellen Microtherm). Lenses directed a Hamamatsu LightningCure 365 nm LED onto the phosphor sample and emission was recorded using an Ocean Optics HR2000+ spectrometer. A type K thermocouple was placed on the cuvette surface to measure sample temperature. Emission spectra were recorded during furnace heating and cooling.

Modulation of Y_2O_3:Eu emission spectra due to pressure and temperature is presented in Figure 1. Several prominent emission peaks are present in the left plot of Figure 1, showing the ruby and phosphor emission observed when compressing then decompressing the DAC. Note

that pressures given in this plot represent a shift in pressure relative to ambient conditions. The rightmost band in these spectra originate from the ruby, exhibiting two peaks. The taller R1 peak location was tracked after fitting an asymmetric pseudo-Voigt profile [2] and the wavelength shift found from this tracking was used to calculate cell pressure using a quadratic equation provided by Piermarini et al. [1]:

$$P = A(\Delta\nu) + B(\Delta\nu^2)$$

In this expression, the fitted constants are $A = 2.735$ and $B = 0.003$. Other prominent peaks include several $^5D0 \rightarrow {}^7FJ$ transitions of Y_2O_3:Eu (J = 0, 1, 2, 3, 4). Of note are the $^5D0 \rightarrow {}^7F1$ peak centered near 590 nm and the prominent $^5D0 \rightarrow {}^7F2$ peak at 611 nm. The former is a magnetic dipole transition and pressure insensitive whereas the latter originates from an electric dipole and is observed to be highly sensitive to pressure [3]. An irreversible shift in the Y_2O_3:Eu spectrum is observed as pressure is increased to the maximum of 17.7 GPa before reducing pressure to ambient. The thermographic response of Y_2O_3:Eu photoluminescence is highlighted in righthand plot of Figure 1 showing an intensity ratio calculation between two integrated spectral bands of the spectrometer data (612.5 ± 7.5 nm and 630 ± 10 nm). This plot shows the calculated ratio as temperature was increased to a maximum of 409 °C then cooled to room temperature. This demonstrates the time integrated thermographic response of Y_2O_3:Eu which also appears to be hysteretic. These results show that Y_2O_3:Eu is a good candidate for dual pressure and temperature sensing within highly dynamic shock compressed environments.

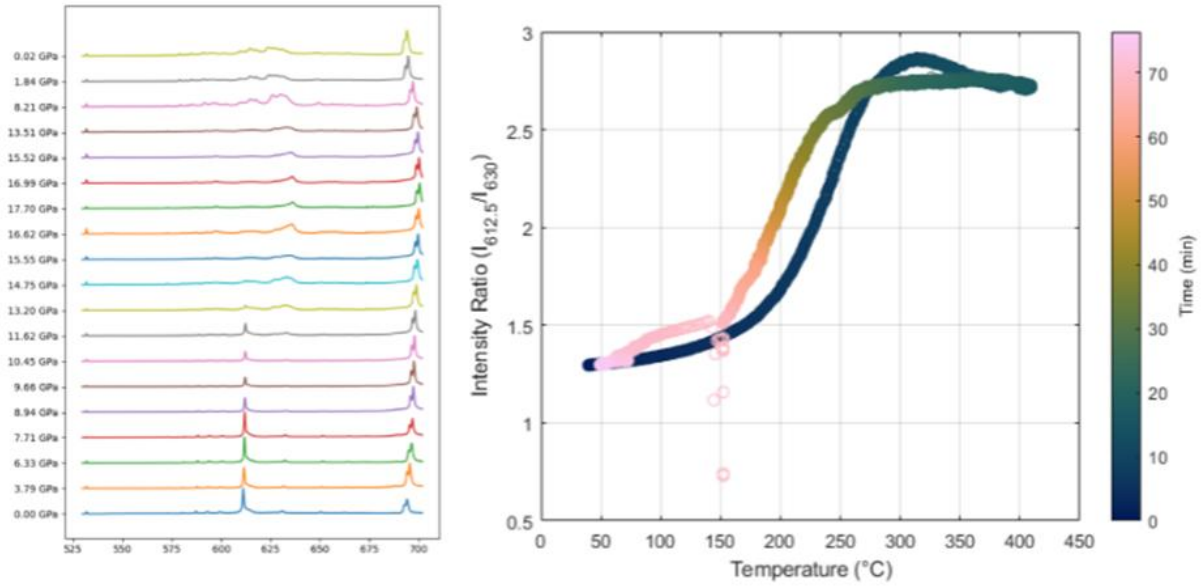

Figure 1. Left: emission spectra of Y_2O_3:Eu as a function of pressure when compressed within a diamond anvil cell. Ruby emission peaks are also present near 690-700 nm and are used to track cell pressure. Right: calculated intensity ratios between two integrated spectral regions (612.5 ± 7.5 nm and 630 ± 10 nm) as temperature of Y_2O_3:Eu powder is increased to 409 °C then cooled to room temperature.

[1] G. J. Piermarini, S. Block, J. D. Barnett, R. A. Forman, J. Appl. Phys. 46 (1975) 2774-2780.

[2] A. L. Stancik, E. B. Brauns, Vib. Spectrosc. 47 (2008) 66-69.
[3] J. Zhang, H. Cui, P. Zhu, C. Ma, X. Wu, H. Zhu, Y. Ma, Q. Cui, J. Appl. Phys. 115(2014) 023502.

Sandia National Laboratories is a multimission laboratory managed and operated by National Technology & Engineering Solutions of Sandia, LLC, a wholly owned subsidiary of Honeywell International Inc., for the U.S. Department of Energy's National Nuclear Security Administration under contract DE-NA0003525. SAND2026-20643A

41. From Errors to Information: Reliability in Luminescence Thermometry for Biology

Nikita Panov, Marina París Ogáyar, Liyan Ming, Erving Ximendes, Riccardo Marin, Daniel Jaque

Facultad de Ciencias, Universidad Autónoma de Madrid, Madrid, Spain,
riccardo.marin@uam.es, daniel.jaque@uam.es

Luminescence thermometry is a very powerful tool to measure temperature without contact and with high spatial resolution. It has clear potential in biology and medicine, for example to monitor temperature inside tissues or even inside cells. However, when we move from ideal conditions to real biological environments, important problems appear. The main issue is reliability. The luminescence signal does not depend only on temperature. It is also affected by many other factors such as light absorption and scattering in tissue, probe concentration, or local chemical conditions. These effects introduce bias and cross-sensitivity, which can lead to wrong temperature readings if they are not properly considered. This is the bad news: in realistic (live) conditions, many luminescent thermometers do not behave as ideal temperature sensors.

But there is also good news. The same effects that generate errors also carry useful information. For example, changes in the emission spectrum caused by tissue absorption or by the local environment can be used to extract information beyond temperature. If properly analysed, these "distortions" can help us to understand the optical properties of the tissue or even its composition.

In this talk, I will show how we can move from trying to eliminate these effects to using them in a smart way. By combining hyperspectral measurements with simple physical models and data analysis tools, it is possible to separate temperature from other contributions and, at the same time, obtain additional information from the system. This approach changes the role of luminescent thermometers. Instead of being only temperature sensors, they can become more complete optical probes, able to provide multiple types of information in complex biological environments.

42. Where Does the Heat Go? Hyperspectral Upconversion Thermometry of Plasmonic Nanowire Networks

Eduardo Martínez[a], Luiz Ferreira[b], Carlos D. S. Brites[c], Ricardo Urbano[b], Luís D. Carlos[c]

[a] Instituto de Nanociencia y Nanotecnología (CNEA-CONICET), Av. Bustillo 9500, S. C. de Bariloche (8400), Río Negro, Argentina
[b] Gleb Wataghin Institute of Physics (IFGW), University of Campinas (UNICAMP), Campinas, Brazil
[c] Phantom-g, CICECO – Aveiro Institute of Materials, Department of Physics, University of Aveiro, 3810–193, Aveiro, Portugal

Light, matter, and heat are inseparable at the nanoscale, yet experimental tools have long treated them as independent variables. In plasmonic and transparent optoelectronic systems, performance is often governed by how electromagnetic energy is converted into heat, making accurate hotspot thermometry essential.

While scanning techniques such as scanning thermal microscopy provide high spatial resolution, their point-by-point acquisition and probe interactions limit their use in complex or dynamic systems. In contrast, luminescence thermometry based on rare-earth-doped upconversion nanoparticles (UCNPs), combined with hyperspectral microscopy, enables fast, wide-field temperature mapping with high sensitivity and sub-diffraction potential.

Here, we present a hyperspectral thermometry platform based on UCNPs integrated with electrically percolated silver nanowire networks, where plasmonic enhancement, nonlinear emission, and heat dissipation are intrinsically coupled.[1-3] Although plasmonic hotspots strongly amplify upconversion emission, they can introduce artifacts in conventional thermometry, raising the key question of whether electromagnetic hotspots correspond to real temperature increases.

By employing ultrasmall anti-thermal-quenching UCNPs, we directly visualize nanoscale thermal hotspots along conductive pathways, resolving temperature gradients of 8 ± 1 K·μm^{-1} with ~88 nm spatial resolution. These results demonstrate that plasmonic and thermal hotspots do not necessarily coincide, establishing hyperspectral upconversion thermometry as a powerful tool for nanoscale heat mapping in advanced optical materials.

[1] E. D. Martínez, et al., Adv. Funct. Mater. 29 (2019) 1807758.
[2] E. D. Martínez, et al., Nanoscale 13 (2021) 18267.
[3] E. D. Martínez, et al., Nanoscale 16 (2024) 18941.

43. Decoding Transient Luminescence with Machine Learning: Toward Autonomous Thermometry

Carlos D. S. Brites

CICECO–Aveiro Institute of Materials, Physics Department, University of Aveiro, 3810-193, Aveiro, Portugal, carlos.brites@ua.pt

Transient luminescence signals encode rich information about dynamic thermal processes, yet extracting meaningful physical parameters from these data remains a major challenge [1,2]. In particular, the determination of the onset time in transient heating curves is highly sensitive to experimental noise and typically relies on manual, operator-dependent signal-processing procedures.

Here, we demonstrate a machine-learning-assisted approach to decode transient luminescence thermometry data and enable autonomous extraction of onset times. Artificial neural networks are trained on a hybrid dataset combining experimental heating curves from Ln^{3+}-doped upconverting nanoparticles with physically motivated synthetic transients, extending the diversity of thermal dynamics beyond experimentally accessible conditions [1].

We show that the accuracy and robustness of onset-time prediction are primarily dictated by the diversity and physical consistency of the training data rather than by the complexity of the neural network architecture. Compared to conventional discrete wavelet transform (DWT)-based analysis, the machine learning models achieve comparable accuracy, with typical errors on the order of a few seconds, while eliminating the need for manual preprocessing and empirical parameter selection [1]. Once trained, the models enable rapid inference with sub-second processing times per transient curve.

This approach transforms transient luminescence thermometry into a scalable, operator-independent methodology, paving the way for real-time thermal sensing and high-throughput analysis [1,3]. More broadly, it establishes a framework for integrating machine learning into time-resolved luminescence measurements, in line with recent advances in data-driven luminescence thermometry and intelligent sensing systems [3,4].

[1] D. J. Sousa, E. Ximendes, L. D. Carlos, C. D. S. Brites, Adv. Intell. Discov. (2026) e202600003.
[2] C. D. S. Brites, R. Marin, M. Suta, et al., Adv. Mater. 35 (2023) 2302749.
[3] W. Xu, C. L. Xu, J. Q. Cui, et al., Opt. Lett. 49 (2024) 606–609.
[4] E. H. Santos, W. F. Silva, E. C. Ximendes, et al., Sens. Actuators A 389 (2025) 11655

Day 1 – Wednesday
24/06/2026
Posters session

1. Mn^{2+}/Mn^{4+} Luminescence Decay Kinetics in Aluminate Phosphors for Frequency-Domain Optical Temperature Sensing

Anatolijs Sarakovskis, Pavels Rodionovs, Guna Krieke, Andris Fedotovs, Janis Trokšs, Ainars Ozols, Uldis Rogulis

Institute of Solid State Physics, University of Latvia, 8 Kengaraga Str. 8, Riga, Latvia, anatolijs.sarakovskis@cfi.lu.lv

Reliable temperature monitoring in environments where conventional contact sensors are difficult to apply requires sensing approaches that are electrically passive, chemically robust, and compatible with remote readout. This work presents the development of a fully optical fibre-based temperature sensing concept intended for operation over an extended temperature range, from at least -150 °C to +350 °C. The proposed approach is based on manganese-activated complex aluminate phosphors and frequency-domain luminescence decay readout, enabling temperature determination through phase-shift measurements rather than intensity alone.

Polycrystalline strontium magnesium aluminate activated with Mn^{2+} and Mn^{4+} was prepared by a high-temperature solid-state synthesis route. Separate compositions containing Mn^{2+} and Mn^{4+} centres were obtained and characterised optically under blue excitation. The Mn^{2+}-related emission appears as a broad green band with a maximum near 525 nm, whereas the Mn^{4+}-related emission is observed as a red band centred near 687 nm. The clear spectral separation of the two emission channels provides the basis for dual-channel optical thermometry and allows the complementary temperature responses to be used within one sensing platform.

Temperature-dependent luminescence decay behaviour was analysed using sinusoidally modulated excitation and phase-shift detection in the frequency domain. The developed readout concept is compatible with optical fibre delivery and collection: excitation light is guided to the sensing element through an optical fibre, while the returning luminescence is separated into green and red channels using dichroic optics. Modulation frequencies in the range of 10–150 Hz were considered for stable phase-sensitive detection.

The results confirm that both manganese centres exhibit pronounced and complementary temperature-dependent phase responses. The Mn^{4+} channel is particularly relevant in the low-temperature region, whereas the Mn^{2+} channel becomes increasingly important at elevated temperatures. Phase-shift sensitivities of up to 0.08 deg/K for the Mn^{4+}-activated material and 0.1 deg/K for the Mn^{2+}-activated material were obtained, demonstrating the suitability of the materials for broad-range optical thermometry. The combined Mn^{2+}/Mn^{4+} strategy therefore extends the useful operating range beyond that of a single luminescent centre and supports continuous temperature readout from cryogenic to high-temperature conditions.

2. Thermographic Phosphor Coatings for Temperature Measurement of an Impinging Jet

Shabnam Mohammadshahi[a], Allianna Chavez[a], Andrea Gallegos Quintana[a]

[a]Department of Mechanical and Aerospace Engineering, New Mexico State University, Las Cruces, NM 88003, USA, shabnam@nmsu.edu.

Accurate surface temperature measurement is important in jet impingement experiments, where conventional contact sensors may disturb the flow field or alter the thermal response of the surface. Thermographic Phosphor Thermometry (TPT) provides a non-contact approach by using phosphor materials whose luminescence response varies with temperature after optical excitation. In this study, Magnesium Fluorogermanate (MFG)-based phosphor coatings were developed and evaluated for surface temperature measurements under impinging jet conditions. MFG particles were mixed with two binder systems, ZAP and hydroxypropyl cellulose (HPC), using a 1:3 mass ratio and deposited on test surfaces by airbrushing. The coated samples were vacuum-dried for 24 hours and thermally cured at 150 °C. The coating quality was assessed based on surface uniformity, optical response, adhesion, and resistance to mechanical damage. The HPC-based coating showed poor bonding and low scratch resistance, while the ZAP-based coating produced a harder and more durable layer. Although some discoloration was observed after curing, the ZAP-based coating was selected for further testing because of its improved mechanical robustness.

Before temperature calibration, the excitation and emission characteristics of the MFG particles were measured using a spectrometer. An ultraviolet LED with a wavelength of 385 nm was used for excitation, and the main emission peak was identified near 655 nm. Lifetime-based calibration experiments were then conducted over a temperature range of 25 °C to 300 °C using a high-speed camera, a 655 ± 10 nm band-pass filter, and K-type thermocouples for reference temperature measurements. The calibrated ZAP-based MFG coating was then applied in an impinging jet experiment to evaluate its practical performance under flow and thermal loading conditions. The results show that binder selection and curing conditions strongly affect coating durability and optical quality. Overall, the ZAP-based MFG coating provides a suitable foundation for TPT-based surface temperature measurements in impinging jet studies.

3. Spectral-Shift Phosphor Thermometry Under Double-Pulsed Excitation

Ömer F. Kadı[a], Mucahit Korkmaz[a], Şahan Aktepe[a], Semih Yurtseven [a], Humbet Nasibli[a]

[a]National Metrology Institute, TÜBİTAK UME, Gebze, Kocaeli, Türkiye
humbet.nasibli@tubitak.gov.tr

Surface temperature, although not rigorously defined under non-equilibrium conditions, remains a key parameter in many industrial, scientific, and biomedical applications. Although contact thermometry provides the highest accuracy under thermal equilibrium conditions, its use in surface measurements is limited by thermal disturbance, point-wise sensing, and unsuitability for moving objects. Infrared techniques enable remote SI-traceable measurements but strongly depend on emissivity and ambient radiation. Consequently, phosphor thermometry has emerged as a promising non-contact technique for harsh environments, moving objects, and fast transient processes [1-3].

In phosphor thermometry, a phosphor-coated surface is optically excited, producing temperature-dependent luminescence whose spectral or temporal characteristics enable temperature determination after calibration. Laser excitation is especially advantageous due to its high energy density, spectral purity, remote delivery capability, and short pulse duration. However, increasing laser pulse energy to improve the phosphorescence signal may lead to phosphor coating damage and laser-induced self-heating, resulting in temperature measurement errors. In this work, a double-pulsed laser excitation approach is proposed for spectral-shift phosphor thermometry to enhance the phosphorescence signal without significantly increasing the energy of a single pulse. Ruby was used as the phosphorescent material and excited with nanosecond laser pulses. Upon optical excitation, Cr^{3+} ions are promoted to higher electronic states and rapidly relax non-radiatively to the metastable ^2E state, from which red emission near 694 nm is generated. Since the $^2E \rightarrow {}^4A_2$ transition has a millisecond-scale lifetime, a second excitation pulse can be applied before the metastable population has significantly decayed, increasing the excited-state population and consequently enhancing the phosphorescence intensity. In our previous studies [4, 5] on decay-time phosphor thermometry, this approach demonstrated approximately a twofold increase in signal intensity without altering the decay-time-based temperature indicator. In the present work, we demonstrate that the same concept can be successfully applied to spectral-shift thermometry. While the second pulse increases the number of emitted photons, the spectral fingerprint of ruby remains unchanged, preserving the temperature-dependent spectral characteristics while significantly improving signal intensity. Experiments performed from room temperature up to approximately 550 °C demonstrate the effectiveness of the proposed approach. The work also presents a detailed description of the experimental setup, including laser sources, timing electronics, spectral measurement system and a furnace system used for phosphor thermometer calibration and validation.

[1] G. Sutton, S. Korniliou, A. Andreu, D. Wilson, Int J Thermophys 43 (2022) 36.
[2] G. Machin et al., Nuclear Engineering and Design, 371 (2021) 110939.
[3] G Sutton et al., Meas. Sci. Technol., 30 (2019) 044002.
[4] O.F. Kadi et al., Meas. Sci. Technol., (2026) In preparation for submission
[5] O.F. Kadi et al., IEEE TIM. (2026) In submission

4. Development of HT Phosphor Thermometry and Calibration Facility at DTI

Henrik Kjeldsen[a,b], Thomas Scrøder Daubjerg[a], Rasmus Degn[a], Christina Kjær Langeland[a], Jan Nielsen[a]

[a]Danish Technological Institute (DTI), Kongsvang Allé 29, 8000 Aarhus C, Denmark
[b]hkje@teknologisk.dk

Phosphor thermometry is especially valuable when accurate, remote, and robust surface temperature measurement is needed. It provides several advantages, such as non-contact measurement, works in harsh environments, suitable for high temperatures, low sensitivity to surface emissivity, good spatial resolution, fast response, and wide temperature range.

DTI has previously developed a phosphor thermometer based on decay-time measurement [1]. This setup is limited to about 500 °C, because the decay time becomes increasingly small as a function of increasing temperature. In order to extend the measurement range to higher temperatures above 1000 °C, a new setup based on intensity-ratio measurement has been designed and constructed. It includes adjustable optics to adjust the sensitivity area from about a mm to averaging over several cm's. In addition, a furnaced-based system for traceable calibration in the range 200 – 1200 °C have been set up.

In the present report, the design and initial tests will be presented.

Reference to a journal publication:
[1] D H Lowe et al 2022 Meas. Sci. Technol. 33 065007

5th International Conference on Phosphor Thermometry
June 24-26th, 2026

11/06/2026

The National Physical Laboratory
Teddington, UK